January 2020

Age Differences In Hippocampal Glutamate Modulation During Associative Learning And Memory: A Proton Functional Magnetic Resonance Spectroscopy (1h Fmrs) Study

Chaitali Anand
Wayne State University

AGE DIFFERENCES IN HIPPOCAMPAL GLUTAMATE MODULATION DURING ASSOCIATIVE LEARNING AND MEMORY: A PROTON FUNCTIONAL MAGNETIC RESONANCE SPECTROSCOPY (^{1}H fMRS) STUDY

by

CHAITALI ANAND

DISSERTATION

Submitted to the Graduate School

of Wayne State University,

Detroit, Michigan

in partial fulfillment of the requirements

for the degree of

DOCTOR OF PHILOSOPHY

2020

MAJOR: NEUROSCIENCE (Translational)

Approved By:

_____

Co-advisor Date

_____

Co-advisor Date

_____

_____

_____

DEDICATION

॥ श्री गणेशाय नमः ॥

(English translation: "Lord Ganesha, I pray to you.")

This work is dedicated to my family. To my Aai, who has always showered her blessings on me from up above. To my Baba, whose words of wisdom resonate with me and whose calm personality has always been my source of strength and composure. To my in-laws, Papa and Mumma, who have been my constant cheerleaders and pillars. To my brother, Ranajeet, with whom I have shared all ups and downs in life and who always makes me laugh. To my ever-supporting husband, Rajit, for his patience, unwavering love, and motivation. Love you.

ACKNOWLEDGEMENTS

"It is good to have an end to journey toward; but it is the journey that matters, in the end"

- Ernest Hemingway.

As I look back and ponder over my years in graduate school in the Translational Neuroscience Program at Wayne State University, I am reminded of everyone who has willingly and sometimes unknowingly made this long and winding path, a journey of immense growth, laughter, love, and learning. I want to take this opportunity to acknowledge them.

First, I sincerely thank my dissertation advisors, Dr. Naftali Raz and Dr. Jeffrey Stanley, for mentoring, challenging, and always encouraging me to think out of the box and overcome new obstacles. I am humbled to have had their support and hope that I have lived up to their expectations. I thank my committee members, Dr. Noa Ofen, Dr. Vaibhav Diwadkar, and Dr. John Woodard for their guidance and encouragement over the past several years. I am enormously grateful for their valuable input during my qualifying exam.

While research work has sometimes yielded successes and has often been frustrating, it was counting the small blessings that helped me persist forward. I am indebted to Caroline for her kindness in always being there for me and helping me with the incessant administrative questions I might have posed. I thank Dalal for being an amazing friend, a confidante, and for always going out of her way to help me scan participants. I thank Cheryl for being a wonderful friend, a confidante, a fun lunchmate, and a fabulous support in lab. I am also very thankful to my lab members and TNPeeps - past and present, for having a very positive influence on many aspects of my academic life and inspiring me to be more creative and seek out new challenges and ideas. Within and outside the TNP, thank you Wafaa, Brian, Andrew, Sophia, Ruta, Zeshan, Shahira, Asadur, Lingfei, Qijing, Roya, Qin, Pushpa, Richa, Drew, Shruti, Shilpa, and Suhasini -

for providing frequent encouragement, much needed coffee-breaks, and comic relief during grad life.

I thank Pavan and Zahid at the MRRF for accommodating my scanning schedule and helping with technical issues at the scanner. Thanks to Sonya, Jennifer, and Cordell at the TNP for their help with managing my grant and funding. I appreciate the support extended to me by Dr. Gail Jensen Summers, Dr. Peter Lichtenberg, Carol Talbott, and Syed Hussain at the Institute of Gerontology. I thank Dr. Wassim Tarraf and Dr. Ana Daugherty for going out of their way to lend advice on statistical analyses and for teaching me the importance of quality work.

Last but not the least, I thank my participants for taking time out of their busy days to participate in my study and help my research. I thank the Translational Neuroscience Program for giving me the opportunity to be a part of them and for supporting my training. I also wish to extend my gratitude towards the National Institutes of Health – National Institute on Aging (NIH NIA) for recognizing the potential of my project and doctoral training by awarding me the NRSA F31 predoctoral fellowship. Thanks also to the Blue Cross Blue Shield of Michigan for taking notice of my work and supporting me with a student award.

This long and challenging journey would not have been possible without the incredible enthusiasm, sacrifices, and love of my dearest family who cheered me on and always encouraged me to be the best person I could be. Their unshakeable faith in me gave me the confidence I needed to believe in myself. In the end, and forever, I thank my loving husband, Rajit, for his unflinching support, immense patience, and for being a constant motivating force pushing me to achieve greater heights and go beyond my limits. He never ceases to amaze me! By far my greatest source of strength came, and continues to come, from Aai, my mother – from her presence through her absence. Thank you for always being there when I look above.

TABLE OF CONTENTS

LIST OF TABLES

LIST OF FIGURES

LIST OF ABBREVIATIONS

^{1}H fMRS	Functional Proton Magnetic Resonance Spectroscopy
^{1}H MRS	Proton Magnetic Resonance Spectroscopy
AD	Alzheimer's disease
ADH	Associative Deficit Hypothesis
ATP	Adenosine Triphosphate
BOLD	Blood Oxygen Level Dependent
CRLB	Cramér-Rao lower bounds
CI	Confidence interval
CSF	Cerebrospinal fluid
E/I	Excitation/Inhibition
EM	Episodic memory
FID	Free Induction Decay
FOV	Field of View
FWHM	Full Width at Half Maximum
GLM	General Linear Model
Gln	Glutamine
Glu	Glutamate
GPC+PC	Glycerophosphocholine + Choline
LCModel	Linear Combination Model
LTP	Long term potentiation
MTL	Medial temporal lobe
NAA	N-acetyl aspartate

NMDA	N-methyl-D-aspartate
PCr+Cr	Phosphocreatine + Creatine
PRESS	Point Resolved Spectroscopy
RF	Radiofrequency
ROI	Region of Interest
SNR	Signal to Noise Ratio
SVS	Single Voxel Spectroscopy
T	Tesla
TA	Acquisition Time
TCA	Tricarboxylic Acid
TE	Echo Time
TR	Repetition Time

CHAPTER 1 ASSOCIATIVE MEMORY FUNCTION IN THE AGING BRAIN

1.1 Public health significance of studying normal aging: Implications towards understanding Alzheimer's disease

Advances in medicine and health care are shifting the demographics worldwide, with the number of individuals over 65 years of age in the US projected to triple from the year 2000 to 2060 (www.census.gov). Longevity, however, comes with a risk of increased occurrence of age-related cognitive deficits imparting tremendous societal, economic, and healthcare burden on patients and their families. About 5.4 million older Americans have cognitive impairments without full-blown dementia, and such impairments affect the quality of life. Aging is also associated with a dramatic rise in the incidence of neurodegenerative disorders such as Alzheimer disease (AD), and indeed is the primary risk factor thereof. Healthcare, financial, and emotional burden, along with the fact that the neuropathology of AD precedes cognitive changes by several years, make it crucial to identify biomarkers of very early disease progression (Rupsingh, Borrie, Smith, Wells, & Bartha, 2011) to help make timely intervention possible. The good news in medicine is that early detection often means early intervention. Clinical trials for AD have focused on drugs targeting cognitive symptoms of the disease, as well as classical AD pathology such as amyloid beta plaques and tau tangles as seen on MRIs. AD diagnosis has also always been based primarily on the detection of these two pathological signatures. However, the amyloid hypothesis of AD has been unsuccessful in producing consistent data on disease prognosis (Makin, 2018), hence, also failing to contribute to the design of effective interventions. Most interventions targeting amyloid plaques have been futile in their attempt to improve cognitive performance and nor have they slowed down the progression of dementia. It is thus, important to target an earlier point in time that precedes the occurrence of amyloid and tau.

While age-related dementia and AD are important concerns, most people undergo 'normal aging' or 'healthy aging' and do not go on to develop dementia. Although cognitive decline is a key manifestation of AD, it is part of normal aging as well. An understanding of the aging process and age differences that underlie cognitive dysfunction are important to be able to identify deviations from normal to pathological aging and to eventually design effective interventions to slow them. This dissertation focuses on an approach towards identifying a plausible functional biomarker of age-related differences in cognition, specifically in associative learning and memory performance. The present study is significant as it contributes, not only to the understanding of age effects on cognition but can also be applied to track cognitive changes in aging and impending dementia.

1.1.1 Associative memory in aging

Memory loss is one of the earliest cognitive impairments observed in normal aging as well as in dementia and is also the one that has received the most attention. However, an intriguing feature of age effects on memory is their variability. Memory is not a single construct but is instead of several types that are differentially vulnerable to the effects of age. Of those, decline in episodic memory (EM) is a hallmark feature of cognitive aging (Rönnlund, Nyberg, Backman, & Nilsson, 2005; Verhaeghen & Marcoen, 1993) and, at its extremes, a defining symptom of AD (Morris & Kopelman, 1986). EM amounts to recollecting experiences that occur in time and space (Rolls, Stringer, & Trappenberg, 2002) and frequently relies on establishing associations between two unrelated stimuli where one stimulus can invoke the other during recall. The ability to use contextual cues linked to the target items for facilitating the retrieval of the latter is a general feature of EM and has been described as environmental support (Craik, 1986). The two-component framework of EM includes an associative component representing the binding processes that combine features of episodes (i.e. the stimuli) to create coherent

representations; and a strategy component made up of cognitive processes that support and regulate memory functions (Shing, Werkle-Bergner, Li, & Lindenberger, 2008). Memory function involves, besides perception of the stimulus; encoding, consolidation, maintenance, and retrieval (Tulving, 1983). Memory encoding involves the pairing of distinct memoranda such as faces with names, objects with locations, or any other contextual features. Making associations between previously unrelated memoranda helps us navigate the world.

Extant literature suggests that in most cases, older adults' EM decline is attributed to impairment in the associative component (Naveh-Benjamin & Mayr, 2018). Older adults are differentially impaired in retrieving *associations* rather than individual items and show disproportionately lower recall for contextual cues that could have been useful in facilitating recall (Old & Naveh-Benjamin, 2008; Spencer & Raz, 1995). This differential impairment has led to the formulation of the associative deficit hypothesis (ADH), which states that impaired binding of individual units of information into associations is the core reason for age-related memory decline (Naveh-Benjamin, 2000). The ADH has been confirmed in paired-associate memory studies utilizing tasks such as learning associations between word-pairs, words-pictures, and faces-names (Bender, Naveh-Benjamin, Amann, & Raz, 2017; Naveh-Benjamin, 2000). Some reports have suggested that deficiencies in associative encoding, more than retrieval, play a larger role in associative and episodic memory dysfunction in the elderly (Friedman, Nessler, & Johnson, 2007; Tromp, Dufour, Lithfous, Pebayle, & Despres, 2015). With the ADH gaining wide acceptance, it still remains unclear what brain mechanisms are responsible for the emergence of this age-related deficit.

1.2 Hippocampal and glutamatergic involvement in associative memory

1.2.1 Role of the hippocampus

Memory function has been linked to the brain's integrity (Ribot, 1882)., with the main brain regions involved in associative encoding and retrieval being the medial temporal lobe (MTL), the prefrontal cortex (PFC), the lateral parietal cortex, and the dorsal anterior cingulate cortex (dACC) (Davachi, 2006; Woodcock, White, & Diwadkar, 2015). However, since the seminal study of the patient H.M. (Scoville & Milner, 1957), the attention of memory researchers has been focused on the hippocampus and surrounding circuitry (Lavenex & Amaral, 2000). The hippocampus is critical for the binding of distinct memoranda and the formation of memory, for temporarily storing memory of individual items and associations, and later transferring them to the neocortex for permanent storage (Eichenbaum, 2001). The unique anatomical location of the hippocampus facilitates the reception of inputs from the association cortices, making it the hub of the associative memory network (Lavenex & Amaral, 2000; Ungerleider, 1995) (Binding of Items and Contexts model, BIC, (R. A. Diana, Yonelinas, & Ranganath, 2007)). For example, the ventral and dorsal visual processing streams ('what' and 'where' pathways) carrying information about the identity and spatial location of an object, respectively, relay it to the lateral and medial entorhinal cortices via the perirhinal and the parahippocampal cortices, respectively (Lavenex & Amaral, 2000), to finally converge at the level of the hippocampus.

Studies on human brain lesions (Burgess, Maguire, & O'Keefe, 2002; Zola-Morgan, Squire, & Amaral, 1986) and animal models (Eichenbaum, Yonelinas, & Ranganath, 2007; Suzuki, 2007) support the view of the hippocampus and connected MTL circuitry as the most important neural substrates of EM in general and associative memory, in particular. Sustained hippocampal activity is required for encoding memories of new items as well as formation and maintenance of associations among them (Davachi & Wagner, 2002; Piekema, Kessels, Mars,

Petersson, & Fernandez, 2006). The importance of the hippocampus in associative memory function is further underscored by the observation of greater hippocampal activation (evidenced by fMRI) during the encoding of associations than of single items (Dennis et al., 2008).

With hippocampal shrinkage being a well-documented feature of normal aging (Raz & Rodrigue, 2006) and one of the earliest foci of neurodegeneration in AD (Braak & Braak, 1995), it stands to reason that memory declines would correlate with hippocampal structural changes. Although there is indeed some limited support for that expectation, the hypothesized associations remain weak and inconsistently replicated (VanPetten, 2004). It is important, also to acknowledge, that aging is a problem of dysfunction and is not characterized by prominent neuronal loss (Morrison & Hof, 1997; Yankner, Lu, & Loerch, 2008). Stereological cell counting methods indicate almost no age-related neuronal loss in the hippocampi of rodents (Rapp & Gallagher, 1996), non-human primates (M.J. West, Amaral, & Rapp, 1993), and humans (M. J. West, 1993). Further, there are no documented age-related changes in the basic cellular characteristics (resting membrane potential, amplitude and duration of action potentials) of hippocampal neurons (Rosenzweig & Barnes, 2003). Given that the changes in hippocampal cellular structure and properties are not prominent in aging, it is important to turn our attention and research focus to the functional molecular mechanisms at the synapse that might deteriorate with age. Indeed, fine synaptic changes and alterations in the neurochemical environment of the synapse can precede the cognitive and gross structural changes that occur as a part of aging and AD, by several years (Walsh & Selkoe, 2004). Since the functional changes underpinning the putative relationship between hippocampal structural integrity and memory remain unclear, investigating age-related differences in neurochemical foundations of memory processes may shed light on the neural mechanism of memory declines in aging.

1.2.2 Glutamatergic neurotransmission in memory function

Investigation of the neural mechanisms of memory function has a long history in experimental and theoretical neuroscience, which links memory formation to cellular structural plasticity (Chen & Tonegawa, 1997; Hebb, 1949) driven by long-term potentiation (LTP, (Bliss & Collingridge, 1993; Kauer, Malenka, & Nicoll, 1988; Lynch, 2004; Nicoll, 2017)). LTP is the cellular mechanism of information storage that modifies the synaptic connections, increases their strength over time, in turn strengthening the encoded memory (Rolls et al., 2002). The necessary condition for LTP and, by implication, memory formation, is the activation of glutamatergic ionotropic N-methyl-D-aspartate (NMDA) receptors that are richly represented in the hippocampus (McEntee & Crook, 1993). Glutamate is the major excitatory neurotransmitter in the mammalian brain, with 80% of cortical neurons being glutamatergic. Glutamatergic NMDA receptors play a role in long term memory formation via synaptic plasticity mediated by LTP (Hebb, 1949). LTP depends on correlated and coincident pre- and post-synaptic activity efficiently supported by NMDA receptors by virtue of being molecular coincidence detectors (Tabone & Ramaswami, 2012). Specifically, *pre-synaptic* depolarization releases glutamate that rapidly diffuses through the synaptic cleft and binds the *post-synaptic* NMDA receptor, bringing about depolarization of the post-synaptic membrane. This depolarization relieves the NMDA receptor of the voltage dependent magnesium (Mg^{2+}) block, thus, allowing the influx of calcium (Ca^{2+}) ions that carry out the downstream events to trigger LTP (Rosenzweig & Barnes, 2003; Tatti, Haley, Swanson, Tselha, & Maffei, 2017). By detecting coincident pre- and post-synaptic depolarization, the NMDA receptors ensure that LTP is restricted to the synapses that display this activity. Increase in excitatory neurotransmission is also accompanied by increased synthesis of glutamate.

Overexpression of NMDA receptors in rodent hippocampi and the ensuing augmentation of synaptic potentiation therein, result in improved spatial learning and memory as assessed using the Morris water maze (Tang et al., 1999). Conversely, selective ablation of NMDA receptors in the hippocampi of adult mice profoundly impairs the recall of associations learned during the water maze task (Magnusson, Brim, & Das, 2010; Morris, Anderson, Lynch, & Baudry, 1986). Pharmacological agents that support the activation of glutamate receptors show a reversal of the cognitive deficit (Müller, Scheuer, & Stoll, 1994). This suggests a dependence of associative recall on NMDA receptor sensitivity and glutamatergic neurotransmission in the hippocampus. A direct relationship between the firing rates of hippocampal glutamatergic neurons and acquisition of new associative memories (Suzuki, 2007) also supports hippocampal glutamatergic involvement in learning and memory.

Delayed induction and inefficient maintenance of LTP occur with aging (G. Diana, Scotti de Carolis, Frank, Domenici, & Sagratella, 1994) and may be supported by well-documented age-associated declines in the number, binding efficiency, and electrophysiological functions of hippocampal NMDA receptors (Magnusson et al., 2010; Müller, Stoll, Scheuer, & Meichelbock, 1994; Rosenzweig & Barnes, 2003). It is in fact suggested that cognitive deficits induced experimentally using NMDA receptor antagonists mimic, in many ways, those seen as a part of age-related cognitive impairments (Müller, Stoll, et al., 1994). Therefore, investigating hippocampal synaptic activity such as glutamate modulation during memory performance may offer a key to understanding age-related memory decline.

1.2.3 Physiological basis of glutamatergic neurotransmission: The Glutamate-Glutamine cycle

It is important to understand the physiological bases of neurotransmission in order to appreciate the glutamatergic dynamics that occur during neuronal engagement. Neuronal response to stimulation prompts changes in neurovascular and neurometabolic processes such as

increase in cerebral blood flow, glycolysis and oxidative metabolism, synthesis of neurotransmitters such as glutamate, as well as increase in neurotransmission (Mergenthaler, Lindauer, Dienel, & Meisel, 2013; Rothman, Behar, Hyder, & Shulman, 2003).

Glucose is the primary source of energy for sustaining the above-mentioned processes under non-fasting conditions. After being taken up by astrocytes (via glucose transporter, GLUT1) and neurons (via GLUT3), glucose undergoes glycolysis to generate pyruvate that then enters the mitochondrial tricarboxylic acid (TCA) cycle of oxidative metabolism. Astrocytes and neurons have their own TCA cycles. Astrocytes, owing to the presence of pyruvate carboxylase, are the only cells that can synthesize new glutamate via α-ketoglutarate (a TCA cycle intermediate), and transfer it to neurons in the form of glutamine. As explained below, pre-synaptic neurons convert glutamine to glutamate and package it into vesicles with the help of vesicular glutamate transporters (vGLUTs). Vesicular glutamate is released into the synaptic cleft upon depolarization induced by increased neuronal activity. Following its release from the pre-synaptic terminal, glutamate binds post-synaptic NMDA receptors to start the processes of LTP generation. Excess synaptic glutamate is taken up by astrocytes to ensure that extracellular levels of glutamate are kept low in order to prevent excitotoxicity. Inside astrocytes, glutamate is converted predominantly to glutamine by glutamine synthetase, an enzyme found only in these cells. Glutamine released by the astrocytes is taken up by the pre-synaptic neuron and converted to glutamate by glutaminase, thus completing the glutamate-glutamine cycle (Rothman et al., 2003; Shen et al., 1999). Glutamate not only acts a neurotransmitter and a metabolic substrate for the TCA cycle, but also as a precursor for glutamine and GABA (the main inhibitory neurotransmitter). The glutamate-glutamine neurotransmitter cycle serves to replenish glutamate

after its release and is thus, crucial for proper regulation of glutamatergic neurotransmission. A simplified schematic of the glutamate-glutamine cycle is depicted in Figure 1.

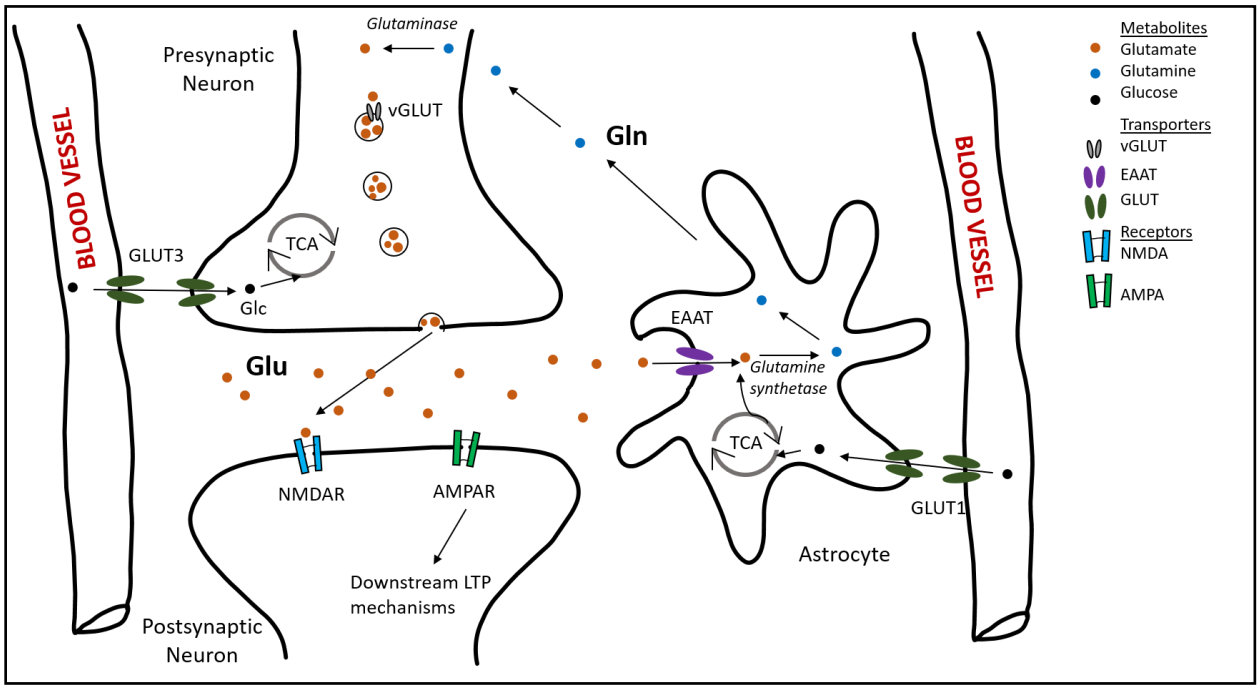

Figure 1. Glutamate-Glutamine cycle. A simplified cartoon of the glutamate-glutamine cycle depicting the main players involved. Glutamate released into the synaptic cleft from the presynaptic neuron binds postsynaptic NMDA receptors (NMDAR) to start the cascade leading to LTP. Extra glutamate in the synaptic cleft is taken up by astrocytes and converted to glutamine, which is released and taken up by the presynaptic neuron. Inside the neuron, glutamine is converted back to glutamate, thus, completing one round of the glutamate-glutamine cycle.

The human brain, comprising only 2% of the total body weight, utilizes 20% of the body's glucose (energy), thus, having the highest energy demand than any other organ in the body (Sokoloff et al., 1977). Majority of the brain's energy is provided by the TCA cycle (oxidative metabolism), with glycolysis playing a transient role. Glycolysis is inefficient since it produces less energy (only 2 ATPs); whereas the TCA cycle produces about 34 ATPs, making it energetically more efficient. The TCA cycle can also operate on its own since amino acids

entering it can continue to cycle and generate energy. Since glutamate is the most abundant excitatory neurotransmitter in the brain, most of the brain's energy is spent on glutamatergic neurotransmission, with almost 80% of the energy obtained from glucose oxidation being used to power the glutamate-glutamine cycle. Even in an awake, resting state, there is ongoing energy (glucose) consumption by the brain, about 20-40% of which is for internal housekeeping processes such as maintenance of resting membrane potentials, and 60-80% for cortical signaling and neuronal activity (Rothman et al., 2003). The glutamate-glutamine cycle is, thus, the major metabolic energy consuming pathway in the human cortex (Shen et al., 1999), with increase in neural activity and energy demand resulting in increased synthesis of glutamate and glutamatergic neurotransmission. Prior investigations have measured the rates of the glutamate-glutamine and the metabolic TCA cycles by tracking the flux of radiolabeled carbon isotope (^{13}C), following infusions of exogenous substrates such as D-glucose, across the intermediates of these cycles (Shen et al., 1999; Sibson et al., 1998). Cell culture studies, as well as ^{13}C magnetic resonance spectroscopy (^{13}C MRS) in rodents and humans, have revealed a tight coupling between the rates of the glutamate-glutamine cycle (i.e. excitatory neurotransmission) and the TCA cycle (oxidative metabolism of glucose) (Hyder et al., 2006; Sibson et al., 1998) (see review (Rothman, De Feyter, De Graaf, Mason, & Behar, 2011)). There is, in fact, a 1:1 stoichiometry where one molecule of glutamate released and cycled requires the oxidation of one molecule of glucose, linking the elevated neuronal spiking activity and excitatory neurotransmission to increased metabolic activity, in order to support cellular energy demands. The neurotransmission and metabolic energy-generating processes in response to neuronal activation and excitatory glutamatergic neurotransmission are thus, tightly coupled. Increases in glutamate levels during neuronal stimulation can be interpreted as a biomarker of task-induced

increases in glutamate, metabolic demand, excitatory neurotransmission, and the ensuing changes in synaptic plasticity.

1.2.4 Excitatory/inhibitory (E/I) balance in the brain

Up to 80% of cortical and hippocampal neurons are excitatory with glutamate as their principle neurotransmitter, and the remaining 20% are inhibitory with γ-aminobutyric acid (GABA) as their main neurotransmitter. Importantly, glutamatergic and GABAergic neurons are closely integrated into neural ensembles within local and long-range circuits, work in concert to process input signals, and drive the brain's excitatory/inhibitory (E/I) balance (Tatti et al., 2017). Neural activity shifts the E/I balance towards a wide spectrum of excitation and inhibition required to meet task demands, eventually taking the brain to new metabolic steady-state levels. The fluctuations in the E/I balance during neuronal stimulation eventually give rise to synaptic remodeling resulting in synaptic plasticity. Synaptic strength and cellular excitability are continually adjusted to maintain the E/I equilibrium and homeostasis, to ensure stable neurotransmission and optimal synaptic performance. Even though the focus of this dissertation is glutamate, it is important to remember that GABA, the dominant inhibitory neurotransmitter, is the complementary player crucial for maintaining the E/I balance. Age-associated changes can be detected at excitatory as well as inhibitory synapses and can lead to disruption of the E/I balance, thus causing instability of the neuronal ensemble to possibly result in age-related cognitive impairment. Owing to the importance of the glutamate and GABA neurotransmitter systems in shifting the E/I balance and evaluating the brain's response to stimulation, it is crucial to employ non-invasive methods to measure the dynamics of these neurotransmitters *in vivo* in humans.

1.2.5 Non-invasive measurement of *in vivo* glutamate levels

Until some years ago, studies of glutamate's role in memory had been restricted to animals, mainly rodent models, and employed invasive techniques such as micro dialysis or ^{13}C MRS to measure levels of metabolites. *In vivo* proton magnetic resonance spectroscopy (^{1}H MRS) that enables the non-invasive quantification of regional brain levels of neurometabolites, including glutamate, has helped translating this research into the human realm (J. A. Stanley, 2002; J. A. Stanley, Pettegrew, & Keshavan, 2000). ^{1}H MRS is an analytical and quantitative technique, an advancement to which, in the form of *functional* ^{1}H MRS (^{1}H fMRS) has been made possible due to improved hardware and magnets with higher field strengths and better signal acquisition schemes (J. A. Stanley & Raz, 2018). ^{1}H fMRS is the only non-invasive technique that can measure, *in vivo*, the temporal dynamics of glutamate *modulation* in response to stimulation. The high temporal resolution afforded by ^{1}H fMRS allows tracking of changes in glutamate levels at a sub-minute time scale. Studies have shown increases in levels of glutamate in the visual (Bednařík et al., 2015; Mangia et al., 2007; Schaller, Mekle, Xin, Kunz, & Gruetter, 2013) and motor (Schaller, Xin, O'Brien, Magill, & Gruetter, 2014) cortices upon stimulation of those areas using appropriate paradigms. Increased modulation of glutamate in the dorsolateral prefrontal cortex has been demonstrated during a working memory task (Woodcock, Anand, Khatib, Diwadkar, & Stanley, 2018). The first study to demonstrate task-related modulation of glutamate in the hippocampus was by Stanley *et al* (J.A. Stanley et al., 2017), where unique temporal dynamics of glutamate were shown to exist during the encoding and retrieval stages of an associative memory task. In that study, characterized by a 54 s temporal resolution, the stages of memory encoding and retrieval were clearly differentiated by the temporal pattern of glutamate modulation. Importantly, that study showed that, early modulation of glutamate, specifically during encoding, predicted faster learning of associations, explained by the early

functional engagement of the hippocampus during encoding. After the initial rise, glutamate levels were shown to decrease and level off, indicating successful consolidation, without the need to elevate glutamate further. Stanley *et al*, thus, established the ability and sensitivity of ^{1}H fMRS to measure task-related temporal dynamics of hippocampal glutamate during cognitive performance. The Stanley *et al* (2017) study was conducted in healthy young adults and formed the basis and motivation of the current dissertation study extended to healthy old adults. It is unknown whether similar unique glutamate dynamics exist during memory encoding and retrieval in the elderly, and whether there are age differences in glutamate modulation during associative memory performance.

Glutamate levels and changes therein that are detected by ^{1}H fMRS in the selected voxel reflect the net cortical output driven by the E/I balance. An increase in synaptic excitability is reflected as a relative increase in glutamate, which is measured by ^{1}H fMRS. Lower excitability, reflected by lower measured glutamate levels, indicates a decrease in excitability balanced by increase in the inhibitory drive due to a shift in the E/I balance. It is thus, important to remember that the glutamate signal measured by ^{1}H fMRS is not a binary brain response to stimulation but reflects a new steady-state achieved by the brain, by shifting the E/I balance, to meet task demands. The use of ^{1}H fMRS also points to the importance of evaluating the dynamics of task-related changes in glutamate (and GABA) for elucidating behaviorally pertinent neural output driven by shifts in the E/I balance. The importance of ^{1}H fMRS is emphasized by reiterating that the association between increased glutamate-glutamine cycling (excitatory neurotransmission) and increased glutamate synthesis (via glucose oxidation) is a fundamental cellular framework that provides the interpretation of glutamate modulation measured by ^{1}H fMRS. Further

information on the principles and methodology of ^{1}H MRS, along with its applications and limitations, are included in Chapter 2.

1.3 Project scope and aims

The selective vulnerability of associative memory to aging has been tested using various paradigms, and the results support the ADH (Naveh-Benjamin, 2000). Possible age effects on the machinery required for LTP induction and maintenance as well as on energy metabolism point to the prospect of age differences in glutamate dynamics contributing to those in memory performance. This might present itself as an inability of older adults to modulate hippocampal glutamate levels in response to memory function. The fact that glutamatergic NMDA receptors richly represented in the hippocampus mediate synaptic plasticity, with increases in hippocampal neuronal spiking coinciding with memory consolidation, and the tight relationship between the metabolic and neurotransmitter pools of glutamate, all together support a direct link between memory consolidation, increased hippocampal neuronal activity, glucose metabolism, glutamate synthesis, and glutamate-glutamine cycling/neurotransmission. This forms the premise of characterizing glutamate dynamics as measured by ^{1}H fMRS under task-active conditions. Relevant to this study is that, levels and temporal dynamics of glutamate during associative memory performance can be measured *in vivo* using ^{1}H fMRS (J.A. Stanley et al., 2017). Moreover, the sub-minute temporal resolution of glutamate measurements allows the characterization of glutamate modulation during the individual stages of memory function (encoding and retrieval) using ^{1}H fMRS.

The main goal of this dissertation was to test the existence of age differences in hippocampal glutamate modulation in response to associative memory function, and their relationship to performance using an object-location associative memory task. This study was developed based on the previous study that demonstrated unique temporal dynamics of glutamate

during memory encoding and retrieval, with early glutamate modulation during encoding predicting faster learning (J.A. Stanley et al., 2017). In the current study, I hypothesized that age differences in hippocampal glutamate modulation do exist and are specific to associative encoding. The previous study (J.A. Stanley et al., 2017) also led me to hypothesize that not only age differences in, but also the timing of, glutamate modulation during encoding is related to associative memory performance. The proposed framework of this investigation is schematically represented in Figure 2. There were three main aims of this dissertation.

1. To evaluate age differences in performance on an object-location associative learning and memory task.
2. (a) To examine age differences in hippocampal glutamate levels during a non-task-active control condition.

   (b) To examine age differences in hippocampal glutamate modulation during associative learning and memory function.
3. To investigate if the timing of glutamate modulation underlies age differences in memory function.

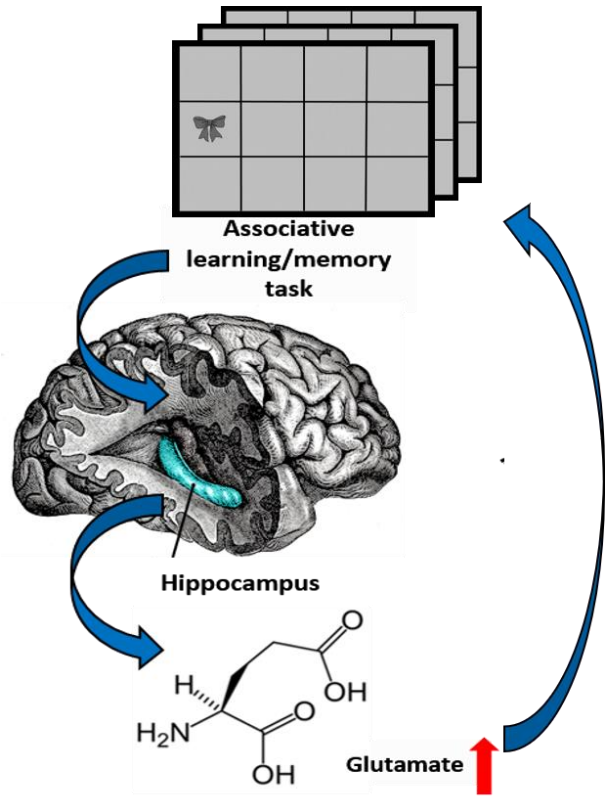

Figure 2. The proposed framework. Associative memory function involving the hippocampus and glutamate results in glutamate modulation that in turn supports task performance.

Glutamate levels during encoding and retrieval in two extreme age groups of healthy young and old adults were recorded while they performed an object-location associative memory task. The first aim of this study sought to confirm age differences in the associative memory task that was further applied to investigate task-induced glutamate modulation. To achieve this aim, it was necessary to first validate and pilot the existing object-location associative memory task (used in the previous study (J.A. Stanley et al., 2017) mentioned above), to test for ceiling effects if any, and appropriately modify the task to allow both age groups to reach their optimum levels of learning. Various learning curve fitting functions were evaluated to appropriately characterize the learning behavior.

The second aim included testing for the relationship between associative memory performance and glutamate levels obtained during a non-task-active control condition i.e. 'control-level glutamate'. The control conditions employed in this study were the flashing checkerboard and fixation cross (see Chapter 3 Methods) that provided steady-state levels of hippocampal glutamate to be compared to glutamate levels acquired during the associative memory task. The second aim also tested for age differences in the *temporal dynamics (modulation)* of glutamate during associative memory performance, as opposed to examining steady-state levels thereof during the control condition. It was hypothesized that age differences in glutamate modulation do exist and show specificity towards memory encoding. The use of proton functional magnetic resonance spectroscopy (^{1}H fMRS) to measure glutamate modulation in different brain regions has been validated using several sensory and cognitive paradigms (see Chapter 2). ^{1}H fMRS is the only non-invasive method for exploring hippocampal glutamate modulation in response to associative memory function.

Finally, this study aimed to investigate a potential functional biomarker of cognitive performance and decline. The third aim of this dissertation, thus, tested whether age differences in glutamate modulation during memory encoding were related to those in memory performance. Based on the previous study (J.A. Stanley et al., 2017) that demonstrated early glutamate modulation being predictive of faster learning in young adults, I hypothesized here, that the timing of glutamate modulation is related to associative memory performance in old adults as well, with early modulation indicating early engagement of the hippocampus, and better performance. In addition, I hypothesized that control-level glutamate is related to associative memory performance. Elucidating such relationships between neurochemicals (specifically an excitatory neurotransmitter such as glutamate) and cognition is critical because it can provide a

better understanding of the possible effects of age on neurotransmission and neurometabolism, which in turn affect cognition in normal as well as pathological aging manifested as AD and other dementia.

This dissertation is structured as follows. The basics of ^{1}H MRS, along with its applications and limitations, are introduced in Chapter 2. Chapter 3 describes the cognitive, neuroimaging, and statistical methods applied in this study to explore the specific aims mentioned above. Chapter 4 describes the results and finally, Chapter 5 summarizes and discusses the findings of this study while also describing limitations and future directions.

CHAPTER 2 INTRODUCTION TO MAGNETIC RESONANCE SPECTROSCOPY

Magnetic Resonance Spectroscopy (MRS) is based on the phenomenon of nuclear magnetic resonance (NMR) and is one of the oldest analytical techniques used to non-invasively measure levels of metabolites in samples such as body tissues. While an extensive review of MRS is beyond the scope of this dissertation manuscript, a summary of relevant concepts is nevertheless provided and more details on the subject can be found elsewhere (De Graaf, 2007; van der Graaf, 2010).

2.1 Evolution of the MRS signal

In NMR, atomic nuclei possessing an internal magnetic moment and a non-zero spin align with the external magnetic field (B_0) to gain angular momentum and precess at their characteristic resonant frequency called Larmor frequency (ω). The Larmor frequency (equation 1) is equal to B_0 times the gyromagnetic ratio – an intrinsic property of the nucleus being studied. The gyromagnetic ratio is the ratio of the magnetic moment to the angular momentum of the nucleus (i.e. spin-1/2 for proton), and for a proton it is approximately 42.58 MHz T^{-1} (megahertz per Tesla).

The Larmor frequency is given by the following equation:

$$\omega = \gamma B_0 \qquad (1)$$

where, γ = gyromagnetic ratio and B_o = external magnetic field.

The evolution of the MRS signal can be explained in brief as follows. Initially, when all nuclei are aligned with the B_0 magnetic field, the net longitudinal magnetization is maximum. Upon exposure to an applied magnetic field (B_1) generated by radiofrequency (RF) pulses and perpendicular to B_0, the nuclei change their orientation away from B_0 and to the transverse plane. T_1 relaxation is the process by which net magnetization that has been tipped by the RF pulse,

returns to equilibrium (longitudinal relaxation). On the other hand, T_2 relaxation is when the transverse magnetization decays after the RF pulse. However, inhomogeneities in the magnetic field result in shortening the T_2, and this effective decay time is called T_2*. During relaxation back to equilibrium, the nuclei produce a decaying RF signal called the free induction decay (FID) that is detected by the receiver coil. This is the time-domain signal since it is dependent on the time taken by the signal to decay (T_2*). Applying a Fourier transform to the time-domain signal provides the frequency components making up the signal and are in the form of peaks along a frequency axis (called the chemical shift axis, see section 2.1.1). This is referred to as a spectrum. At a given frequency, the area under each peak is proportional to the number of nuclei that contribute to the signal at that frequency, and thus, proportional to the concentration of the metabolite that contains those nuclei of interest. It is important that the spectrum be made of sharper, taller, and well-separated peaks, leading to better resolution. The shape of the peak is strongly affected by the decay rate of the FID, where a slower decay results in taller and narrower peaks and a faster decay results in shorter and broader peaks. The area under the peak and the measured concentration of the metabolite always remain the same irrespective of the shape of the peak.

Although MRS can detect any nucleus with a magnetic moment, such as proton, phosphorus, carbon (^{1}H, ^{31}P, ^{13}C); the most commonly studied nucleus for biological applications is the proton (hydrogen nucleus, ^{1}H) owing to its high sensitivity and high natural abundance in the body. The majority of metabolites involved in cellular function including components of the cell membrane as well as neurotransmitters contain protons, making it possible to investigate them simultaneously using proton MRS (^{1}H MRS). ^{1}H MRS can reliably detect metabolites with concentrations equal to or greater than 0.5 to 1 mmol/kg wet weight

(w.w.). (Govindaraju, Young, & Maudsley, 2000). Accurate identification and quantification of the proton-containing metabolites depend on *a priori* knowledge, as well as efficient separation and resolution of the peaks that in turn depend on several factors that are described in brief below.

2.1.1 Chemical shift

^{1}H MRS provides a chemical profile, or an *in vivo* non-invasive "biochemical biopsy", of a selected region of interest (ROI) in an organ, owing to its capacity to resolve and quantify specific proton-containing chemical species. Brain metabolites such as N-acetyl-aspartate (NAA), glycerophosphocholine + choline (GPC+PC), Phosphocreatine + creatine (PCr+Cr), glutamate (Glu), and myoinositol (mI) can be conveniently measured using ^{1}H MRS. Each metabolite is characterized by spin groups such as -CH, -CH_2, -CH_3, NH_3 depending on its chemical structure. The unique chemical structure of each metabolite and the electron cloud around the nucleus of interest (here, proton) produces a shielding effect that modifies, and decreases the strength of, the local magnetic field experienced by the nucleus (Figure 3). For instance, water has a simple chemical structure (H_2O) and thus, experiences the least shielding effect; whereas lipids with more complex structures experience more shielding. Shielding causes identical nuclei to experience different local magnetic fields, resonate at different frequencies, resulting in their separation from one another along the frequency axis - called the 'chemical shift' axis.

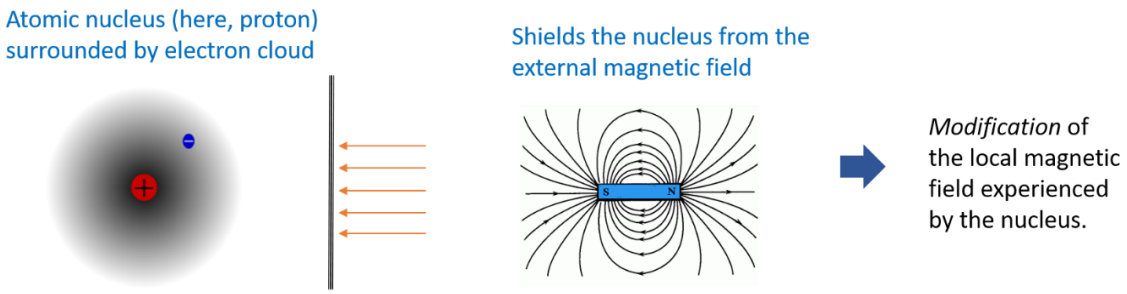

Figure 3. Effect of shielding on chemical shift. A schematic explaining the shielding of a proton by its electron cloud resulting in the modification of the local magnetic field experienced by the proton.

Metabolites are thus, identified by their unique chemical shifts along the frequency axis of the spectrum. For instance, although glutamate and myoinositol, both are proton-containing metabolites, their unique chemical structure and environment will make them occupy different positions on the chemical shift axis owing to the different local magnetic fields that they experience. Chemical shift scales with magnetic field strength, with higher strengths affording more separation (in Hz) and resolution of the metabolites. The frequencies along the chemical shift axis are presented as parts per million (ppm). Table 1 lists the major metabolites identifiable using ^{1}H MRS, along with their chemical shifts.

2.1.2 Scalar (J) coupling

Spectral peaks are either prominent singlets as in NAA, choline, creatine, or can also be split to give doublets, triplets or multiplets. This splitting of spectral peaks occurs due to the 'through-bond' interaction between adjacent spin groups on the same molecule. This phenomenon is called J coupling. It provides information about the distance and angle of chemical bonds between two spin groups within the metabolite. The J coupling constant determines the spacing between the subpeaks in a multiplet. Unlike chemical shift, J coupling is

not dependent on the strength of the external magnetic field. Table 1 lists the major metabolites identifiable using ^{1}H MRS, along with their spin groups, multiplicity, and chemical shifts.

Table 1. List of common proton-containing metabolites. The following are common proton-containing metablites observed *in vivo,* with their spin groups, multiplicity, and chemical shift positions (Govindaraju et al., 2000).

Metabolite	Spin group	Multiplicity	Chemical shift (ppm)
myoinositol (mI)	CH	doublet	3.52
	CH	triplet	3.61
GPC + PC	$N(CH_3)_3$	singlet	3.18
	CH_2	multiplet	4.05
	CH_2	multiplet	3.5
PCr + Cr	$N_2(CH_3)$	singlet	3.03
	CH_2	singlet	3.91
	NH	singlet	6.65
GABA	CH_2	multiplet	3.01
	CH_2	quintet	1.89
	CH_2	triplet	2.28
Glutamine	CH	triplet	3.75
	CH_2	multiplet	2.13
	CH_2	multiplet	2.45
	NH_2	singlet	6.82
Glutamate	CH	doublet	3.74
	CH_2	multiplet	2.03
	CH_2	multiplet	2.35
NAA	CH_3	singlet	2.01
	CH	doublet	4.38
	CH_2	doublet	2.67
	NH	doublet	7.82
Lactate	CH	quartet	4.09
	CH_3	doublet	1.31

Note: Glycerophosphocholine + choline: GPC+PC, Phosphocreatine + creatine: PCrCr, N-acetyl aspartate: NAA. Only a few main representative spin groups per metabolite are mentioned. For an extensive list refer to (Govindaraju et al., 2000).

2.1.3 Signal acquisition scheme

Single voxel spectroscopy (SVS) uses three slice selective RF pulses in the presence of three orthogonal B_0 gradients to select a voxel at the intersection of the three slices. These orthogonal RF pulses generate a spin echo of the spins inside the voxel. One should make sure that the voxel is placed appropriately in the region while minimizing contamination from the adjacent tissue. Voxel placement can become tricky when acquiring signal from more internal and convoluted brain regions such as the hippocampus. One of the two SVS sequences commonly used (and applied in this study) is Point Resolved Spectroscopy (PRESS). PRESS utilizes three RF pulses: a 90º pulse followed by two 180º pulses, with each pulse having a slice-selective gradient along one of the three principle axes (X, Y, Z). This ensures that only the protons in the cuboid created at the intersection of the gradients experience the three RF pulses.

2.1.4 Assuring the MRS signal quality

2.1.4.1 Water suppression

Since water is the largest contributor to the number of protons in the body, signals arising from it must be efficiently suppressed to allow the detection of metabolites that are at much lower concentrations. Water suppression is done using methods such as variable power and optimized relaxation delays (VAPOR) (Tkáć & Gruetter, 2005) that utilize a very narrow bandwidth selective for the frequency of water. In addition, outer volume suppression (OVS) is performed to improve the definition of the ROI by eliminating the signals coming from outside the voxel as well as from lipids (Tkáć & Gruetter, 2005). In the current study, VAPOR and OVS were implemented as a part of the acquisition sequence (PRESS).

2.1.4.2 Shimming

Improved resolution of the metabolite spectra depends not only on the magnetic field strength, but also on the homogeneity of the magnetic field in the voxel. Even though higher

magnetic field strength affords better spectral resolution and chemical shift dispersion, it is accompanied by the issue of possible magnetic field inhomogeneity due to factors such as voxel placement near air-filled cavities (sinuses) and increase in iron deposition due to old age, for instance. Poor magnetic field homogeneity results in variable magnetic field strength in the ROI, thus, creating large variances in precession frequencies. This results in broader and overlapping peaks in the frequency domain and weakens the ability of MRS to resolve the spectra. In shimming gradients through shim coils are iteratively adjusted to optimize the homogeneity of the magnetic field over the voxel of interest. It is mostly automated but may be complemented with manual adjustments. Automated shimming is done using algorithms such as Fast Automatic Shim Technique using Echo-planar Signal readout for Mapping Along Projections (FASTESTMAP) (Gruetter & Tkác, 2000). Manual adjustment of gradients through the shim coils might be required especially in challenging situations such as imaging an ROI in an aging brain. Brains of the elderly have higher iron accumulation in regions such as the hippocampus (Haacke et al., 2005) resulting in higher B_0 inhomogeneity. Manual shimming, although time-consuming, is necessary for acquisition of cleaner spectra. Poor shimming can result in broad spectral peaks leading to lower accuracy in quantifying metabolites.

2.1.4.3 Signal averaging

SVS, as its name suggests, can acquire signal only from a single localized ROI at a time. It requires averaging of multiple scans to improve the signal to noise ratio (SNR), resulting in a spectrum of good quality. Noise scales inversely with the square-root of the number of signal averages and signal scales directly with the number of signal averages. Although averaging prolongs acquisition, its effect on reducing noise makes it a critical aspect of MRS.

Additional factors critically affect the quality of the MRS signal. A larger voxel size is preferred owing to low concentrations of the metabolites of interest; however, at the expense of

partial volume. Higher magnetic field strength reduces the degree of spectral overlap by increasing the chemical shift dispersion, leading to better and more accurate spectral resolution and better SNR. In fact, at very high field strengths (7T and higher) greater spatial resolution can be achieved by employing smaller voxels while minimizing the problem of partial volume of different tissue types (gray matter, white matter, CSF) within the localized voxel. The echo-times (TE) used in MRS studies may be long (> 135 ms) to acquire only the prominent singlets (NAA, GPC+PC, PCr+Cr) or short (< 35 ms) to acquire singlets as well as multiplets (glutamate, glutamine, myoinositol). TE depends on the decay time constant, T_2, which is different for different metabolites. Longer TE will not be able to capture the signal from metabolites with shorter T_2 values since the signal will have already decayed. On the other hand, at short TE, all metabolites will have maximum signal since less time will be available for them to undergo T_2 decay. The shortest TE thus results in the smallest T_2 losses. The repetition time (TR) should be optimized to allow enough time between excitations to ensure sufficient relaxation of the signal before the next excitation. TR depends on the relaxation time constant, T_1, which is different for different metabolites. Ideally, the TR must be at least three (preferably five) times the longest T_1 to allow full recovery of the signal. If TR is not optimum, the observed signal will have an amplitude that is lower than a fully relaxed signal (J. A. Stanley et al., 2000). This is called partial saturation. TRs between 2-5 seconds are considered optimal.

2.2 MRS data processing and fitting

2.2.1 Eddy-current, phase, and shift corrections

Eddy currents are electrical currents induced by a rapidly changing magnetic field due to a conducting material moving in the magnetic field and can cause time-varying shifts in the main magnetic field. Eddy currents generate a decaying signal with varying amplitude and phase. Thus, the acquired signal is no longer a pure MR signal, but a distorted FID, which upon Fourier

transformation can result in imperfect spectra. During data acquisition the signal from water is suppressed. However, a separate water-unsuppressed spectrum is acquired from the same voxel after data acquisition, using the same data acquisition parameters. Phase information from the water-unsuppressed spectrum is used to correct the water-suppressed spectra (Klose, 1990) by cancelling the influence of the Eddy currents. Acquisition of this extra water-unsuppressed spectrum requires about 2-4 averages and adds about half a minute to the overall procedure but helps improve spectral quality.

The signal is made of real (absorption) and imaginary (dispersion) components that are 90º out of phase with each other. After Fourier transform, phase correction is applied to the spectrum to bring all peaks into the absorption mode. Phasing thus, applies an adjustment to the spectrum to display the optimal spectral form and is mostly automated on many MRI scanners. Phasing can be zero-order (frequency independent) and first-order (frequency dependent). Zero-order phase correction is applied equally to all peaks in the spectrum and is done by adjusting the phase correction factor until all peaks are aligned in the same direction. Frequency-dependent phase errors occur during the delay between excitation and signal reception, where after being tipped into the transverse plane, the nuclei start dephasing based on their frequencies. Such errors are corrected using first-order phasing where the phase correction factor changes according to the different frequencies. In addition, frequency errors that might be caused due to temporal drifts in B_0 can be corrected by moving a reference peak of the spectrum to its theoretical position, or entering a numeric value at the scanner control panel

2.2.2 Spectral fitting

Spectral fitting can be performed either in the time-domain or in the frequency-domain. For the current study, spectral fitting was done in the frequency-domain. Precise and accurate quantification of metabolites requires that the metabolite peaks not only be well-resolved but

also have a narrow linewidth (full-width half-maximum, FWHM). Any user-bias that may accompany spectral enhancements is avoided by employing a fully automated processing and fitting approach. The most common curve-fitting approach for MRS is LCModel (Provencher, 1993). Acquired *in vivo* spectra are analyzed as a linear combination (LC) of the spectra from the LCModel simulated basis set of 20 metabolites. LCModel fitting incorporates *a priori* knowledge of the chemical shifts, J-coupling constants, lineshape function, number of peaks, phase, and amplitude of the basis set and ensures improved specificity of resolving overlapped resonances (peaks).

The uncertainty in spectral fitting, i.e. the difference between acquired and modeled spectra, is expressed as a Cramér-Rao lower bound (CRLB) value (Cavassila, Deval, Huegen, van Ormondt, & Graveron-Demilly, 2001). CRLB is the threshold of the error associated with model fitting and reveals uncertainties in the fit. CRLB can be expressed either as a percentage (relative CRLB) or as an absolute value (Kreis, 2016). Relative % CRLB values have been routinely used as a quality filter for spectra; however, the thresholds are arbitrarily determined, leading to a possible bias. Spectra with CRLB values higher than a certain threshold indicate less reliable measures and are commonly excluded from further analyses. The CRLB threshold can depend on the study as well as on the ROI from which spectra are acquired. It is optimum to use absolute CRLB values, measured in comparison to a control group or to normal metabolite levels, as quality control criteria. The absolute CRLB value is determined based on a cutoff set at the mean CRLB plus two standard deviations obtained from a control population (Kreis, 2016). This means spectra with CRLB values more than this cutoff will be excluded from analyses.

LCModel fitting of data may or may not be followed by further spectral averaging to achieve improvements in the SNR. Averaging is mainly done for experiments with block designs

where consecutive blocks of the stimulation can be averaged to further improve the SNR. This will be explained in detail in the 'image post-processing and quantification of the spectra' section of Chapter 3.

2.3 Absolute quantification of metabolite levels

Absolute concentrations of metabolites in mmol/kg.w.w. are calculated as:

$$[metabolite] = [reference] * \frac{S(metabolite)}{S(reference)} * (1 - f_{CSF}) \quad (2)$$

where, [metabolite] and [reference] are the concentrations (number of protons) in the metabolite and reference, respectively, S is the signal amplitude, and f_{CSF} is the fraction of CSF in the sample tissue volume. The 1 - f_{CSF} adjustment factor is for partial volume correction, and also corrects for the fact that the metabolites are almost all concentrated in the gray and white matter.

The reference is a compound of known concentration against which the areas occupied by metabolite peaks are compared and metabolite concentrations are quantified. The unsuppressed water signal collected from the same voxel during data acquisition is the reference used for the absolute quantification of metabolites. The concentration of water is calculated based on the tissue segmentation (gray and white matter) information that is obtained from structural T_1-weighted (e.g. MPRAGE) image processing. The concentration of pure water is 55.6 moles/l. The total tissue water is assumed to be (J. A. Stanley, Drost, Williamson, & Thompson, 1995):

$$[H_2O] = ((0.81 * f_{GM}) + (0.71 * f_{WM})) * 55.6 * 10^3 \text{ mM} \quad (3)$$

where, f_{GM} and f_{WM} are fractions of gray and white matter in the sample tissue volume, respectively. The concentration of pure water is 55.6, and 0.81 and 0.71 are the fractions of MR-visible water in gray and white matter, respectively (Ernst, Kreis, & Ross, 1993; J. A. Stanley et

al., 1995). Corrections for signal attenuation due to T_1 and T_2 relaxation effects are also applied as:

$$S(metabolite_{relaxed}) = \frac{S(metabolite)}{\exp\left(-\frac{TE}{T_2}\right)*\left(1-\exp\left(-\frac{\mathrm{TR}}{\mathrm{T_1}}\right)\right)} \quad (4)$$

where, S(metabolite$_{relaxed}$) is the fully relaxed signal of the metabolite and S(metabolite) is the observed signal of the metabolite (Gasparovic, 2006)

Metabolite concentrations can also be expressed as a ratio to an internal reference metabolite, which most of the times is total creatine. However, it is misleading to assume that total creatine levels always remain constant (Kreis, Ernst, & Ross, 1993), since they can change during various stages of development as well as during pathology.

2.4 Applications of ^{1}H MRS

So far, the most popular method to examine the neural correlates of the brain's response to stimulation has been fMRI that is based on the Blood Oxygen Level Dependent (BOLD) signal. Although characterized by better spatial and temporal resolution, the BOLD signal is a proxy for neuronal response. It increases upon neuronal activation and cannot differentiate between the contribution of excitatory and inhibitory activity. Neuronal activity induced by stimulation includes processes such as increased glucose oxidation, generation and propagation of action potentials as well as neurotransmitter release. It is important to employ an approach that is specific to the investigation of excitatory and inhibitory processes involving glutamate and GABA neurotransmitters, respectively, since the maintenance of the brain's E/I balance is crucial for neuronal function (Letzkus, Wolff, & Luthi, 2015; Tatti et al., 2017)). ^{1}H MRS is the only neuroimaging technique that can non-invasively measure neurometabolite levels; and despite lacking the spatial resolution of other neuroimaging techniques, can provide valuable complementary information.

As an analytical and a quantitative technique, ^{1}H MRS finds wide applications in clinical as well as research settings. In clinical applications, ^{1}H MRS data are collected during resting conditions (without any behavioral constraints imposed) and static levels of metabolites are compared between clinical populations and healthy controls. In research, the technique finds applications not only in the comparison of static metabolite levels between groups, but importantly, also in investigating dynamic changes (modulation) in levels of metabolites, especially neurotransmitters, in response to neural activity. The latter approach that incorporates sequential acquisition of MR spectra over time, has led to the coining of the term ^{1}H *functional* MRS (^{1}H fMRS) to highlight the importance of assessing functional changes in steady-state metabolite levels (J. A. Stanley & Raz, 2018). Thus, while ^{1}H MRS provides data on static levels of metabolite, ^{1}H fMRS records data when behavioral constraints are imposed which lead to new steady states of metabolites in response to the stimulation. These behavioral constraints can be stimuli such as a fixation cross, a flashing checkerboard, or a cognitive task for instance (Lynn, Woodcock, Anand, Khatib, & Stanley, 2018). ^{1}H fMRS can thus also provide information about the temporal change in metabolite levels in the specific ROI. Radiolabeled ^{13}C MRS applications mentioned briefly in Chapter 1 are a form of fMRS; the only limitation being the requirement of injecting a radiolabeled ligand, thus, making it an invasive approach.

Recently, ^{1}H fMRS is finding applications in cognitive neuroscience research. The ^{1}H MRS signal acquired from an ROI during rest (in the absence of any stimulation) reflects the static levels of the metabolites, including neurotransmitters like glutamate, whose associations with behavioral perturbations are unclear. However, associations between such static neurotransmitter levels and cognitive performance have indeed been reported, where cognitive performance measured outside the scanner was simply correlated with glutamate levels

(Nikolova, Stark, & Stark, 2017; Spurny et al., 2020; Thielen et al., 2018). Since neuronal response to any kind of stimulation (sensory, motor, cognitive) involves a constant adjustment of neurotransmitter levels to maintain the E/I balance (J. A. Stanley & Raz, 2018), assessment of the temporal dynamics of neurochemical levels is more important than that of static levels. As previously mentioned, ^{1}H *functional* MRS (^{1}H fMRS) is the only non-invasive technique that can measure *in vivo* glutamate modulation in response to stimulation (motor, sensory, or cognitive) of a localized region in the brain, with a high temporal resolution that allows tracking of glutamate levels at a sub-minute time scale. Significant modulation of glutamate in the occipital cortex upon visual stimulation (Mangia et al., 2007), in the motor cortex during a finger tapping task (Schaller et al., 2014), in the dorsolateral prefrontal cortex during a working memory task (Woodcock et al., 2018), and in the hippocampus during an associative memory task (J.A. Stanley et al., 2017) corroborate the utility of ^{1}H fMRS as a technique to measure modulation of glutamate in response to stimulation. In fact, the Stanley *et al* study also demonstrated the specificity of glutamate modulation to different memory stages, underscoring the ability of ^{1}H fMRS to capture the temporal behavior of the glutamate signal.

2.4.1 ^{1}H MRS in studying aging

^{1}H MRS has been used to compare metabolite levels in animal models of aging and AD as well as in human participants. Low medial temporal levels of glutamate have been demonstrated in rodent models of AD (Febo & Foster, 2016) and in healthy aged rodents (X. Zhang et al., 2009). Low glutamate and high glutamine levels, leading to a low Glu/Gln ratio, have been documented in the hippocampi and sensorimotor cortices of aged rats (Harris et al., 2014). It can be speculated that higher glutamine levels with aging are related to increases in the number of astrocytes as indicated by age-related increases in myoinositol (a glial marker) (Kaiser, Schuff, Cashdollar, & Weiner, 2005). In humans, age-related reduction in hippocampal

and cortical glutamate (Hädel, Wirth, Rapp, Gallinat, & Schubert, 2013) has been reported in older adults with mild cognitive impairment as well as in those with AD, compared to their healthy age-matched counterparts (Antuono, Jones, Wang, & Li, 2001; Rupsingh et al., 2011) (for a review see (Haga, Khor, Farrall, & Wardlaw, 2009)).

Static levels of glutamate measured in the absence of any behavioral constraint have been associated with age-related differences in cognition and behavior. For instance, the combined levels of hippocampal glutamate and its precursor and breakdown product - glutamine - have been linked to out-of-scanner verbal memory performance in healthy old adults (Nikolova et al., 2017). Low levels of striatal glutamate in the elderly have been associated with poor performance on a visuomotor task (Zahr et al., 2013). Whereas these and other studies hint at glutamatergic dysfunction as one of the factors in age-related cognitive decline, they fail to address the neurotransmitter *dynamics* taking place during cognitive performance (such as memory encoding and retrieval) (J.A. Stanley et al., 2017) that may be crucial for pinpointing the mechanisms of cognitive dysfunction. The current dissertation study aims to fill this gap by investigating age differences in the temporal dynamics of hippocampal glutamate during associative memory function using a paradigm adapted from Stanley *et al* (J.A. Stanley et al., 2017).

The importance of ^{1}H MRS in studying aging, age-related changes, and age differences in levels of neurometabolites is underscored by the fact that the signal generated by MRS is not susceptible to the effects of neurovascular coupling. This is a critical point of comparison to the most commonly used fMRI BOLD signal, which depends on the contrast generated by cerebral blood flow and cerebral rate of oxygen metabolism, thus, being dependent on neurovascular coupling and affected by the aging cerebral vasculature. Functional MRI studies that investigate

age effects, do so by assuming age-invariant coupling of the neural activity to the BOLD signal. However, neurovascular coupling changes with age (D'Esposito, Zarahn, Aguirre, & Rypma, 1999) owing to age differences in the vascular reactivity, elasticity, and other characteristics of the vascular bed as well as age-related increases in vascular pathology. The BOLD response is confounded by such events and, thus, its interpretation when assessing age effects might not reflect true changes in brain activity or metabolism (D'Esposito, Deouell, & Gazzaley, 2003). In contrast, ^{1}H MRS provides direct information about the levels and changes in neurochemicals (including excitatory and inhibitory neurotransmitters such as glutamate and GABA) involved in neurotransmission and metabolism, providing an avenue to assess the functional changes in the brain (J. A. Stanley & Raz, 2018).

2.5 What does the ^{1}H fMRS signal mean?

One would like to believe that the changes in glutamate levels observed using ^{1}H fMRS reflect the increase in glutamate released in the synapse. However, owing to poor spatial resolution, ^{1}H fMRS quantifies metabolites in the entire tissue rather than at the finer cellular level. ^{1}H fMRS cannot distinguish between the compartments that the signal arises from and is assumed to capture the glutamate signal from all cellular compartments (neurons, glia, synaptic cleft, presynaptic vesicles) in the ROI. Task-related modulation of glutamate levels, thus, reflects the net change in glutamate within the chosen voxel.

It is unlikely that the signal measured by fMRS reflects synaptic glutamate molecules involved in neurotransmission. The overwhelming majority of glutamate is intracellular – about 10 mM, compared to only 0.5 - 1.0 μM extracellular glutamate (Erecinska & Silver, 1990). In addition, the timescale of synaptic glutamate turnover is very brief with glutamate staying in the synaptic cleft for less than 5 ms before binding to post-synaptic receptors or transporters (Clements, Lester, Tong, Jahr, & Westbrook, 1992). Thus, ^{1}H fMRS measures glutamate that is

almost exclusively located inside the cells and nearly all the changes observed in glutamate are assumed to have a metabolic basis. This is congruent with the 1:1 stoichiometry between neuronal glucose oxidative metabolism (TCA cycle) and the glutamate-glutamine cycle of neurotransmission, where each molecule of glutamate recycled requires the oxidation of one molecule of glucose (see Chapter 1). This indicates that the metabolic and neurotransmitter pools of glutamate are closely linked and are indistinguishable by ^{1}H MRS.

Glutamate levels in a cortical region (or a specific voxel), and task-induced changes therein, as quantified by the ^{1}H MRS signal reflect the net E/I status of that region. An increase in glutamate during stimulation indicates more excitability, whereas glutamate reduction indicates a gradual decrease in excitability or a gradual increase towards the inhibitory drive. Although ^{1}H fMRS at 3T cannot measure GABA reliably, it is important to remember that the two neurotransmitter systems are highly integrated in neuronal ensembles and respond to stimulation by driving the shift in the brain's E/I balance. The dynamic equilibrium of excitation and inhibition always strives to maintain the E/I balance in the brain to give rise to new metabolic states required to meet task demands.

2.6 Limitations of single voxel MRS

The SNR for MRS studies depends on the voxel size due to low concentrations of the metabolites within the voxel. However, large voxels bring with them the problem of partial volume, where data are collected from surrounding tissue that might be inactive. In addition, since only one ROI can be studied at a time, neurochemical changes occurring in other regions involved in stimulus processing cannot be captured simultaneously. For instance, as described in Chapter 1, memory function involves not only the hippocampus, but also the association cortices such as the prefrontal cortex; and these neural correlates might be differentially involved during

the various stages of memory function. Single voxel MRS precludes the simultaneous investigation of neurochemical changes in these regions during memory performance.

Signal averaging, an integral part of MRS data acquisition, ensures higher SNR but lengthens the experimental time, thereby increasing the risk of participant fatigue and loss of attention. This can affect the true change in neurochemistry observed. The high sensitivity of the MRS signal to magnetic field inhomogeneity makes shimming an essential part of data acquisition. Shimming can further lengthen the experiment time in challenging situations such as aging research where ROIs have undergone atrophy or have high iron accumulation (J. A. Stanley & Raz, 2018).

An important thing to note while interpreting the effect size of MRS data is the wide range of changes in levels of glutamate observed upon neuronal activation. The observed glutamate levels depend on numerous aspects of the study design: block vs event-related design, type of stimulus, region being investigated, to name a few (for a summary of studies with stimuli used and effect size observed see (Lynn et al., 2018)). Noxious as well as visual stimuli tend to elicit larger changes in glutamate levels compared to cognitive stimuli, where changes can also range from 2.6% to 12% depending on the paradigm used and the region studied (Mullins, 2018). This discrepancy has been interpreted as, a more salient stimulus eliciting a larger glutamate response. The mean change in glutamate, aggregated from studies using various stimulus paradigms, ROIs, field strengths and so on, is about 7% (Mullins, 2018). The expected optimal effect size with MRS research, thus, remains an open question.

CHAPTER 3 METHODS

3.1 Power Analysis

I based the power analysis on a previous study that compared age differences in hippocampal glutamate levels measured during rest (Kaiser et al., 2005) as well as a study by our group that characterized hippocampal glutamate modulation during associative memory function in young adults (J.A. Stanley et al., 2017). G*Power version 3.1 was used to conduct power analysis.

3.1.1 Age-related difference in levels of hippocampal glutamate measured during a control condition

In a study by Kaiser *et al*, young participants (n = 11) had 13% (1.24 mM/kg.w.w.) more glutamate in their motor cortices than the old (n = 13) with a standard deviation of 0.863 (Cohen's d = 1.44) (Kaiser et al., 2005). For the current study, assuming age differences in hippocampal glutamate levels to be at least half as much as in the Kaiser *et al* study, i.e. 0.62 mM/kg.w.w, and a medium to large effect size (Cohen's d = 0.70), a total sample size of 68 (34 in each group) was required to achieve 80% power for a two-sided t test for independent groups.

3.1.2 Age-related difference in hippocampal glutamate modulation during associative learning and memory

A previous study in our lab (J.A. Stanley et al., 2017) utilizing the object-location associative learning and memory task in healthy young participants observed mean hippocampal glutamate levels of 13.4 mM/kg.w.w., and about 11% and 7.7% task-related increases in glutamate in fast and slow learners, respectively. In the current study on age differences, the primary dependent variable in the repeated measures analysis was glutamate level, with control-level glutamate as the continuous covariate, and age group as the between-subject categorical variable. To improve the SNR of the hippocampal glutamate signal three consecutive blocks out of the 12 encoding blocks were averaged to give four measures for encoding. A similar

averaging approach was applied to the retrieval blocks. This created four block triads per task stage. Refer to Figure 8 for a schematic of the averaging approach. The averaging approach was analogous to the one used in the previous study (J.A. Stanley et al., 2017). The within-subject factors were task stage (encoding, retrieval) and block triad number (1-4). For a between-within interactions repeated measures GLM analysis assuming a small to medium effect size f = 0.2, Bonferroni corrected type I error rate = 0.006, the sample size required to achieve 80% power was 56 (i.e. 28 per age group). Based on the analysis in 3.1.1 and allowing for possible attrition and exclusions, I decided to recruit a total sample of 72, with equal numbers of young and old adults.

3.2 Participants

Participants for this study were recruited through the Wayne State University online advertising system, flyers distributed across the campus, and word-of-mouth referrals. Note that this study was conducted on a sample of convenience that is unlikely to represent the general population of young and old adults. One hundred and four people responded to the advertisements and called the lab for additional information about the study. Twenty-five people were excluded based on an initial screening conducted via a telephone interview. All eligible participants at this stage completed an additional and detailed health questionnaire to screen for history or current diagnosis of neurological and psychiatric disorders, cardio- and cerebro-vascular disease, endocrine disorders, diabetes, cancer, head trauma with loss of consciousness for more than five minutes, and claustrophobia. Additional exclusion criteria were: recreational drug and alcohol abuse and treatment thereof, alcohol consumption (excess of three drinks per day), and history or current use of anxiolytics and antidepressants. Pregnant and lactating women, as well as those with intrauterine contraceptives were excluded from the study. Participants diagnosed with hypertension and taking anti-hypertensive medications were

included in this study, as were those who reported treatment for abnormal levels of thyroid hormones. In addition, the participants underwent standard metal screening. All participants were right-handed (scores over 75% on the Edinburgh Handedness Questionnaire) (Oldfield, 1971) and completed the Center for Epidemiologic Studies questionnaire to rule out current depression (CES-D; cut-off = 15) (Radloff, 1977).

After the extensive health screening, 61 participants were deemed eligible and provided informed consent in accordance with the Wayne State University Institutional Review Board guidelines. Cognitive impairment was screened for by using the Mini Mental State Examination (MMSE; cut-off = 27) (Folstein, Folstein, & McHugh, 1975). Every participant's systolic and diastolic blood pressure was measured at the beginning of the session via an aneroid sphygmomanometer (MDF Calibra) with a standard blood pressure cuff on the left arm with the participant seated in a comfortable position. The sample was on average normotensive, defined as having blood pressure below 140 mm Hg systolic and 90 mm Hg diastolic. Vision correction was provided to participants in need using MRI compatible glasses and lenses that matched their prescription. Once the participant was inside the scanner, and before scanning commenced, sample images and instructions were displayed, and participants' accurate identification thereof was confirmed to ascertain vision correction.

As depicted in Figure 4, out of the 61 participants scanned, two were excluded from analyses because of incidental findings such as arachnoid cysts, and nine (five young and four old) were excluded owing to poor data quality due to head motion. In this study, for glutamate spectra collected from the hippocampus, the CRLB value was set to 16% (J.A. Stanley et al., 2017) and the block triads with higher CRLB values were excluded. An additional four participants (one young and three old), who had one of the four block triads excluded due to high

CRLB values, were omitted from data analysis. Note that this was a more stringent criterion employed in the current study, whereas other groups exclude only individual poor spectra.

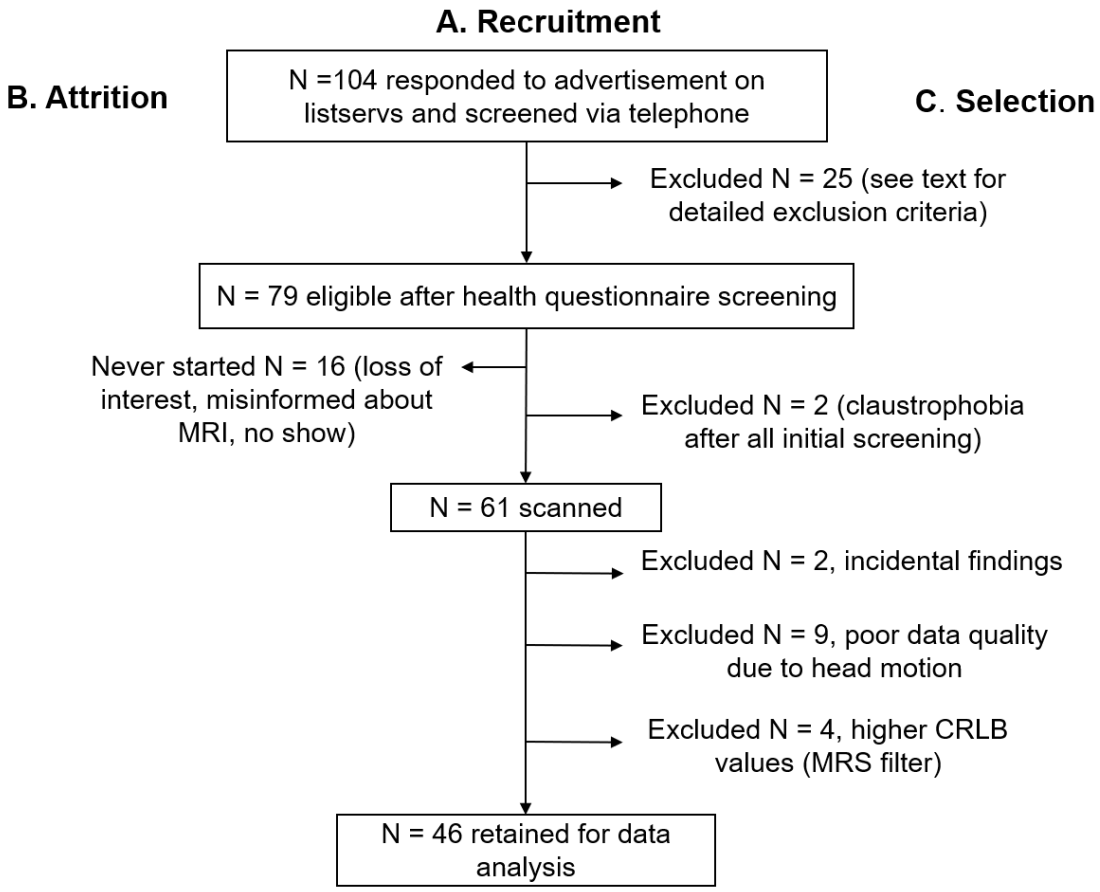

Figure 4. Participant recruitment flow chart.

The sample analyzed here, thus, consisted of 46 participants including 32 healthy young (21 to 30 years, M = 25.37, SD = 2.9, 16 women) and 14 healthy old (60 to 70 years, M = 65.25, SD = 3.2, 8 women) adults. Descriptive demographic statistics of the sample are listed in Table 2. Note: The recruitment occurred during the years 2018, 2019, and 2020 but was not completed because of the COVID-19 pandemic, with ensuing restrictions preventing additional accrual of the sample; hence the lack of balance between the two age groups.

Table 2. Demographic profile of the final sample analyzed. Values indicate mean ± 1 standard deviation

	Old	**Young**	***t***	χ^2	***p***
N	14	32			
Age (years)	65.25 ± 3.2	25.37 ± 2.9	-	-	-
% Women	57%	50%	-	0.19	0.65
% Caucasian	85%	55%	-	6.78	< 0.05
Average education (years)	18.2 ± 1.7	16.6 ± 1.6	< 1	-	0.9
Average MMSE	29.3 ± 0.7	29.2 ± 0.9	0.18	-	0.86
Average systolic BP (mm/Hg)	125.8 ± 10.4	116.4 ± 7.9	3.65	-	< 0.005
Average diastolic BP (mm/Hg)	83.1 ± 8.4	77 ± 6.7	3.06	-	< 0.005

Note: MMSE = Mini Mental State Examination, BP = Blood Pressure

3.3 Associative learning and memory task

The object-location paired-associates task used in this study was adapted and modified from a human analogue of spatial tasks in animal studies of hippocampal associative learning (Diwadkar et al., 2008). Previous studies have shown that this task produces hippocampal glutamate modulation that demonstrates unique temporal dynamics during memory encoding and retrieval (J.A. Stanley et al., 2017). Before the MRS study, I conducted a pilot study in a mock MRI scanner, to modify and optimize the original associative memory task. The modifications sought to allow more time for learning to occur in both age groups, and to help choose the level of task difficulty that minimizes celling effects while demonstrating group differences.

3.3.1 Piloting of the object-location associative learning and memory task

A separate pool of participants was recruited for this task optimization study via listservs and flyers posted across the Wayne State University campus, and the sample included twenty young (21-30 years, M = 23.7, SD = 2.4, 12 women) and eight old (60-70 years, M = 64.6, SD = 2.2, 5 women) adults who met the inclusion and exclusion criteria previously mentioned.

The original associative memory task ((Diwadkar et al., 2008; Wadehra, Pruitt, Murphy, & Diwadkar, 2013), also employed in (J.A. Stanley et al., 2017)) consisted of alternating blocks of memory encoding and retrieval. During encoding, black and white line drawings of nine unique and familiar objects were presented one at a time in each of the nine squares of a 3×3 grid. The objects were chosen from the Snodgrass and Vanderwart line-drawings set and familiarity was equalized among them based on the reported norms (Snodgrass & Vanderwart, 1980). During the encoding stage that was 27 seconds long each of the nine objects was presented for 3 seconds in its unique location on the grid. During the retrieval stage (also 27 seconds long), instead of the object, a black square was presented once in each of the nine locations and served as a cue for the participant to recall the object that was earlier presented in the cued location. Cued recall was chosen instead of free recall, because it imposes stronger demands on the associative memory network (Kan, Giovanello, Schnyer, Makris, & Verfaellie, 2007). Participants vocalized their responses during encoding and retrieval and were instructed to choose monosyllabic names for the objects to reduce head motion. If unable to recall the object or make their best guess about what the object might be, participants were instructed to say “no”. A ‘non-zero’ response meant vocalizing a correct answer, an incorrect answer, or saying “no” as instructed. All responses were scored in real-time as well as audio-recorded so that the score could be checked against the recorded responses. Each encoding and retrieval stage

was followed by a rest period of 27 seconds, where participants were instructed to focus on a fixation-cross presented on the screen. Blocks of encoding-rest-retrieval-rest made up one epoch, and eight such epochs were presented. The object-location associations remained constant; however, the order of presentation of objects and cues was random (Figure 5).

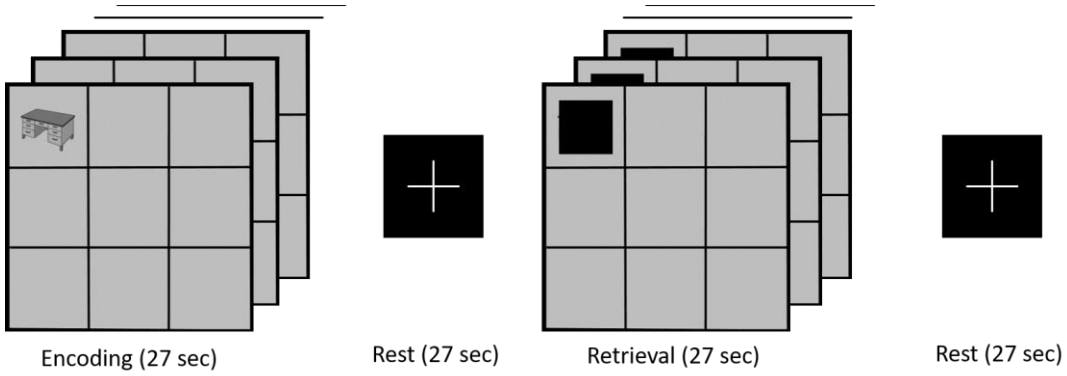

Figure 5. A schematic depicting the original 3 × 3 object-location paired-associates task (Diwadkar et al., 2008). Encoding-rest-retrieval-rest made up one epoch and eight such epochs were presented as a part of the task.

The following modifications were made to the above-described task for piloting:

(i) *Blocking of memory rehearsal.* The passive rest period after each encoding and retrieval block was replaced with a block of counting backwards by one, from a randomly chosen number between 40 and 80, programmed into the task. Participants were instructed to count aloud backwards for 20 seconds at a calm and steady pace of one number per second. The purpose of the counting task was to provide articulatory suppression (Baddeley & Hitch, 1974; Salamé & Baddeley, 1989) and prevent active rehearsal during memory maintenance; especially since encoding and retrieval required articulation of the responses, and also to remove potential variability among subjects in memory rehearsal and use

of strategies. In addition, this also ensured that all participants performed a controlled mental activity during memory maintenance.

(ii) *Task-length.* The task was lengthened by extending it from eight to 12 epochs to provide more opportunity for older adults to reach an asymptote.

Figure 6. Mock MRI scanner used to simulate the MR environment.

This pilot study was conducted in an adult-size mock MRI scanner that is routinely used for preparing patients for real imaging procedures (Figure 6). It mimics the actual MRI scanner environment, including the bed, the magnet housing, and the head-coil frame. A laptop displaying the associative memory task depicted in Figure 5 was placed behind the bore of the mock scanner to project the stimuli on to a mirror attached to the mock head-coil. To simulate the scanner noise, a pre-recorded ^{1}H MRS sequence, recorded during a phantom scan in a real scanner, was played throughout the mock-scanning session from speakers located behind the bore of the mock scanner. I added the mock-scanner condition to the pilot study to include an

exploratory analysis of the effects of the MR-scanner environment on performance of the memory task, since little attention has been paid to this aspect of lab-based cognitive testing.

There are substantial differences between conventional cognitive testing procedures and their implementation in the MRI scanner, including a noisy environment, supine position, and tight quarters, to name a few. All these factors may affect cognitive performance by adding stress and distraction from the task (Kobald, Getzmann, Beste, & Wascher, 2016). To date, the effects of MRI scanner environment on cognitive performance have been examined in a handful of studies and almost always in research designs that focused on one factor at a time (Jacob et al., 2015; Kobald et al., 2016; Koch et al., 2003), without assessing the effect of interactions among factors. Since it is possible that these factors act in concert instead of in isolation, a study-design that includes a combination of two or more of them is more appropriate. As illustrated in the schematic in Figure 7, the effects of a within-subject variable 'setting' (task performed while seated at a desk or while lying supine inside the mock MRI scanner) and a between-subject variable 'noise' (presence or absence of simulated MRI scanner noise) on associative memory performance were compared between the two age groups. Participants were asked to lie down on the scanner table with their head placed inside the bore. As is typical in an actual MRI protocol, participants' heads were supported by padding to prevent sudden movements. Participants were explicitly told that the experiment is conducted in a mock scanner, as the absence of a real magnetic field does not affect behavior (van Maanen, Forstmann, Keuken, Wagenmakers, & Heathcote, 2016); and the mock environment is associated with equal levels of anxiety (McGlynn, Smitherman, Hammel, & Lazarte, 2007) and stress (Lueken, Muehlhan, Evens, Wittchen, & Kirschbaum, 2012) as in the real scanner. In each experimental condition (at the

desk and in the mock scanner), participants performed 12 epochs of encoding-counting-retrieval-counting. The entire session, including consenting and screening, lasted approximately 1.5 hours.

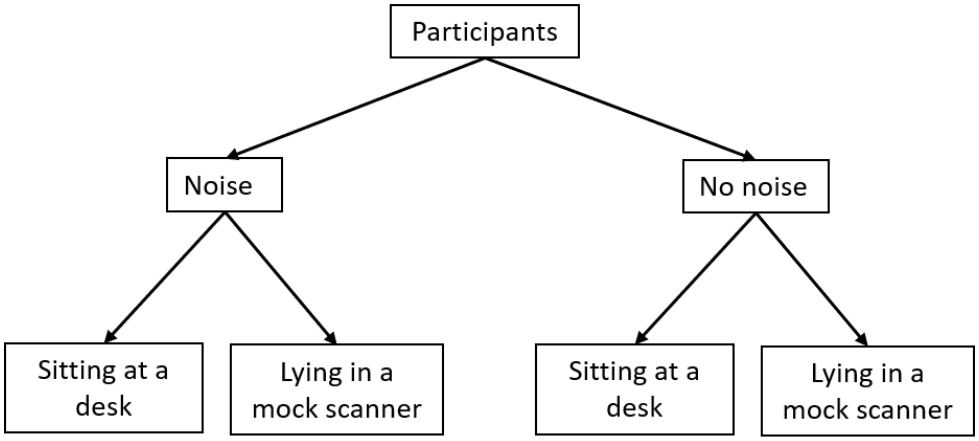

Figure 7. Schematic of the mock-scanner pilot study design.

(iii) *Task-complexity.* Ceiling effects were noted in the modified version of the task, with 100% asymptotes achieved by several participants despite blocking memory rehearsal. The task-complexity was, therefore, increased to allow age differences in performance while avoiding ceiling effects. The optimal level of task-complexity would induce the least amount of boredom (due to the task being too easy) and frustration (due to the task being too difficult), but at the same time would allow learning to gradually occur. Two versions of the original task with different levels of difficulty - (a) grid size: 3 × 4 (12 objects, 2.67 seconds per object) and (b) grid size: 4 × 4 (16 objects, 2 seconds per object) were created and characterized. The duration of each retrieval cue during the two complex tasks matched that of object presentation, respectively. Both versions of the task

included 12 epochs of encoding-counting-retrieval-counting and were performed only in the scanner in the presence of noise.

3.3.2 Final object-location associative learning and memory task

For the dissertation study investigating age differences in hippocampal glutamate modulation during associative memory, I chose the 3 × 4 grid version of the task with 12 epochs of encoding-counting-retrieval-counting. Task-related changes in levels of glutamate are normally compared to those obtained during a control condition. While the cognitive task is intended to modulate glutamate levels during performance, the control condition is expected to provide steady-state and less variable measures thereof. The most commonly used control conditions are fixation cross and flashing checkerboard, with some studies utilizing simple eyes-open or eyes-closed conditions (Lynn et al., 2018). The steady-state glutamate levels, and variability therein, depend on the control condition chosen.

For the current study, the associative memory task was preceded by a fixation cross (5:26 min) followed by a 2-Hz flashing checkerboard (5:26 min). These two conditions served as task-free and non-hippocampal control conditions for assessing the steady-state, control levels of hippocampal glutamate between the age groups. Inside the scanner, participants viewed the fixation cross followed by the checkerboard projected from a monitor on to the mirror attached to the head coil. While viewing, they were instructed to not think of anything specific and let their mind wander.

The schematic task representation (Figure 8) depicts the relevant conditions and the time course of a trial within the associative memory task. The associative memory task was programmed using Neurobehavioral systems Presentation software (version 17) and lasted for 19:12 minutes. At the encoding stage, participants viewed a 3 × 4 grid projected from a monitor

on to the mirror attached to the head coil. In each of the 12 squares of the grid, a unique object appeared one at a time, and stayed in its location for 2.67 seconds before the next object appeared in its unique location. The objects appeared in their locations at random. Randomization of occurrence precluded primacy or recency effects that would be brought about by presentation of the objects in any specific order. Each encoding block lasted about 32.04 seconds (2.67 seconds per object, 12 objects). As in the pilot study, objects came from the Snodgrass and Vanderwart line-drawings set (Snodgrass & Vanderwart, 1980). Participants responded by vocalizing the name of the object and were instructed to choose monosyllabic words for the object names in order to reduce head motion inside the scanner.

The memory retrieval stage lasted 32.04 seconds and included presentation of the same 3 × 4 grid. However, instead of objects, a black square appeared once in the location on the grid where the object appeared at encoding. It served as a cue for the participant to recall and vocalize the name of the object that they had seen during the encoding stage. The black square stayed on for 2.67 seconds before the next one appeared in a randomly chosen location that was occupied by a different object during the encoding stage. If unable to recall the object or make their best guess about what the object might be, participants were instructed to say “no”. A ‘non-zero’ response meant vocalizing a correct answer, an incorrect answer, or saying “no” as instructed. All responses were scored in real-time as well as audio-recorded so that the score could be checked against the recorded responses.

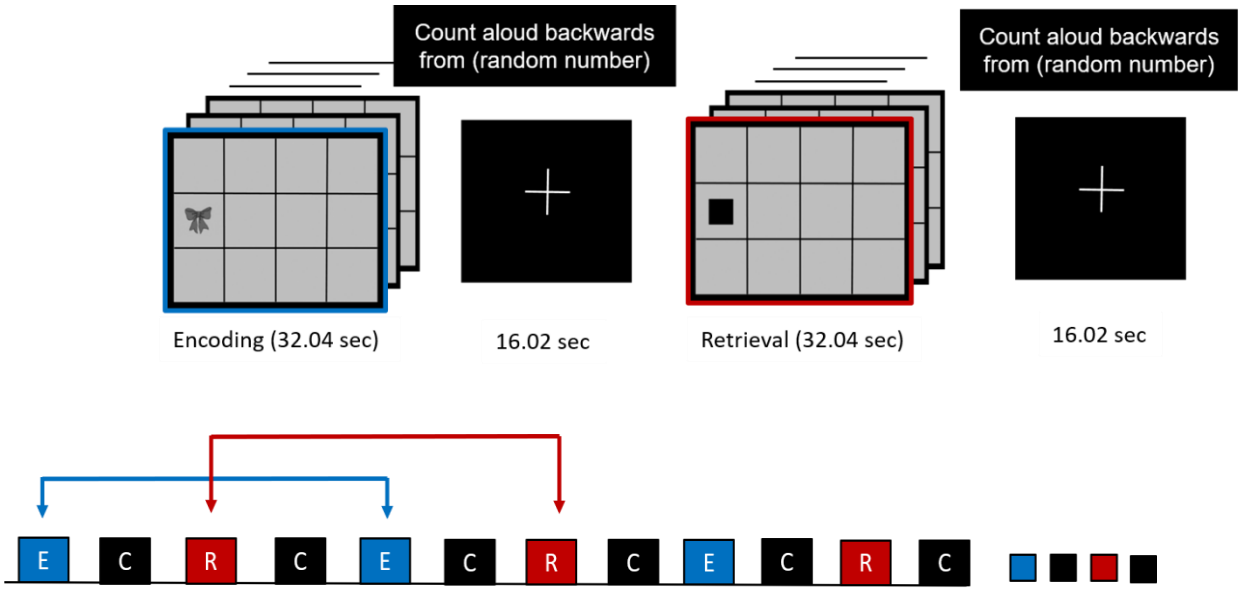

Figure 8. Object-location associative learning and memory task. The top panel shows a schematic of the 3 × 4 object-location paired-associates task. The bottom panel shows the playout of the task with each epoch made up of blocks of encoding (E) -counting (C) - retrieval (R) - counting (C). The entire task consisted of 12 such epochs.

As in the pilot study, each encoding and retrieval stage was followed by a buffer task, in which the participants counted aloud backwards by one from a random number between 40 and 80, chosen by the randomization programmed in the task. Each counting condition lasted 16.02 seconds. Participants were instructed to count at a calm and steady pace of one number per second. The purpose of the buffer task was to engage all participants in a uniform controlled activity designed to suppress the articulatory loop (Baddeley & Hitch, 1974; Salamé & Baddeley, 1989), prevent active rehearsal during the memory maintenance interval between encoding and retrieval, and suppress use of strategies. In addition, this also ensured that all participants performed a controlled mental activity during memory maintenance. Learning of the object–location association pairs was assessed over 12 encoding-counting-retrieval-counting epochs. Prior to scanning, each participant received detailed instructions regarding the associative memory task and practiced for one trial of encoding, counting, and retrieval on a

laptop outside the scanner. The goal of this short demonstration was to familiarize the participant with the task format before performing it in the scanner. During this one trial, the timing of presentations of objects and cues matched those of the in-scanner task to familiarize the participant with the presentation speed.

At the end of the task, when the participant stepped out of the scanner and was back in the control room, a cognitive test assessing free recall of the objects was conducted. The participant was provided with a sheet of paper with the 3 × 4 grid drawn on it. They were instructed to visualize the objects that were presented to them on the grid while performing the in-scanner task and write the object names in the appropriate location on the grid drawn on the paper. This was a single trial test with no time limit or recall order imposed on the participant.

3.4 Neuroimaging protocol

As detailed in the neuroimaging protocol below, ^{1}H MRS spectra were continuously collected when the participants performed the task inside the scanner.

3.4.1 Signal acquisition

All imaging was performed on a 3 Tesla (3T) MRI system (Siemens MAGNETOM Verio^{TM}) with a 32-channel receive-only head coil. All scans were collected in the morning between 9:00 am and noon to standardize the time of scanning, and the imaging protocol was identical for each participant. A scout image (TA = 9.2 sec) was followed by a structural T_1 MPRAGE scan collected in the axial plane. The T_1 MPRAGE covered the whole brain and had a resolution of 1 × 1 × 1 mm^3 with the following parameters: TR = 2.15 sec, TE = 3.53 ms, TI = 1100 ms, GRAPPA = 2, flip-angle = 8^0, FOV = 256 × 256 × 160 mm^3, 160 axial slices, pixel resolution = 1 × 1 × 1 mm^3, acquisition time = 4:59 min.

To proceed with ^{1}H MRS scans, a 3.0 × 1.8 × 1.3 cm^3 (7.02 cm^3) voxel was prescribed in the unilateral (side randomized) anterior hippocampus of the participant (Figure 9). Hippocampal

side was randomized across participants because of the nature of the associative memory task used in this study. The task included aspects of spatial, visual, as well as verbal memory owing to object-location associations that had to be encoded and retrieved via vocalization. The right hippocampus in involved in spatial memory, whereas the left in verbal memory (Ezzati et al., 2016; Kelley et al., 1998). Owing to possible individual variability in utilizing these domains, an effect of hemispheric differences on hippocampal glutamate levels was not hypothesized. The anterior hippocampus was chosen because of its involvement in spatial and associative memory (Schacter & Wagner, 1999). Hippocampal voxel was manually placed for each participant's scan. Prior to the ^{1}H MRS acquisition homogeneity of the magnetic field in the hippocampal voxel was optimized (shimmed) using FASTESTMAP (Tkáć & Gruetter, 2005). Before the beginning of the MRS sequence, a trigger-pulse time-locked the presentation of the stimulus with the acquisition of the spectra. The ^{1}H MRS scans were acquired using the point-resolved spectroscopy (PRESS) sequence with outer volume saturation (OVS) for improved localization and reduced signal contamination from outside the hippocampal voxel, high bandwidth slice-selective RF pulses for minimal chemical shift displacement, and VAPOR for water suppression and a clean spectral baseline. The ^{1}H MRS scans were continuously acquired approximately every 16 seconds as the participants performed the task. For the control conditions (fixation cross and flashing checkerboard) and the task with 12 sets of encoding-counting-retrieval-counting epochs, the acquisition parameters were as follows: TR = 2.67 sec, TE = 23 ms, 6 averages/spectrum, bandwidth = 2 kHz, 2048 complex data points.

Twenty ^{1}H MRS spectra were collected during each of the control conditions (fixation cross and flashing checkerboard). Seventy-two spectra were collected during the associative memory task. Each spectrum indicated a single measurement comprising of 6 averages, totaling

16.02 sec per averaged spectrum. Thus, per encoding and retrieval block, each of which were 32.04 seconds long, there were two measurements (16.02 + 16.02 sec) or two averaged spectra. The 16.02-second-long counting condition comprised of only one measurement or one averaged spectrum. A fully relaxed water-unsuppressed spectrum (TR = 10 sec, TE = 23 ms, 2 averages) was acquired from the same voxel as part of the absolute quantification approach. These water-unsuppressed spectra were acquired after the fixation cross condition and after the checkerboard + associative learning task condition to be used as an internal reference for the quantification of MRS data.

3.4.2 Image post-processing and quantification of the spectra

Prior to quantification, each spectrum was frequency- and phase-corrected. Eddy current effects were corrected using the unsuppressed water signal (Klose, 1990). FreeSurfer and FSL tools were used to correct the B_1 field, extract images, segment into tissue volume maps (CSF, gray and white matter), and estimate the tissue fractions within each voxel (Jenkinson, Beckmann, Behrens, Woolrich, & Smith, 2012). The water-unsuppressed signal, gray and white matter, and CSF values from the tissue segmentation procedure (FAST) (Y. Zhang, Brady, & Smith, 2001), along with T_1 and T_2 relaxation values, were used to quantify absolute values of the neurometabolites (mmol/kg.w.w) (Gasparovic, 2006; J. A. Stanley et al., 1995).

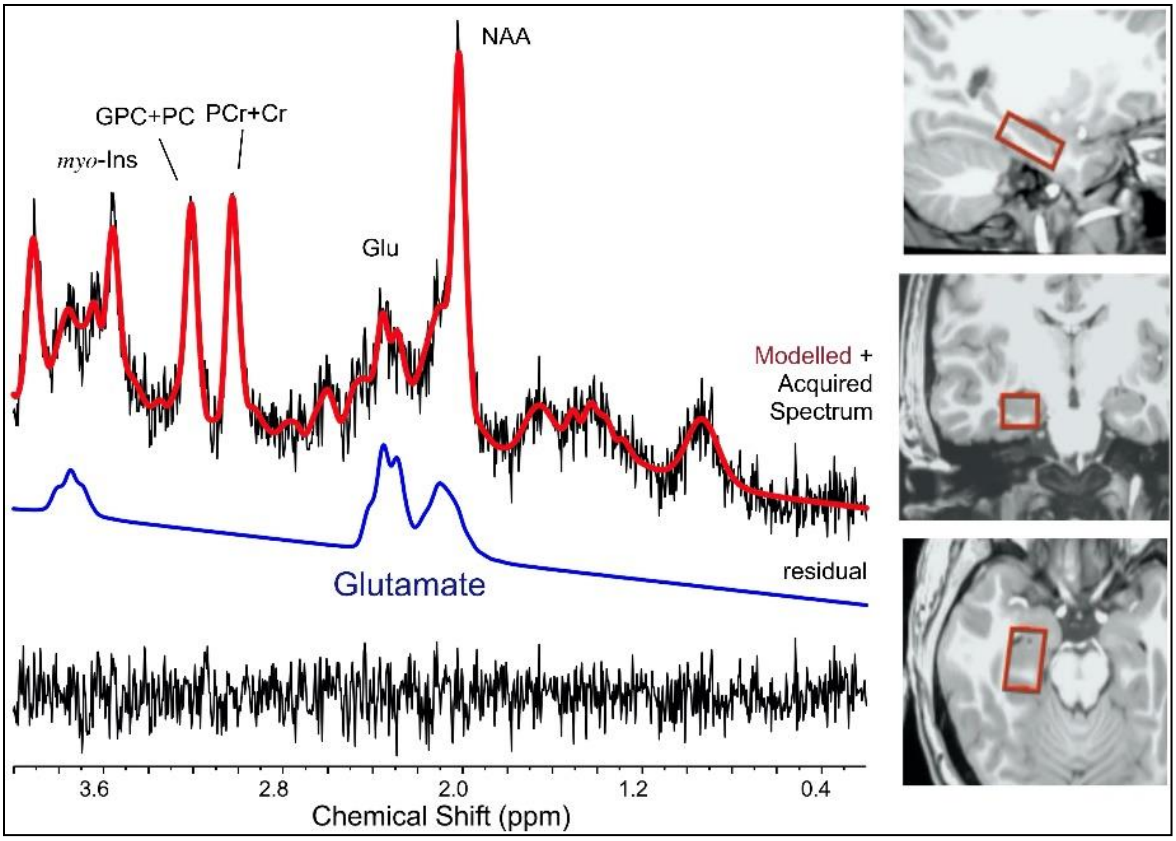

Figure 9. An example ^{1}H MRS spectrum. Acquired (black) and modeled (red) *in vivo* ^{1}H MRS spectrum from the right hippocampus (96 sec temporal resolution). Raw (black line) and LCModel fit (red line) signal are displayed above the estimated spectral peaks for Glu (blue line). The residual signal (i.e. noise) and chemical shift (ppm) are displayed at the bottom of the figure. The panel on the right side shows from top to bottom: sagittal, coronal, and axial views of the MRS voxel placed in the head/body of the hippocampus.

The ^{1}H fMRS acquisition in the hippocampus had a temporal resolution of 16.02 seconds. Thus, each encoding and retrieval block contained two measures (2 × 16.02 = 32.04) and the two counting conditions were one measure each (16.02 seconds). However, the SNR in the hippocampus was very low and prompted combining the signal from three (spectral tripling) consecutive encoding blocks (2 spectra per block), with a similar combination scheme applied to retrieval blocks. Spectral averaging was performed after phase and frequency correction of individual spectra and this improved the SNR from 4 ± 0.75 to 9.04 ± 1.65. This resulted in a

series of four outcome measures for each stage, giving a temporal resolution of 96 sec. Averaging fewer blocks would have improved the temporal resolution while sacrificing SNR. Thus, even though spectral tripling afforded only four total time points per memory stage, the more-than-doubled SNR ensured greater confidence in the signal.

Completely automated post-processing of ^{1}H fMRS data and quantification of neurometabolites was performed using Linear Combination (LC) Model (version 6.3) with a simulated basis-set for *a priori* knowledge (Provencher, 1993). The first spectrum from the fixation cross and checkerboard conditions, each, was excluded from analysis due to a possible T_1-saturation effect (De Graaf, 2013). Spectral fitting was assessed via the Cramér-Rao lower bound (CRLB) value. It is the threshold of the error associated with model fitting and reveals uncertainties in the fit i.e. the difference between acquired and modeled spectra (Cavassila et al., 2001). Spectra with CRLB values higher than a certain threshold indicate less reliable measures and are characterized by less optimal peak separation as well as more noise in the fitting. Higher CRLB values are associated with low SNR, low glutamate, and high FWHM. Spectra with high CRLB values are commonly excluded from further analyses. For the current study, the CRLB was set at a threshold of 16% for hippocampal glutamate (J.A. Stanley et al., 2017) and spectral triplets with CRLB values more than 16% were discarded since that indicated an unacceptable fit in LCModel. An example of a ^{1}H MRS spectrum obtained from the right hippocampus is shown in Figure 9 above.

Although the focus of the current investigation was glutamate, levels and dynamics of GABA, the major inhibitory neurotransmitter, are an important subject of inquiry as well. Both, glutamate and GABA, play a collaborative role in maintaining the brain's E/I balance. However, reliable quantification of GABA requires possibly higher magnetic field strength as well as

special spectral editing techniques that can resolve the GABA resonance (Rothman, Petroff, Behar, & Mattson, 1993). Thus, only data on glutamate analyses are reported.

3.5 Modeling of behavioral data

Each participant's behavioral data were collected during the cued-retrieval stage of the associative learning and memory task and were expressed as percent correct responses out of a maximum of 12 per block of retrieval. Considering the individual variability in the behavioral data, it is critical to choose an optimal model function to fit the data and characterize the learning curve. Model fitting was evaluated for five different functions commonly mentioned in literature: single-parameter linear and negatively accelerating exponential functions that optimize the slope, three-parameter logistic and Gompertz functions that optimize the asymptote, inflection point and slope, and four-parameter Richards function that optimizes an additional parameter called shape. The linear and negatively accelerating exponential functions did not capture the learning behavior and did not allow for individual variability in the learning curves. In addition, these functions also demonstrated weaker goodness of fit. Both the three-parameter functions, logistic and Gompertz, were equally suitable for these data. Such three-parameter families of curves (Vieira & Hoffman, 1977), and more so, the Gompertz function, have been extensively used for modeling growth data (Winsor, 1932). The Gompertz function is a special case of the logistic function where the inflection point is at 37% of the upper asymptote, instead of at 50%, thus, making the former more asymmetric. Most growth processes are not symmetric around the inflection point (Vieira & Hoffman, 1977), and in line with that property, in our data, with a maximum of 12 objects, learning seemed to occur earlier in the task. Learning rates in most participants were higher initially and later gradually decreased as performance approached the asymptote, indicating an asymmetrical 'S' shaped learning curve. Although, the four-parameter Richards function can flexibly accommodate different growth patterns owing to the shape

parameter (Birch, 1999), a criticism about this function is the lack of interpretability of the shape parameter (Zwietering, Jongenburger, Rombouts, & van 't Riet, 1990).

Goodness of fit measures (χ^2, R^2, and RMSE) were compared among all five fits. The Gompertz and Richards functions, both, fit the data well. However, a model that optimally describes the data using fewer parameters is recommended over a model with additional parameters. The three-parameter model is conceptually simpler than the four-parameter model and its solution is more stable since the parameters are less correlated. I, therefore, selected the Gompertz function to fit the learning data (Gompertz, 1825; Zwietering et al., 1990). The Gompertz function optimized three parameters that are expected to capture the salient characteristics of the learning process in each individual: asymptote (maximum attained score reflecting the associative learning proficiency), slope (learning rate), and point of inflection (transition from steeper to shallower slope in growth and learning curve models). The Gompertz function is given as:

$$y = ae^{-e\left(-\frac{t-c}{r}\right)} \quad (5)$$

where a = asymptote, t = time (block), r = slope (learning rate), c = inflection point (displacement about the x-axis indicating the block when learning rate transitions from fast to slower). The curve fitting was implemented in Matlab (MathWorks, 2013), using the lsqnonlin function.

With respect to data on the single trial free-recall test conducted after the scanning session, the performance was scored as the number of correct object-location associations recalled out of total 12. Only accurate object-location pairs were scored as correct responses.

3.6 Statistical Analyses

3.6.1 Mock scanner pilot study

The data were analyzed using a GLM approach with age group (young, old), location (scanner, desk), noise (present, absent) as categorical two-level independent variables, and a vector of the Gompertz learning curve parameters (asymptote, learning rate, and inflection point) as the dependent variable. For assessing the effects of task complexity, the predictors of performance were age group and grid size.

3.6.2 Associative learning and memory dissertation study

3.6.2.1 Cognitive data analyses.

The vector of Gompertz function parameters served as the dependent variable, with age group (young, old) and sex (male, female) being the categorical two-level independent variables. A GLM analysis assessed the age and sex differences in the Gompertz function parameters. Correlation analyses evaluated the strength of associations between the free recall score and each of the learning curve parameters.

3.6.2.2 Glutamate level analyses.

Glutamate levels used in these analyses are absolute levels and not ratios to total creatine, as are reported in most studies. Age differences in mean levels of glutamate achieved throughout the encoding, retrieval, and the control conditions were evaluated using the GLM approach. Age group (young, old), sex (male, female), and hippocampal side (left, right) were the between-subject factors, whereas task stage (encoding, retrieval, control condition) was the within-subject factor. Age differences in hippocampal glutamate modulation were investigated via GLM repeated measures ANOVA (using PROC MIXED in SAS). Glutamate level served as the dependent variable, with age group (young, old), sex (male, female), hippocampal side (left, right) as between-subject factors. Task stage (encoding, retrieval) and block triad (1-4) were the

within-subject factors. Glutamate levels during the control condition, centered at the sample mean, served as a continuous covariate. Huynh-Feldt correction was applied to account for violation of the assumption of sphericity in tests of interactions. If a significant age group × task stage × block interaction was found, it was followed by assessment of the task stage where the age group × block was the interaction of interest. Further post-hoc analyses were conducted to determine the block at which age differences were significant. In addition, the effect of block triad within each task stage was assessed for each age group to examine significant glutamate modulation.

A variable called 'adjusted-glutamate' was calculated, where task-related levels of glutamate at each block triad were adjusted for mean levels of glutamate during the control checkerboard condition via analysis of covariance adjustment (Jack et al., 1989). The adjusted values are calculated as:

$$Glu_{adj} = Glu_{obs} - \beta[Glu_{con} - mean(Glu_{mean\_con})] \quad (6)$$

where, Glu_{adj} and Glu_{obs} are the adjusted and observed concentrations of glutamate in a participant, Glu_{con} is the participant's control-level glutamate, Glu_{mean_con} is the average control-level glutamate across all participants, and β is the unstandardized regression coefficient. As the relationship between control-levels of glutamate and glutamate at each block triad for each task stage did not differ between the age groups (all control-level glutamate × age group interactions were non-significant), the same control-glutamate correction was applied to the entire sample. This correction reduces any bias due to individual differences in control-levels of glutamate. 'Adjusted-glutamate' was used only for visualization of the results (i.e. Figure 13).

3.6.2.3 Relationship between glutamate and cognitive performance.

GLM analyses with age group and control-level glutamate as predictors were conducted on the Gompertz function parameters to investigate whether age differences in control-level glutamate affected memory performance. To investigate the relationship between glutamate modulation and memory performance, two glutamate modulation parameters were defined for each participant: the maximum level of glutamate achieved during encoding (called 'Glu-max') and the block triad at which Glu-max was achieved (called 'block-max'). A GLM analysis was then conducted with a multivariate vector of the three Gompertz function parameters as the dependent variable. Age group (young, old), sex (male, female), and block-max were the independent variables. Correlation analyses evaluated the strength of associations between the free recall score and control-level glutamate as well as between free-recall score and Glu-max.

3.6.2.4 Neurochemical specificity.

Age differences as well task-specific temporal differences were investigated for the other well-resolved main ^{1}H MRS visible metabolites (NAA, PCr+Cr, GPC+PC, myoinositol) to confirm neurochemical specificity of the associative memory paradigm with respect to glutamate.

CHAPTER 4 RESULTS

4.1 Mock scanner study

Gompertz function showed successful fit (average R^2 of 0.98) for cognitive data in both age groups and for both conditions (desk, scanner). Compliance with task instructions was high, with about 93% non-zero responses across the entire sample. Overall, the young performed better than the old and had a significantly higher asymptote: F (1, 26) = 7.45, p = 0.011. With respect to setting, a trend was noted for older adults to have a lower asymptote than the young when the task was performed inside the scanner compared to at the desk: F (1, 50) = 4.04, p = 0.055. Simulated MRI noise did not affect performance in either age group. Ceiling effects were observed for performance in the 3 × 3 version of the grid, with 12 out of the 20 young and five out of the eight old adults achieving 100% asymptotes. Task complexity was, therefore, increased in a dose-response manner using 3 × 4 and 4 × 4 grid versions of the task. In a separate group of participants that were tested for effects of task complexity operationalized as grid size, it was noted that the 4 × 4 grid significantly and adversely affected learning rate [F (1,11) = 12.69, p = 0.016] and inflection point [F (1,11) = 40.29, p = 0.001]. Thus, the less complex 3 × 4 grid was chosen for the final associative memory task used in the dissertation (see Methods section 3.3.2); and all following results - behavioral and neuroimaging - are based on data collected using the 3 × 4 grid version of the task.

4.2 Age differences in associative learning and memory performance in the dissertation study

The Gompertz function showed acceptable fit to the cognitive data for both age groups, with an average R^2 of 0.92 and 0.84 for the young and old, respectively. Compliance with task instructions was high, with 96% non-zero responses across the entire sample. Performance increased across the retrieval blocks for all participants. Young adults performed better than their

older counterparts as demonstrated by significant age differences in the asymptote: F (1,44) = 6.32, p = 0.015, Cohen's d = 0.80, 95% CI for Cohen's d: 0.16/1.45. Inflection point [F (1,44) = 1.15, p = 0.11] and slope [F (1, 44) = 0.14, p = 0.71] did not differ between the groups. However, the effect size for inflection point (Cohen's d = 0.34, 95% CI: -0.29/0.98) was greater than that for the slope (Cohen's d = 0.17, 95% CI: -0.51/0.75). There was no difference between men and women for any of the Gompertz function parameters, nor was there any significant interaction between sex and age group. Learning curves modeled using the Gompertz function as well as age group differences in the three parameters are shown in Figure 10. Table 3 includes mean and standard deviation values for the Gompertz function parameters.

Table 3. Gompertz function parameters for the two age groups (mean ± 1 standard error)

Gompertz function parameter	**Old**	**Young**
Asymptote (% correct)	84.98 ± 5.11	94.71 ± 1.29
Inflection Point (block number)	3.68 ± 0.52	3.18 ± 0.23
Learning Rate	0.43 ± 0.06	0.41 ± 0.03

There were no age differences in the free recall score obtained at the end of the entire MRI scanning session (t < 1). However, within age groups, free-recall performance was positively associated with the asymptote in old adults (Pearson's r = 0.58, p = 0.028, F (1) = 14.36, p = 0.03) and negatively associated with the inflection point in the young adults (Pearson's r = - 0.42, p = 0.026, F (1) = 4.55, p < 0.012).

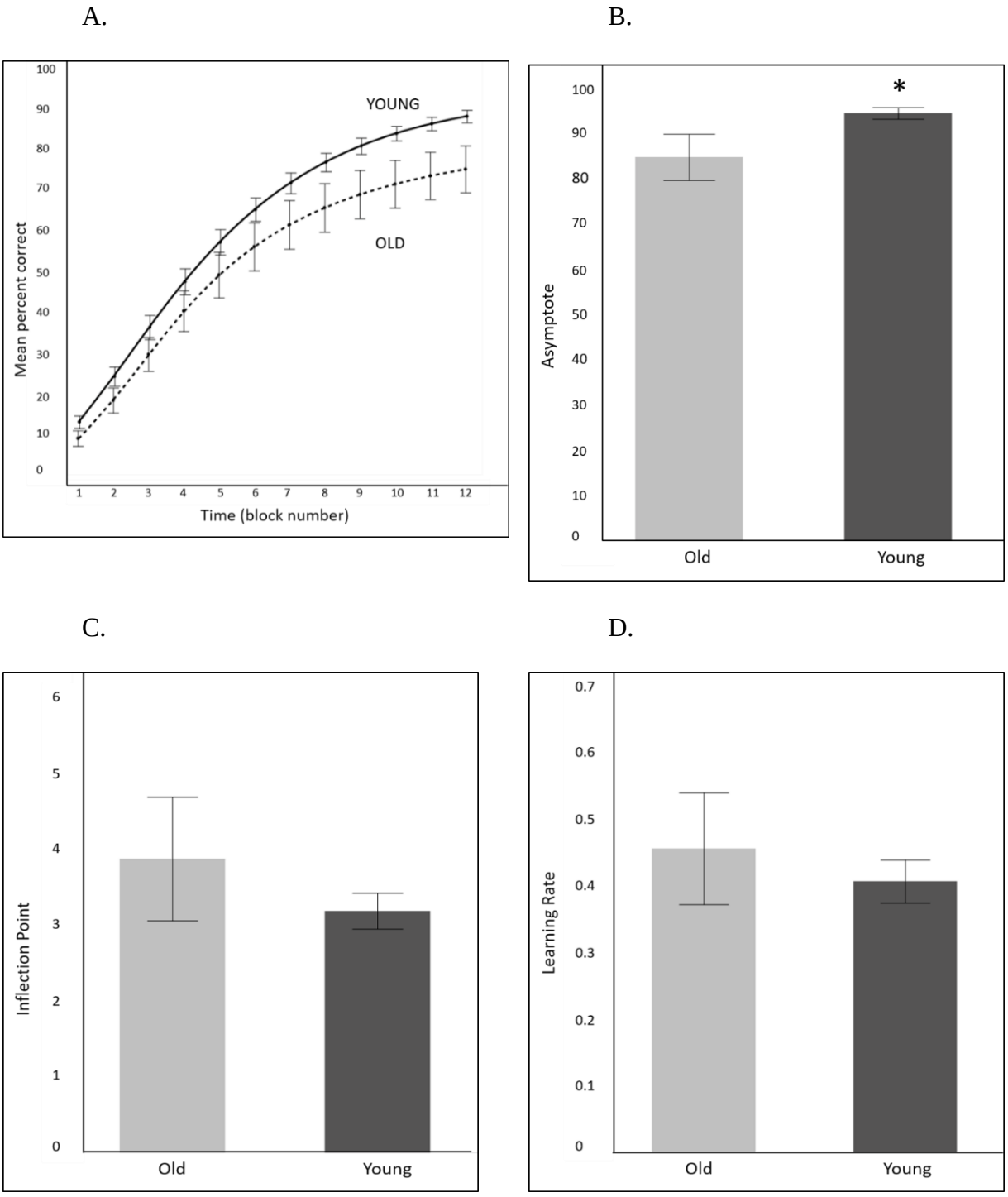

Figure 10. Age differences in the associative learning and memory task. Gompertz function modeled learning curves for both age groups (dashed line: old, solid line: young) (A), Mean age group differences in asymptote (B), inflection-point (C), and learning-rate (D) (light gray: old, dark gray: young). Error bars indicate ± 1 standard error. (* $p < 0.05$).

4.3 ^{1}H fMRS results

4.3.1 Spectroscopy data quality check

Signal averaging of the acquired ^{1}H MRS spectra into triplets (block triads) made of consecutive encoding and retrieval blocks more than doubled the SNR from 4 ± 0.75 to 9.04 ± 1.65 but reduced the temporal resolution to about 96 seconds. Although the range of values of LCModel fit characteristics (SNR, FWHM, and CRLB) across the entire sample was within acceptable limits of data quality, younger adults demonstrated higher SNR and lower FWHM and CRLB compared to the old (all $p < 0.001$), indicating better data quality. However, across age groups and task stages the average SNR (9.26 ± 1.71), FWHM (8.27 Hz ± 1.78), CRLB (8.08 ± 1.71) for glutamate were deemed optimal. LCModel fit characteristics averaged across block triads per task stage for each age group are presented in Table 4. The abovementioned LCModel indices did not differ significantly between the task stages for each age group, thus, indicating an absence of bias due to differences in spectral quality between task stages.

Table 4. LCModel fit characteristics by task stage and age groups.

LCModel fit characteristic	**Checkerboard**		**Encoding**		**Retrieval**	
	Old	**Young**	**Old**	**Young**	**Old**	**Young**
SNR	8.8 ± 2	9.7 ± 1.4	8.6 ± 1.9	9.4 ± 1.3	8.5 ± 1.9	9.4 ± 1.4
FWHM (Hz)	8 ± 1.4	7.6 ± 1.6	8.8 ± 1.9	8 ± 1.8	8.9 ± 1.9	8.2 ± 1.9
CRLB (%)	8.7 ± 2.1	7.5 ± 1.2	8.8 ± 1.7	7.2 ± 1.1	8.8 ± 1.7	7.5 ± 1.3

Note: The values are mean ± 1 standard deviation. SNR = signal to noise ratio, FWHM = fullwidth at half of maximum, CRLB = Cramér-Rao lower bound

The average absolute concentration of glutamate across the entire task was 8.4 ± 1.19 mmol/kg, and that of glutamine was 2.97 ± 1.01 mmol/kg. The unilateral anterior hippocampal voxel, in which ^{1}H MRS signal was recorded, contained more gray matter by volume in the young participants (60.5 ± 0.06%; range 46% to 74%) than in their older counterparts (45.2 ± 0.07%; range 33% to 60%); t (44) = 6.65, $p < 0.000$.

4.3.2 Age differences in steady-state hippocampal glutamate levels at the control condition

The levels of hippocampal glutamate during both task-free control conditions (fixation cross and flashing checkerboard) did not differ between young and old participants ($F < 1$) and there was no difference between the sexes ($F < 1$). The flashing checkerboard was chosen as the control condition to be used in further analyses because of lesser variability in steady-state levels of glutamate associated with this condition (Lynn et al., 2018). The glutamate levels under the flashing checkerboard stimulation for each age group are illustrated in Figure 11. Unilateral hippocampus (side randomized) was chosen since at the inception of the study there was no hypothesis regarding the effect of hemispheric differences on hippocampal glutamate levels during associative memory performance. However, a significant age group × side interaction [F (1) = 7.89, p = 0.047] was noted for control-level glutamate, with older adults demonstrating higher levels of glutamate in the left hippocampus compared to the right. No hemispheric differences in control-level glutamate were observed in the young.

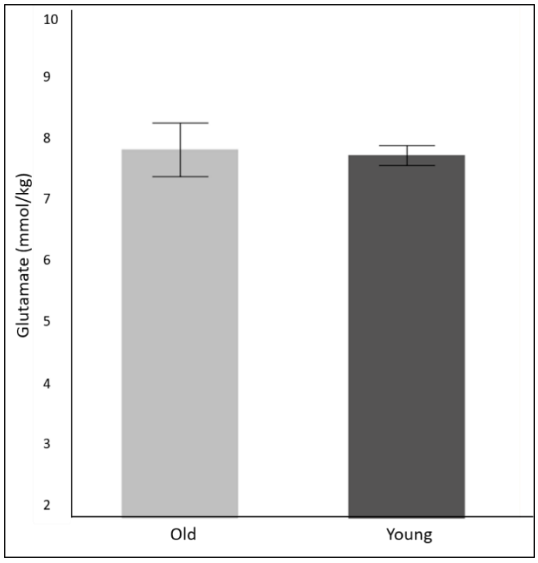

Figure 11. Age differences in control-level glutamate. (light gray: old, dark gray: young). Error bars indicate ± 1 standard error.

4.3.3 Age differences in mean hippocampal glutamate levels during associative memory task

During memory encoding, young adults displayed higher levels of mean hippocampal glutamate compared to their older counterparts: F (1, 182) = 8.36, p = 0.004, with a small to medium effect size (Cohen's d = 0.35, 95% CI: 0.15/0.68). In contrast, mean hippocampal glutamate during memory retrieval did not differ between the age groups (F < 1) (Figure 12). Within the young group, hippocampal glutamate levels during encoding showed a non-significant trend to exceed those during retrieval [F (1, 250) = 3.36, p = 0.07], with no task stage dependent differences in the old group. There were no sex differences in mean glutamate levels at any task stage. Mean levels of hippocampal glutamate for both age groups during the control condition, encoding, and retrieval are presented in Table 5.

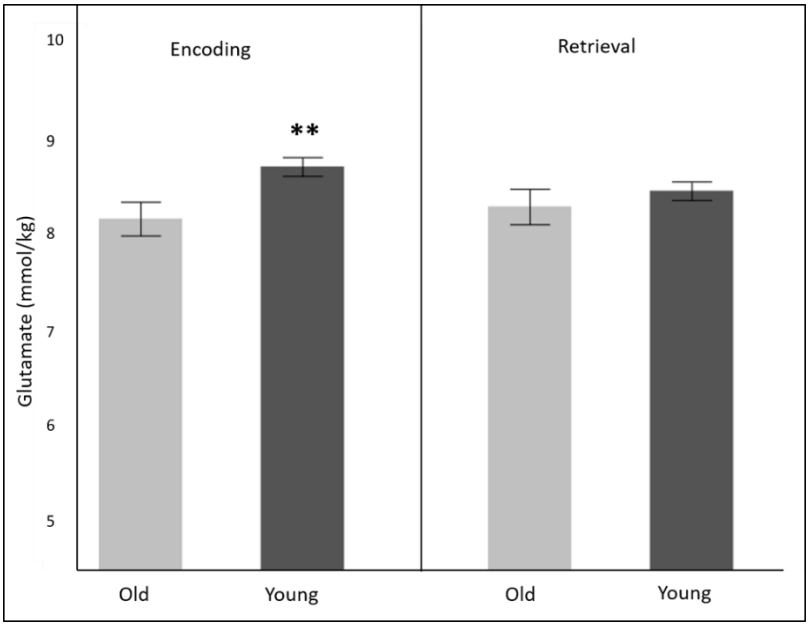

Figure 12. Age differences in mean glutamate levels during associative memory performance. Significant age differences in hippocampal glutamate levels during memory encoding but not retrieval (light gray: old, dark gray: young) (** $p < 0.005$). Error bars indicate ± 1 standard error.

Table 5. Mean hippocampal glutamate levels (mmol/kg) for both age groups during the control condition, encoding, and retrieval stages (mean ± 1 standard deviation).

Task stage	**Old**	**Young**
Checkerboard (control condition)	7.8 ± 1.5	7.7 ± 0.9
Memory Encoding	8.2 ± 1.3	8.8 ± 1.1
Memory Retrieval	8.3 ± 1.4	8.5 ± 1.1

In addition, for both age groups across both task stages, the main effect of side was significant [$F(1) = 12.7$, $p = 0.004$]. The left hippocampus evinced higher mean glutamate levels during encoding as well as retrieval across both age groups.

4.3.4 Age differences in hippocampal glutamate modulation during associative memory task

A repeated measure general linear model (GLM) analysis was conducted, with glutamate levels as the dependent variable, age group, sex, and hippocampal side as categorical between-subject variables, trial stage and block as within-subject (repeated) measures. Mean-centered control level glutamate was the continuous covariate. The full model also included all first-order interactions as well as the highest order age group × task stage × block triad interaction. A reduced model was evaluated after the removal of non-significant interactions. Significant main effects of age group [F (1, 308) = 7.39, p = 0.009, Cohen's d = 0.87, 96% CI: 0.22/1.52], hippocampal side [F (1, 308) = 5.01, p = 0.017, Cohen's d = 0.72, 95% CI: 0.07/1.36], and control-level glutamate [F (1, 308) = 26.19, p < 0.000], as well as significant age group × task stage × block triad interactions [F (11, 308) = 2.48, p = 0.002] were noted. Young adults demonstrated higher mean glutamate levels than the old. In both age groups, the left hippocampus showed higher levels of glutamate throughout encoding and retrieval.

To assess whether the age group × block triad interaction was restricted to the encoding stage as hypothesized, this interaction was explored by subsidiary GLM analyses conducted separately for encoding and retrieval stages. A trend level age group × block triad interaction was indicated for glutamate modulation during encoding [F (3, 132) = 2.41, p = 0.05] but not for retrieval (F <1). In addition, this difference emerged during the second and last quarters of encoding. Post hoc analyses showed that young adults demonstrated higher glutamate levels compared to the old during the second (block numbers 4, 5, and 6) (Cohen's d = 0.9, 95% CI: 0.25/1.56) and fourth (block numbers 10, 11, and 12) block triads (Cohen's d = 0.43, 95% CI: -0.16/1.12) of encoding. Age differences for all retrieval block triads were non-significant (Figure 13).

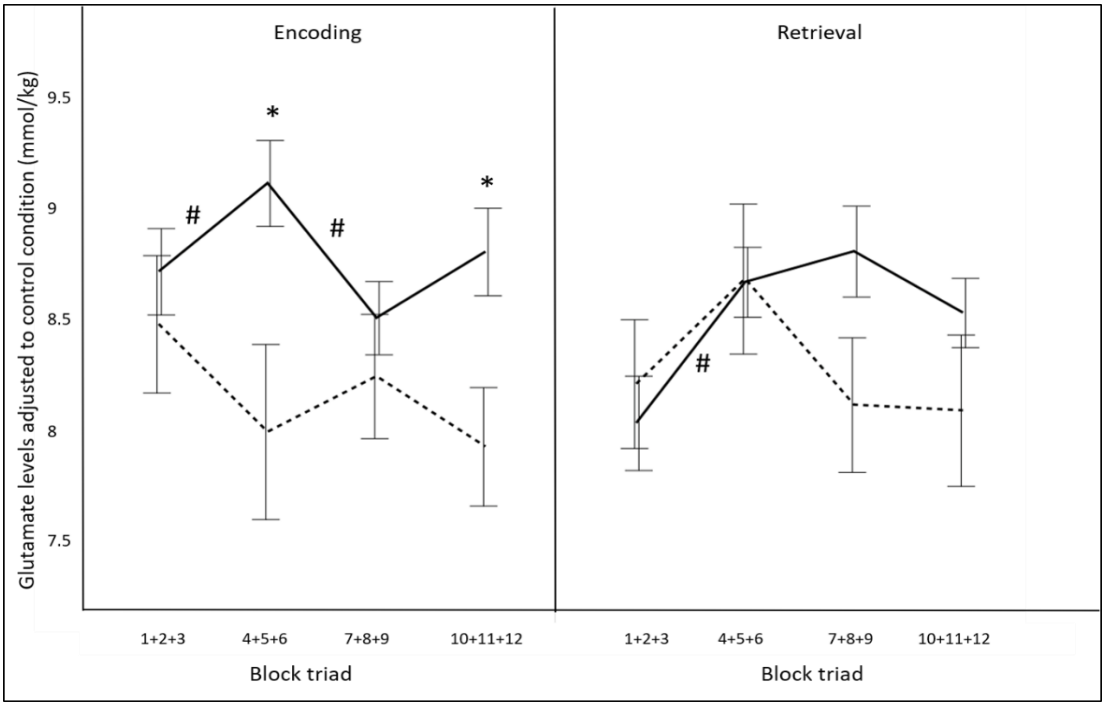

Figure 13. Age differences in glutamate modulation during associative memory performance. Age differences in hippocampal glutamate modulation were specific to memory encoding (dashed line: old, solid line: young). Post-hoc analysis revealed the age differences to be significant in the second and fourth block-triads of memory encoding. Within-group differences in glutamate levels between block triads are indicated by hash sign (#). (* $p < 0.05$). Error bars indicate ± 1 standard error.

With respect to glutamate modulation *within* each age group; young adults demonstrated differences in glutamate levels between the first and second (Cohen's d = 0.34, 95% CI: -0.21/1.02), as well as the second and third (Cohen's d = 0.58, 95% CI: -0.05/1.23) block triads of encoding, and between the first and second (Cohen's d = 0.46, 95% CI: -0.17/1.1) block triads of retrieval (Figure 13). No such differences in mean glutamate levels across time were noted in the elderly.

4.3.5 Relationship between glutamate levels and cognitive performance

Across both age groups, control-level glutamate did not explain associative memory performance and was unrelated to any of the Gompertz function parameters. The effect of the

timing of glutamate response during encoding on performance was investigated. Old adults who evinced maximum levels of glutamate (Glu-max) at a later block triad (block-max) during encoding demonstrated non-significant trends towards a later inflection point [F (1, 42) = 3.61, p = 0.06] (Figure 14 A) and a slower learning rate [F (1, 42) = 2.96, p = 0.09] (Figure 14 B).

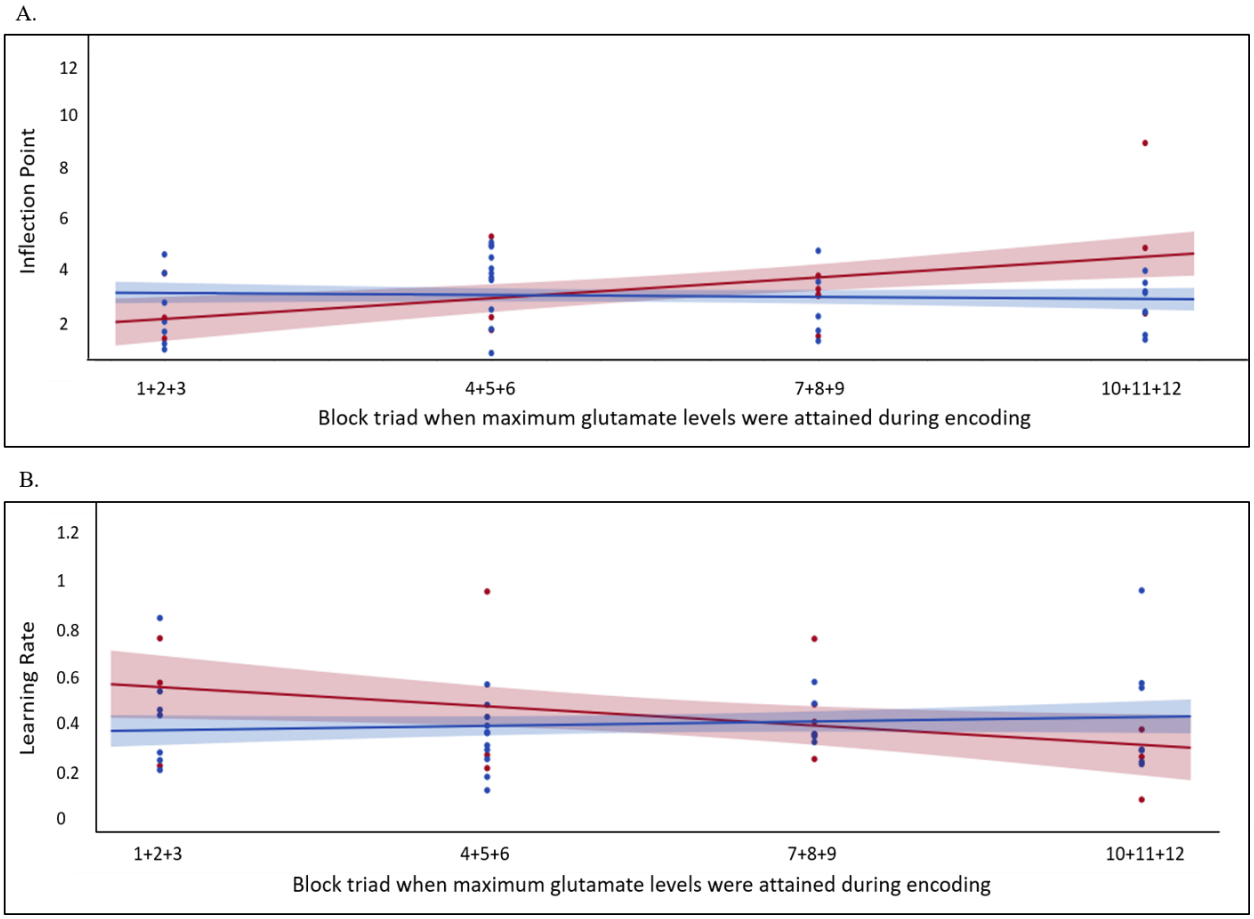

Figure 14. Effect of glutamate modulation on memory performance. Old adults (red) with later glutamate modulation showed a trend towards a later inflection point (A) and slower learning rate (B). No effect of the timing of glutamate modulation was observed in the young (blue).

No such relationships were observed for young adults (blue line in Figure 14), nor did glutamate levels obtained during retrieval show an association with the learning curve parameters in either age group. In addition, Glutamate levels at any stage did not show an association with the free recall score for either age group.

4.3.6 Neurochemical specificity

With respect to age differences in the other ^{1}H MRS-observable metabolites, old adults had higher mean levels of PCr+Cr [F (1,42) = 4.32, p = 0.021], GPC+PC [F (1,42) = 14.36, p < 0.000], and myoinositol [F (1,42) = 9.68, p = 0.002] compared to the young. No age differences were noted in NAA (F < 1). Importantly, for both age groups, the observed temporal effects during encoding and retrieval were specific to glutamate, with no significant differences in levels of the other metabolites at any block triad (supplementary figure S 1). GABA could not be reliably measured since it is present at very low concentrations and special spectral editing techniques are required to be able to resolve the GABA peak reliably.

4.3.7 BOLD effect

The BOLD effect that occurs due to increases in the concentration of oxygenated blood in the task-active ROI reduces the spectral linewidth (i.e. FWHM) and affects signal amplitude. Earlier ^{1}H fMRS investigations have noted a significant BOLD effect as a function of task (Mangia et al., 2007; Schaller et al., 2013). In the current study, for either age group, the FWHM did not significantly differ across any task stage relative to the control condition (all F < 1).

CHAPTER 5 DISCUSSION

Episodic and associative memory impairment is one of the most common age-related cognitive deficits and can be exacerbated in conditions such as Alzheimer's disease (AD). Glutamate, the primary excitatory neurotransmitter involved in cognitive processes, including associative memory, is reduced in several key brain regions in AD (Butterfield & Pocernich, 2003) and in normal aging. Characterizing age effects on the modulation of glutamate in response to a cognitive task has the potential of providing new insights on age differences in neurotransmission-capacity related to cognitive decline. Proton functional magnetic resonance spectroscopy (^{1}H fMRS) is the only neuroimaging technique that can non-invasively measure changes in levels (temporal modulation) of metabolites, *in vivo*, in response to functional activation. Specifically, investigation of the temporal dynamics of neurotransmitter levels in response to neuronal activation can shed light on the shift in the brain's E/I balance that may be dysregulated in aging and age-related neuropathology. The identification of altered dynamics of task-related glutamate modulation in the elderly has the potential to provide an effective framework to test better-targeted therapies to decelerate, if not reverse, the impending cognitive decline.

The present study demonstrated, for the first time, the existence of age differences in hippocampal glutamate modulation that may underlie those in associative memory performance, with a specificity towards impaired associative encoding. As has been observed before in studies of associative learning, older adults performed significantly worse than their younger counterparts. Despite the absence of age differences in hippocampal glutamate levels during a control condition, modulation of hippocampal glutamate during memory encoding was higher in young adults compared to the old, in whom it was almost absent. Delays in glutamate elevation

seemed to negatively affect older adults' memory performance. In addition, the task-related modulation was specific to glutamate, with no temporal changes observed in the levels of other metabolites (NAA, GPC+PC, PCr+Cr, myoinositol). This neurochemical specificity of the associative memory task with respect to glutamate is an important finding that ascertains the role of glutamate in subserving memory performance as well as being sensitive to the different stages of memory function. The main observations and the possible underlying mechanisms are unpacked in the ensuing sections.

5.1 Interpretation of Results

5.1.1 Age differences in associative memory performance

Old adults demonstrated significantly lower asymptote than the young, indicating lower associative memory proficiency. A non-significant later inflection point among the elderly may suggest a possible delay in the acquisition and consolidation of memory for the object-location associations. This is in line with the ADH (Naveh-Benjamin, 2000), which posits that older adults are disproportionately deficient in tasks of associative memory. The ADH is based on observations that although their memory for individual items might be unimpaired, older adults perform worse than the young on tests of associative memory that require the creation and retrieval of links between the associated memoranda. Indeed, the free-recall test administered after the scanning session showed no age differences indicating similar item memory in the young and old. Among the old adults, those who demonstrated proficient associative memory inside the scanner performed better on the free recall test. Young adults who demonstrated an earlier inflection point (i.e. an earlier transition from presumably less consolidated to more consolidated learning) during in-scanner performance, scored higher on the free recall test.

In addition to the biological age effects, it is important to consider certain aspects of the study design that may underlie the observed age differences. This study differed from the Stanley

et al study, in that, the resting condition that would have allowed memory rehearsal was replaced by a backward-counting task. This task was included to intentionally suppress the articulatory loop and block memory rehearsal, specifically the individual variability that comes with it. However, interference in memory rehearsal that takes place during the rest period may result in disruption of memory consolidation (Ravishankar et al., 2019). An age-related difficulty in retaining the object-location associations in the absence of rehearsal may have contributed to the older adults' weaker performance noted here (Gick, Craik, & Morris, 1988). It has been shown using the older version of the object-location task (Diwadkar et al., 2008), that during the rest period the functional connectivity between regions involved in associative learning gradually changes as proficiency on the task increases (Ravishankar et al., 2019). Although lack of an opportunity to rehearse can plausibly underlie age differences in associative memory, one study has demonstrated absence of age differences in the articulatory loop processing (using digit-span and word-span tasks) (Fisk & Warr, 1996) that is required for rehearsal. If this holds true, it is possible that the age differences in associative memory seen in the current study are true differences therein.

Another factor that may have affected performance on the task was time to recall. It is possible that the time (2.67 seconds) provided for encoding as well as recalling an object in the cued location was insufficient for the old adults and might have taxed their processing capacities, thus, penalizing them on memory performance. Studies on associative learning have demonstrated that older adults' poorer performance is related to inefficient memory encoding, which in turn may be explained by deficiencies in processing speed. In fact, about 50 to almost 100% of age-related variance in associative learning is shared with processing speed (Salthouse, 1994, 1996). Slower processing speed results in weaker encoding of an association, the

representation of which is labile and may be susceptible to interference by processing of the immediate next association. A stable representation allows more information to be retained, whilst new is being acquired. Thus, even though 12 rounds of encoding and retrieval were presented to each participant to allow strengthening of the associations, weak representations of the associations may have resulted in delayed strengthening thereof, and hence a later inflection point in the elderly. The possibility that processing speed may have been a factor was also surmised from the feedback on task-speed received from the participants after the scanning session. For some participants, performance on the exploratory free-recall paper-pencil test given post-scan was better than in-scanner performance. Since this test did not impose any time limit it can be assumed that task-speed may have contributed to weaker in-scanner performance for some individuals. However, on the other hand, it cannot be denied that 12 trials, instead of a single presentation of the object-location associations inside the scanner may have resulted in better free recall performance.

5.1.2 Evidence of age differences in glutamate modulation during associative memory performance, despite none in steady-state control-level glutamate

In the current study, no age differences were observed in control levels of hippocampal glutamate. Previous studies have documented age differences in glutamate levels, albeit in different ROIs (motor cortex, basal ganglia) (Hädel et al., 2013; Kaiser et al., 2005; McEntee & Crook, 1993; Sailasuta, Ernst, & Chang, 2008). In those studies, age effects were noted in NAA levels as well, with a positive relation between glutamate and NAA. NAA is a putative neuronal marker and thus, lower glutamate and NAA were attributed to age-related neuronal loss. However, there is no wide-spread neuronal loss in normal aging (Morrison & Hof, 1997; Yankner et al., 2008). Accordingly, along with a lack of age differences in glutamate, the current study did not observe differences in levels of NAA either. It is also important to remember that

the exclusion criteria imposed in the current study (see Chapter 3, participants section) are more stringent than most other groups use. This reflects the selection of a very healthy group of old adults, and so a lack of age differences in control levels of glutamate can be expected. Hemispheric differences were noted only in the old adults, where glutamate levels were higher in the left compared to the right hippocampus.

During the associative memory task, significant age differences in hippocampal glutamate modulation emerged and were specific to the encoding stage. During encoding, the young adults evinced higher and earlier glutamate modulation, levels of which returned to initial values with a non-significant rise towards the end. The initial increase in glutamate during retrieval in this group, stabilized later. Glutamate modulation during encoding and retrieval was non-significant to almost absent in the elderly, as confirmed by a lack of differences in glutamate levels between the block triads within each memory stage. The initial ramp-up of glutamate in the young suggests that there is rapid deployment of a glutamate-driven process that dissipates once a stable performance level (probably due to better and earlier memory consolidation) is reached. This can be explained by the following two scenarios.

5.1.2.1 Reduced neuro-metabolism and neurotransmission in the elderly

The demands of encoding might have driven an increase in hippocampal excitatory neural activity that was indicated by glutamate elevation. Task-induced surges in glutamate possibly reflect increases in glutamate synthesis and glutamatergic neurotransmission as well as glucose utilization and oxidative metabolism in the regions responsive to the specific task-related stimulation. Owing to the large voxel that contains intra- and extracellular space, the ^{1}H fMRS signal cannot distinguish between the compartment (intracellular versus extracellular) and the cell type (glia versus neurons) that glutamate is being measured from. In addition, glutamate signal arising from neurotransmission and metabolic processes cannot be separated. Hence, the

task-related increase in glutamate captured by the ^{1}H fMRS signal indicates higher *net* formation of glutamate reflecting increased excitatory neurotransmission and oxidative metabolism to meet the energy demand of higher neuronal activity. This has been a consensus among extant ^{1}H fMRS literature, since, a tight coupling has been demonstrated between the glutamate neurotransmitter cycling and the rate of glucose oxidation (De Graaf, Mason, Patel, Rothman, & Behar, 2004; Rothman et al., 2011; Sibson et al., 1998; Sonnay, Duarte, Just, & Gruetter, 2016). Therefore, the task-related changes in glutamate, as detected by ^{1}H fMRS, probably reflect increased metabolism as well as excitatory neurotransmission in the young in response to associative encoding. This indicates the attainment of a new metabolic steady state reflecting the neural response leading to shifts in the local E/I balance. On the other hand, an absence of apparent glutamate modulation in the elderly may signal age-associated decrease in metabolism, neurotransmission, or a combination of both.

A recently published study (Crofts, Trotman-Lucas, Janus, Kelly, & Gibson, 2020) demonstrated significant reduction in glutamate modulation during sensory forepaw stimulation in aged rodents. The authors hypothesized that age-related impairment in the glutamate-glutamine cycle in these animals might have affected further glutamate release, thus leading to a net decrease in glutamate levels. About a 30% age-associated reduction in the rate of the neuronal TCA cycle as well as the glutamate-glutamine cycle have been documented (Boumezbeur et al., 2010). Age-related glucose hypometabolism may also play a role here. Under non-fasting conditions, the brain depends nearly entirely on glucose as its main substrate for energy production. The mitochondrial metabolism of glucose via the TCA cycle is the primary source of this energy (ATP). Mitochondrial dysfunction that occurs with aging (Raz & Daugherty, 2018) can underlie impairment in glucose metabolism and disrupt energy supply in

the brain. Importantly, levels and rates of cerebral glucose metabolism in the hippocampus have been shown to predict gradual decline from normal cognition to AD (Lin & Rothman, 2014; Mosconi, 2005).

5.1.2.2 The effects of age on the constituents of the synapse

There is a constellation of molecular mechanisms transpiring at the synapse that drives shifts in E/I balance in response to neural stimulation. It is possible that an age-related impairment in any of these mechanisms (elucidated below) could lead to a dysfunction in the ability to modulate the E/I equilibrium, thus affecting functioning.

Age-related reduction in the density and binding efficiency of the glutamatergic NMDA receptors (Magnusson et al., 2010), glutamate transporters, or even lower depolarization-induced release of glutamate during LTP (Lynch, 2004) can affect glutamate modulation individually or in concert. Decline in the number of NMDA receptors in the hippocampus and the cortex has been documented in several species and seems to be the most robust effect of age at the synapse. Spatial memory deficits in aging rodents have been associated with impaired NMDA receptor function as well (Menard et al., 2015). Western blot analyses of synaptic excitatory and inhibitory proteins in aged monkeys has shown a reduction in NMDA as well as GABA(a) receptor subunits suggesting an age-related effect on both components of the E/I machinery (Williams, Pinto, Irwin, Jones, & Murphy, 2009). Imbalances in the receptors and decreased post-synaptic density in prefrontal cortices of aged rodents (Majdi, Ribeiro-da-Silva, & Cuello, 2009), and reduced excitation and increased inhibition in prefrontal cortices of aged monkeys (Luebke, Chang, Moore, & Rosene, 2004) have also been documented. Like in the prefrontal cortex, similar effects of aging are possible at the hippocampal synapses as well. Reduced levels of stimulated glutamate release and of vGLUT proteins have been documented in AD-type and aged wild-type rodents (Minkeviciene et al., 2008). Diminished *in vivo* glutamate release in aged

rats (Stephens, Quintero, Pomerleau, Huettl, & Gerhardt, 2011), as well as from hippocampal slice preparations of aged rats (review by (Segovia, Porras, Del Arco, & Mora, 2001)) support the possibility of age-effects on vGLUT function that may affect vesicular glutamate packaging and subsequent glutamate release.

As suggested in Figure 15, the synapse affords several target mechanisms that underlie the observed age-related absence of glutamate modulation as measured by ^{1}H fMRS in the current study. These mechanisms include, but are not limited to, age-related loss of the entire synapse, impaired NMDA receptor density and kinetics, reduced levels of vGLUT, weakened release of pre-synaptic glutamate, and mitochondrial dysfunction as reflected by impaired TCA cycle (Yankner et al., 2008).

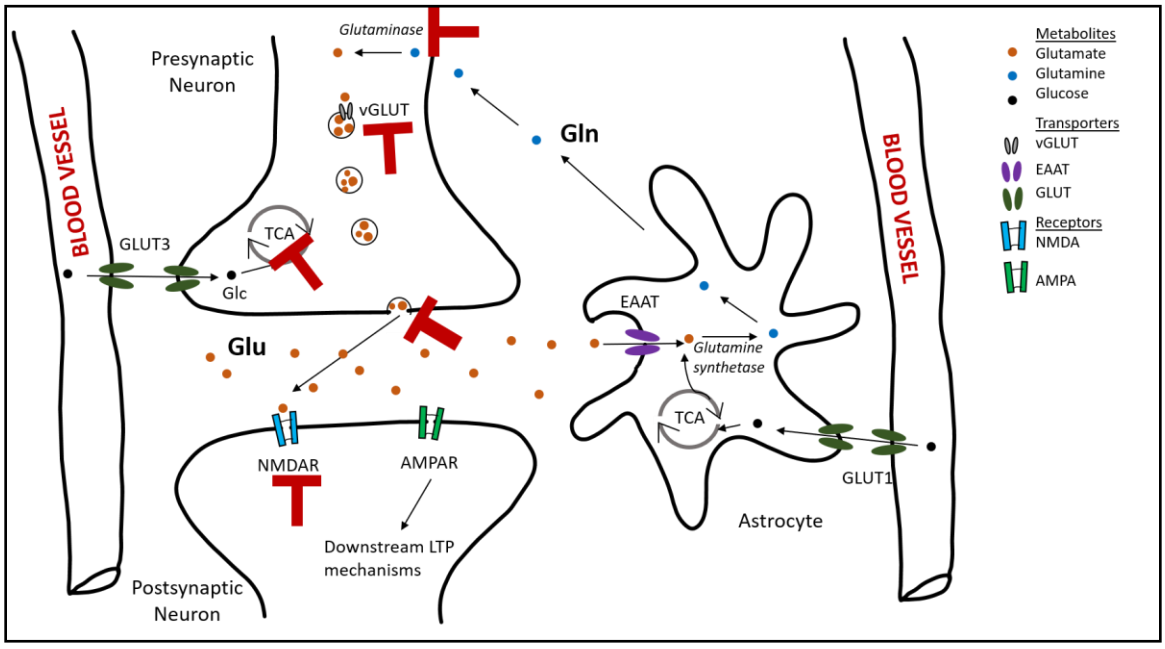

Figure 15. Effects of age on the glutamate-glutamine cycle. Adapted from Figure 1 of this dissertation, this simplified cartoon illustrates the hotspots (marked by bold red 'T') at the synapse that are some of the targets of aging and can individually or in concert impair the glutamate-glutamine cycle leading to weaker glutamate modulation in the elderly.

Indeed, it can be appreciated that the synapse is an inherently complex environment affording several targets for the effects of age to manifest themselves on, and possibly contribute to the nature of the glutamate signal as measured by ^{1}H fMRS.

In the current study, although glutamine levels could not be reliably measured (owing to its low SNR and high CRLB values), an exploratory assessment indicated that in the elderly, glutamine evinced a pattern complementary to glutamate specifically during encoding (supplementary figure S 2). Similar age-related decrease in glutamate but increase in glutamine – although in different ROIs, was also noted by Kaiser *et al* (Kaiser et al., 2005). Glutamine is a precursor to glutamate. A possible increase in glutamine at the expense of glutamate modulation in the elderly might suggest age-related dysfunction of the glutamate-glutamine cycle (Boumezbeur et al., 2010). Increases in glutamine could also be due to reduced glutaminase activity (reduced breakdown of glutamine), or due to NMDA receptor hypofunction that has been shown to potentiate glutamine synthetase activity (increased formation of glutamine) (Jelen, King, Mullins, & Stone, 2018).

5.1.3 Glutamate modulation and associative memory performance

The present study provides the first evidence of age differences in hippocampal glutamate modulation specifically during associative encoding (Figure 13). Notably, the timing of glutamate modulation, indicated by the block triad ('block-max') at which glutamate levels were the highest during *encoding* ('Glu-max'), may be related to older adults' associative memory performance. Older adults who demonstrated a delayed rise in glutamate levels demonstrated a trend to suffer a later inflection point and a slower learning rate with no effect on their asymptote. This may indicate that early elevation in glutamate in response to memory encoding may play a more important role in enabling faster acquisition of memories rather than affecting the final memory capacity (i.e. the asymptote). Early glutamate increase plausibly reflects early

hippocampal engagement during memory encoding, since initially in the process of learning the hippocampus is assumed to be rapidly engaged in acquiring new associations. Interestingly, a coincidence was noted between possible age differences in the inflection point around the second block triad (combination of blocks 4, 5, and 6) (see Table 3) and those in glutamate modulation also around the same time point (see Figure 13). This further points to the possibility that earlier and higher glutamate modulation in the young may underlie better associative memory function. Owing to the low sample size and high variability in the learning curve parameters in the group of old adults, the data on the effect of block-max demonstrate trend-level effects.

As mentioned in Chapter 1, LTP is the cellular mechanism of information storage and memory encoding. Two steps in the process of LTP are crucial – induction and maintenance. Hippocampal LTP induction depends on glutamate-mediated activation of post-synaptic NMDA receptors. It has been speculated that maintenance of LTP might be supported by the persistent enhancement of glutamate release (Richter-Levin, Canevari, & Bliss, 1995). Remember that this persistent increase in glutamate release is assumed to be accompanied by shifts in neuronal circuitry to maintain the E/I balance, as well as efficient extra-synaptic glutamate clearance to prevent excitotoxicity. Assuming this possibility, the early increase in encoding-related glutamate in the young participants, followed by a return to and stabilization around initial levels, may reflect LTP maintenance subserving memory consolidation and better associative memory performance. Lack of glutamate increase in the elderly indicates a possible dysfunction in the LTP induction as well as maintenance mechanisms.

A critical feature of cognitive biomarker studies is indeed the elucidation of the relationship between the biomarker and cognitive function. Previous studies that have reported associations between brain glutamate levels and cognitive performance, have done so by

correlating out-of-scanner performance with static levels of glutamate measured in specific ROIs using ^{1}H MRS (Nikolova et al., 2017; Thielen et al., 2018). However, such correlations fail to unveil the neurotransmitter dynamics during cognitive functioning that may be central for comprehending the finer mechanisms of memory dysfunction. In contrast to those reports, the current study did not detect any effect of control-level hippocampal glutamate on the out-of-scanner free recall test for either age group, and nor was control-level hippocampal glutamate related to any of the in-scanner learning curve parameters.

The advent of functional ^{1}H MRS (^{1}H fMRS) has made it possible to track changes in neurotransmitters in real time during neuronal stimulation. Indeed, this technique has been successfully applied in younger adults and patients with schizophrenia to investigate glutamate dynamics in the dorsolateral prefrontal cortex during working memory performance (Woodcock et al., 2018), and in the hippocampus during object-location association memory formation (J.A. Stanley et al., 2017). The latter study demonstrated the existence of unique temporal dynamics of glutamate during encoding in fast and slow young learners and indicated that the timing of glutamate modulation during encoding may matter for the acquisition of object-location associations. Brain-behavior relationships can be complicated to model as they operate on different scales. Statistically elucidating such relationships becomes an intriguing challenge since a cognitive behavioral outcome mostly follows an established model, whereas the behavior of the biomarker is a biological and molecular process possibly driven by feedback and thresholds. Increase in neuronal activity during learning results in increased glutamate synthesis and cycling that is manifested as an increased glutamate signal in ^{1}H fMRS. Thus, a linear relation between glutamate levels and memory score seems like a possibility – but up to a certain threshold. Although an increase in glutamate following neuronal stimulation is an optimum response, a

persistent increase may signal inefficiency of the neuronal ensemble. Instead, feedback from the glutamatergic system and well as an adjustment to the E/I equilibrium makes sense, where, as learning approaches an asymptote, glutamate levels stop rising and instead reduce to initial levels. The attainment of asymptotic performance during learning and memory mostly indicates successful memory consolidation without further need to be supported by increases in glutamate.

The current study was based on the hypothesis that age differences in glutamate modulation would be specific to associative encoding. Although extant literature has emphasized deficits in binding during encoding as the underlying factor in associative memory impairment, deficits related to the retrieval process are possible as well. The approach applied in the current study, in fact, allows investigation of individual task stages (encoding or retrieval) where functional impairments indeed may lie.

This study did not hypothesize hemispheric effects on hippocampal glutamate levels during associative memory performance owing to the nature of the task that involved vocalization of the object-location pairs during encoding and retrieval. The task thus probed spatial, visual, as well as verbal memory, characterized by differential involvement of the left and right hippocampi. Therefore, ^{1}H MRS voxels were placed in unilateral hippocampi with side randomized across participants. However, higher levels of glutamate in the left hippocampus were observed throughout the encoding and retrieval stages in both age groups. It is possible that higher left-lateralized hippocampal activation occurred due to the verbal nature of encoding and retrieval in the current associative memory task, characterized by a vocal response. A few studies have demonstrated stimulus-specific hemispheric specialization of the hippocampus, with the right and left hippocampi being involved in spatial (or non-verbal) and verbal memory encoding, respectively (Ezzati et al., 2016; Kelley et al., 1998).

5.2 Study Limitations

The findings reported here should be interpreted in the light of the limitations in study design and sampling. First, it is a cross-sectional study investigating two intentionally chosen healthy and extreme age groups (young: 21 to 30 years and old: 60 to 70 years), and like any cross-sectional study it cannot speak to true age-related change and individual differences therein (Raz & Lindenberger, 2011). Although these data demonstrate interesting trends, the small and unbalanced sample size precludes definite results. It is thus, necessary to recruit additional older adults and continue with data collection, to be able to confirm the observed trends.

Second, with respect to study design, all MRI scans were collected between 9:00 am and noon to keep time of scanning constant. However, this constraint might have failed to capture some participants' performance during their best time of the day (Maylor & Badham, 2018). In addition, no information was collected about participants' sleep quality the night before as well as caffeine-intake status – variables which may affect attention and hence, memory performance, thus adding to individual variability. The objects and cues during memory encoding and retrieval were presented for a very short time (2.67 sec). Thus, in the absence of rehearsal, task-presentation speed may have taxed the processing speed capacities of some participants, affecting their memory performance. Older adults' poorer performance on the task may in fact be related to slower processing speed (Park et al., 1996; Salthouse, 1994, 1996) rather than weaker memory function. Age differences in processing speed were not measured and thus, its effect on associative memory performance could not be assessed here. Other cognitive domains that were not measured but can affect associative memory performance are attention, working memory capacity, and inhibitory processing (Spencer & Raz, 1995).

Third, with respect to the technique, the large voxel used in this study may induce possible partial volume effects that are common in single-voxel MRS studies. However, the

influence of partial volume effects on the findings were minimized by ensuring individualized placement of the hippocampal voxel and including only within-subject analyses across conditions during the assessment of temporal modulation of glutamate. Being a single-voxel study, the technique also precluded measuring and comparing metabolites from a control area of the brain not involved in associative learning and memory function. In addition, associative memory function depends on the fronto-hippocampal network (Simons & Spiers, 2003) with support from other cortical regions; and thus, poor performance on associative tasks may be related to the impaired functioning of these regions as well. Since single voxel ^{1}H fMRS precludes the investigation of other ROIs, future multivoxel MRS studies will help augment our understanding of the entire system involved in successful encoding and retrieval.

Finally, owing to a lower field strength (3T) this study lacked the ability to reliably quantify other relevant molecules such as GABA, glutamine, or lactate. It is important that future studies quantify these metabolites, along with glutamate, since neurotransmission and neurometabolism function via an interplay between these metabolites.

5.3 Future Directions

This dissertation is only the first step towards probing and understanding age differences in task-related glutamatergic modulation that might serve as a plausible biomarker of cognitive deficit. The findings in this study open up several exciting avenues for future investigations.

First, the observed age differences in glutamate modulation during associative memory function should be confirmed with tasks using different stimuli such as word-pairs and faces-names that have been described in extant literature on age-related associative deficits (Bender et al., 2017; Naveh-Benjamin, 2000). The results of this cross-sectional investigation should be further leveraged in developing a long-term follow-up study to examine the utility of variations in task-related glutamate modulation as an early biomarker of cognitive decline, and possibly be

later extended to include participants with mild cognitive impairment and AD. The etiology and pathophysiology of AD being complex, non-invasive investigations of age effects on neurotransmission can contribute towards the identification of early diagnostic biomarkers of AD. This is a crucial aspect of AD research especially for implementing timely interventions at the preclinical stages of the disease.

Associative learning is subserved by the fronto-hippocampal circuitry and the different stages of memory function can activate these regions differentially. During encoding and retrieval, there is an interplay between other cognitive domains such as attention and inhibition that call upon other brain regions. Future studies should involve a multivoxel, multi-ROI investigation of the temporal dynamics of glutamate during encoding and retrieval.

The current investigation informs on changes in net glutamate levels i.e. a combination of intracellular, extracellular, neuronal, and glial stores of glutamate. At the molecular level the observed age differences can be explained by a myriad of possible underlying mechanisms, such as age-related reduction in the number and binding efficiency of NMDA receptors (Magnusson et al., 2010) and transporters (Minkeviciene et al., 2008), and a reduction vesicular release of glutamate (Lynch, 2004) (as also outlined in Figure 15). Future analyses can, thus, include genomics and proteomics to assess the different players that glutamate levels depend on. Testing participants for polymorphisms of the genes coding for NMDA receptors and glutamate transporters can also shed light on finer details of glutamatergic function.

5.3.1 Possible therapeutic targets in the glutamatergic system

An understanding of glutamatergic dysfunction underlying cognitive deficits may pave way to design therapeutic and interventional approaches. Considering the numerous players involved at the synapse and in the glutamatergic system, interventional research has been directed towards targeting any one or a combination of them. In addition to direct genetic

manipulation, pharmacological drugs targeting the glutamatergic systems are also being tested and developed. For instance, NMDA receptor function can be elevated by application of its exogenous agonists. Although L-glutamate, an agonist, has not been suggested because of the risk of excitotoxicity, D-cycloserine, a partial agonist at the glycine binding site of the NMDA receptor has indeed shown to elevate the receptor's function only till its maximum physiological capacity, thus avoiding neurotoxicity (Jones, Wesnes, & Kirby, 1991). Partial modulation of the NMDA receptor by D-cycloserine has shown improved spatial memory in aged rats (Dauvermann, Lee, & Dawson, 2017). Although partial agonists of the NMDA receptor have demonstrated positive effects in humans (Müller, Scheuer, et al., 1994), conclusive evidence of the benefits of such agents in human cognition is still lacking and more research in this direction is necessary.

5.4 Conclusions

This study demonstrates, for first time, existence of age differences in hippocampal glutamate modulation during associative memory function and their specificity to associative encoding. This phenomenon may underlie the observed age differences in the performance of the associative memory task. The modulation of hippocampal glutamate in response to memory function can be construed as the result of increased metabolic demand and excitatory neurotransmission required by the processes of encoding, accompanied by a shift in the brain's E/I balance to serve the task demands. The observed absence of glutamate modulation in the elderly is endorsed by their deficits in associative encoding as well as by a possible age-related reduction in brain energy regulation and neurotransmission, as well as possible age effects on maintaining the E/I equilibrium. Hippocampal atrophy, a part of normal as well as pathological aging, is not a reliable biomarker of the earlier stages of impending dementia. Thus,

identification of a functional biomarker of cognitive performance is necessary, and investigation of age differences in task-related glutamate modulation may contribute towards it.

Supplementary figures

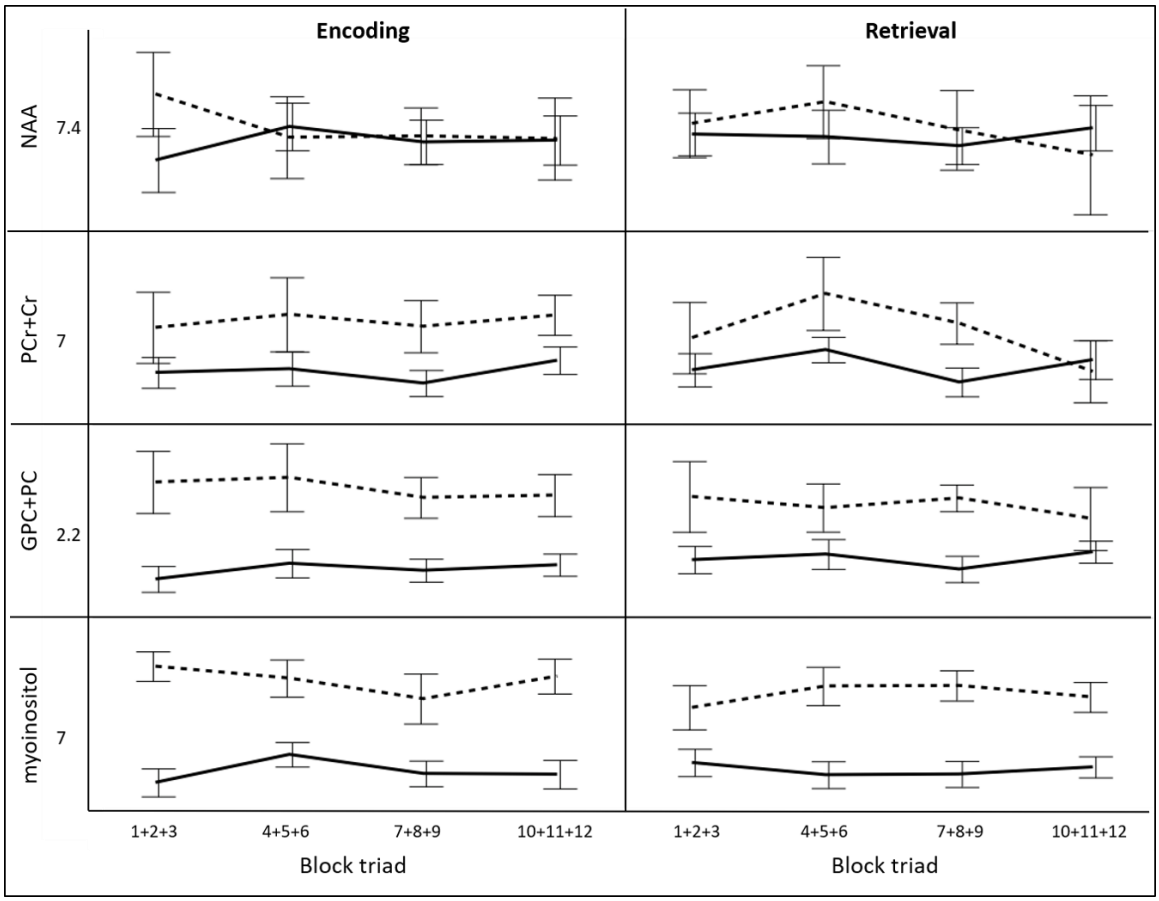

S 1. Neurochemical Specificity. Levels of other main metabolites detected by ^{1}H MRS. NAA, PCr+Cr, GPC+PC, and myoinositol did not show temporal modulation across encoding and retrieval in both age groups (dashed line: old, solid line: young). The numbers on the Y axis are overall mean levels of these metabolites after collapsing across age groups and the two task stages. Error bars indicate ± 1 standard error.

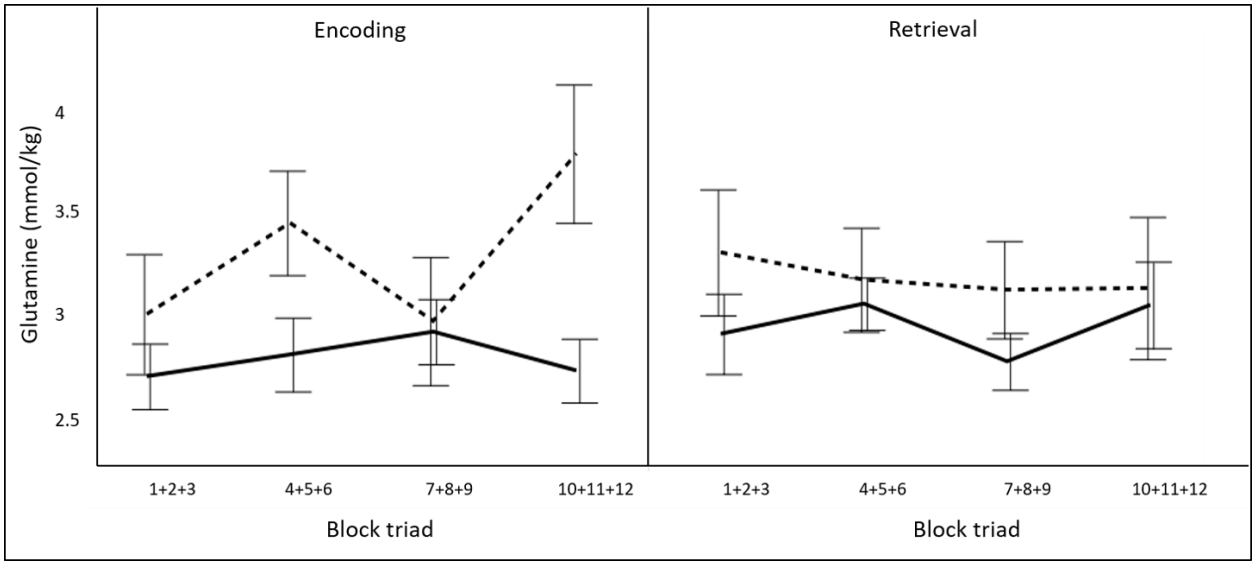

S 2. Age differences in glutamine levels across encoding and retrieval (dashed line: old, solid line: young). Error bars indicate ± 1 standard error.

REFERENCES

Antuono, P. G., Jones, J. L., Wang, Y., & Li, S. J. (2001). Decreased glutamate + glutamine in Alzheimer's disease detected in vivo with (1)H-MRS at 0.5 T. *Neurology, 56*(6), 737-742. doi:10.1212/wnl.56.6.737

Baddeley, A. D., & Hitch, G. J. (1974). Working memory. . In G. A. Bower (Ed.), *The psychology of learning and motivation: Advances in research and theory* (pp. 47-89): New York: Academic Press.

Bednařík, P., Tkáč, I., Giove, F., DiNuzzo, M., Deelchand, D. K., Emir, U. E., . . . Mangia, S. (2015). Neurochemical and BOLD responses during neuronal activation measured in the human visual cortex at 7 Tesla. *J Cereb Blood Flow Metab, 35*(4), 601-610. doi:10.1038/jcbfm.2014.233

Bender, A. R., Naveh-Benjamin, M., Amann, K., & Raz, N. (2017). The role of stimulus complexity and salience in memory for face-name associations in healthy adults: Friend or foe? *Psychol Aging, 32*(5), 489-505. doi:10.1037/pag0000185

Birch, C. P. D. (1999). A New Generalized Logistic Sigmoid Growth Equation Compared with the Richards Growth Equation. *Annals of Botany, 83*, 11.

Bliss, T. V., & Collingridge, G. L. (1993). A synaptic model of memory: long-term potentiation in the hippocampus. *Nature, 361*(6407), 31-39. doi:10.1038/361031a0

Boumezbeur, F., Mason, G. F., De Graaf, R. A., Behar, K. L., Cline, G. W., Shulman, G. I., . . . Petersen, K. F. (2010). Altered brain mitochondrial metabolism in healthy aging as assessed by in vivo magnetic resonance spectroscopy. *J Cereb Blood Flow Metab, 30*(1), 211-221. doi:10.1038/jcbfm.2009.197

Braak, H., & Braak, E. (1995). Staging of Alzheimer's disease-related neurofibrillary changes. *Neurobiol Aging, 16*(3), 271-278; discussion 278-284.

Burgess, N., Maguire, E. A., & O'Keefe, J. (2002). The human hippocampus and spatial and episodic memory. *Neuron, 35*(4), 625-641. doi:10.1016/s0896-6273(02)00830-9

Butterfield, D. A., & Pocernich, C. B. (2003). The glutamatergic system and Alzheimer's disease: therapeutic implications. *CNS Drugs, 17*(9), 641-652.

Cavassila, S., Deval, S., Huegen, C., van Ormondt, D., & Graveron-Demilly, D. (2001). Cramer-Rao bounds: an evaluation tool for quantitation. *NMR Biomed, 14*(4), 278-283. doi:10.1002/nbm.701

Chen, C., & Tonegawa, S. (1997). Molecular genetic analysis of synaptic plasticity, activity-dependent neural development, learning, and memory in the mammalian brain. *Annu Rev Neurosci, 20*, 157-184. doi:10.1146/annurev.neuro.20.1.157

Clements, J. D., Lester, R. A., Tong, G., Jahr, C. E., & Westbrook, G. L. (1992). The time course of glutamate in the synaptic cleft. *Science, 258*(5087), 1498-1501. doi:10.1126/science.1359647

Craik, F. I. (1986). *A functional account of age differences in memory*: Amsterdam: Elsevier Science.

Crofts, A., Trotman-Lucas, M., Janus, J., Kelly, M., & Gibson, C. L. (2020). A longitudinal, multi-parametric functional MRI study to determine age-related changes in the rodent brain. *Neuroimage, 218*, 116976. doi:10.1016/j.neuroimage.2020.116976

D'Esposito, M., Deouell, L. Y., & Gazzaley, A. (2003). Alterations in the BOLD fMRI signal with ageing and disease: a challenge for neuroimaging. *Nat Rev Neurosci, 4*(11), 863-872. doi:10.1038/nrn1246

D'Esposito, M., Zarahn, E., Aguirre, G. K., & Rypma, B. (1999). The effect of normal aging on the coupling of neural activity to the bold hemodynamic response. *Neuroimage, 10*(1), 6-14. doi:10.1006/nimg.1999.0444

Dauvermann, M. R., Lee, G., & Dawson, N. (2017). Glutamatergic regulation of cognition and functional brain connectivity: insights from pharmacological, genetic and translational schizophrenia research. *Br J Pharmacol, 174*(19), 3136-3160. doi:10.1111/bph.13919

Davachi, L. (2006). Item, context and relational episodic encoding in humans. *Curr Opin Neurobiol, 16*(6), 693-700. doi:10.1016/j.conb.2006.10.012

Davachi, L., & Wagner, A. D. (2002). Hippocampal contributions to episodic encoding: insights from relational and item-based learning. *J Neurophysiol, 88*(2), 982-990. doi:10.1152/jn.2002.88.2.982

De Graaf, R. A. (2007). *In vivo NMR spectroscopy : principles and techniques.* Chichester, West Sussex, England;

Hoboken, NJ: John Wiley & Sons.

De Graaf, R. A. (2013). *In Vivo NMR Spectroscopy: Principles and Techniques.* West Sussex: John Wiley & Sons.

De Graaf, R. A., Mason, G. F., Patel, A. B., Rothman, D. L., & Behar, K. L. (2004). Regional glucose metabolism and glutamatergic neurotransmission in rat brain in vivo. *Proc Natl Acad Sci U S A, 101*(34), 12700-12705. doi:10.1073/pnas.0405065101

Dennis, N. A., Hayes, S. M., Prince, S. E., Madden, D. J., Huettel, S. A., & Cabeza, R. (2008). Effects of aging on the neural correlates of successful item and source memory encoding. *J Exp Psychol Learn Mem Cogn, 34*(4), 791-808. doi:10.1037/0278-7393.34.4.791

Diana, G., Scotti de Carolis, A., Frank, C., Domenici, M. R., & Sagratella, S. (1994). Selective reduction of hippocampal dentate frequency potentiation in aged rats with impaired place learning. *Brain Res Bull, 35*(2), 107-111. doi:10.1016/0361-9230(94)90089-2

Diana, R. A., Yonelinas, A. P., & Ranganath, C. (2007). Imaging recollection and familiarity in the medial temporal lobe: a three-component model. *Trends Cogn Sci, 11*(9), 379-386. doi:10.1016/j.tics.2007.08.001

Diwadkar, V. A., Flaugher, B., Jones, T., Zalanyi, L., Ujfalussy, B., Keshavan, M. S., & Erdi, P. (2008). Impaired associative learning in schizophrenia: behavioral and computational studies. *Cogn Neurodyn, 2*(3), 207-219. doi:10.1007/s11571-008-9054-0

Eichenbaum, H. (2001). The long and winding road to memory consolidation. *Nat Neurosci, 4*(11), 1057-1058. doi:10.1038/nn1101-1057

Eichenbaum, H., Yonelinas, A. P., & Ranganath, C. (2007). The medial temporal lobe and recognition memory. *Annu Rev Neurosci, 30*, 123-152. doi:10.1146/annurev.neuro.30.051606.094328

Erecinska, M., & Silver, I. A. (1990). Metabolism and role of glutamate in mammalian brain. *Prog Neurobiol, 35*(4), 245-296.

Ernst, T., Kreis, R., & Ross, B. D. (1993). Absolute quantification of water and metabolites in the human brain. I. Compartments and water. *J Magn Reson, 102*, 8.

Ezzati, A., Katz, M. J., Zammit, A. R., Lipton, M. L., Zimmerman, M. E., Sliwinski, M. J., & Lipton, R. B. (2016). Differential association of left and right hippocampal volumes with verbal episodic and spatial memory in older adults. *Neuropsychologia, 93*(Pt B), 380-385. doi:10.1016/j.neuropsychologia.2016.08.016

Febo, M., & Foster, T. C. (2016). Preclinical Magnetic Resonance Imaging and Spectroscopy Studies of Memory, Aging, and Cognitive Decline. *Front Aging Neurosci, 8*, 158. doi:10.3389/fnagi.2016.00158

Fisk, J. E., & Warr, P. (1996). Age and working memory: the role of perceptual speed, the central executive, and the phonological loop. *Psychol Aging, 11*(2), 316-323. doi:10.1037//0882-7974.11.2.316

Folstein, M. F., Folstein, S. E., & McHugh, P. R. (1975). "Mini-mental state". A practical method for grading the cognitive state of patients for the clinician. *J Psychiatr Res, 12*(3), 10.

Friedman, D., Nessler, D., & Johnson, R., Jr. (2007). Memory encoding and retrieval in the aging brain. *Clin EEG Neurosci, 38*(1), 2-7.

Gasparovic, C. (2006). Use of tissue water as a concentration reference for proton spectroscopic imaging. *Magn Reson Med, 55*, 1219-1226.

Gick, M. L., Craik, F. I., & Morris, R. G. (1988). Task complexity and age differences in working memory. *Mem Cognit, 16*(4), 353-361. doi:10.3758/bf03197046

Gompertz, B. (1825). On the nature of the function expressive of the law of human mortality, and on a new mode of determining the value of life contingencies. *Philosophical Transactions of the Royal Society of London, 115*, 513-583.

Govindaraju, V., Young, K., & Maudsley, A. A. (2000). Proton NMR chemical shifts and coupling constants for brain metabolites. *NMR Biomed, 13*(3), 129-153. doi:10.1002/1099-1492(200005)13:3<129::aid-nbm619>3.0.co;2-v

Gruetter, R., & Tkác, I. (2000). Field Mapping Without Reference Scan Using Asymmetric Echo-Planar Techniques. *Magn Reson Med, 43*, 5.

Haacke, E. M., Cheng, N. Y., House, M. J., Liu, Q., Neelavalli, J., Ogg, R. J., . . . Obenaus, A. (2005). Imaging iron stores in the brain using magnetic resonance imaging. *Magn Reson Imaging, 23*(1), 1-25. doi:10.1016/j.mri.2004.10.001

Hädel, S., Wirth, C., Rapp, M., Gallinat, J., & Schubert, F. (2013). Effects of age and sex on the concentrations of glutamate and glutamine in the human brain. *J Magn Reson Imaging, 38*(6), 1480-1487. doi:10.1002/jmri.24123

Haga, K. K., Khor, Y. P., Farrall, A., & Wardlaw, J. M. (2009). A systematic review of brain metabolite changes, measured with 1H magnetic resonance spectroscopy, in healthy aging. *Neurobiol Aging, 30*(3), 353-363. doi:10.1016/j.neurobiolaging.2007.07.005

Harris, J. L., Yeh, H. W., Swerdlow, R. H., Choi, I. Y., Lee, P., & Brooks, W. M. (2014). High-field proton magnetic resonance spectroscopy reveals metabolic effects of normal brain aging. *Neurobiol Aging, 35*(7), 1686-1694. doi:10.1016/j.neurobiolaging.2014.01.018

Hebb, D. O. (1949). The organization of behavior. *Wiley, New York*.

Hyder, F., Patel, A. B., Gjedde, A., Rothman, D. L., Behar, K. L., & Shulman, R. G. (2006). Neuronal-glial glucose oxidation and glutamatergic-GABAergic function. *J Cereb Blood Flow Metab, 26*(7), 865-877. doi:10.1038/sj.jcbfm.9600263

Jack, C. R., Jr., Twomey, C. K., Zinsmeister, A. R., Sharbrough, F. W., Petersen, R. C., & Cascino, G. D. (1989). Anterior temporal lobes and hippocampal formations: normative volumetric measurements from MR images in young adults. *Radiology, 172*(2), 549-554. doi:10.1148/radiology.172.2.2748838

Jacob, S. N., Shear, P. K., Norris, M., Smith, M., Osterhage, J., Strakowski, S. M., . . . Eliassen, J. C. (2015). Impact of functional magnetic resonance imaging (fMRI) scanner noise on

affective state and attentional performance. *J Clin Exp Neuropsychol, 37*(6), 563-570. doi:10.1080/13803395.2015.1029440

Jelen, L. A., King, S., Mullins, P. G., & Stone, J. M. (2018). Beyond static measures: A review of functional magnetic resonance spectroscopy and its potential to investigate dynamic glutamatergic abnormalities in schizophrenia. *J Psychopharmacol, 32*(5), 497-508. doi:10.1177/0269881117747579

Jenkinson, M., Beckmann, C. F., Behrens, T. E., Woolrich, M. W., & Smith, S. M. (2012). Fsl. *Neuroimage, 62*(2), 782-790. doi:10.1016/j.neuroimage.2011.09.015

Jones, R. W., Wesnes, K. A., & Kirby, J. (1991). Effects of NMDA modulation in scopolamine dementia. *Ann N Y Acad Sci, 640*, 241-244. doi:10.1111/j.1749-6632.1991.tb00226.x

Kaiser, L. G., Schuff, N., Cashdollar, N., & Weiner, M. W. (2005). Age-related glutamate and glutamine concentration changes in normal human brain: ^{1}H MR spectroscopy study at 4 T. *Neurobiol Aging, 26*(5), 665-672. doi:10.1016/j.neurobiolaging.2004.07.001

Kan, I. P., Giovanello, K. S., Schnyer, D. M., Makris, N., & Verfaellie, M. (2007). Role of the medial temporal lobes in relational memory: neuropsychological evidence from a cued recognition paradigm. *Neuropsychologia, 45*(11), 2589-2597. doi:10.1016/j.neuropsychologia.2007.03.006

Kauer, J. A., Malenka, R. C., & Nicoll, R. A. (1988). NMDA application potentiates synaptic transmission in the hippocampus. *Nature, 334*(6179), 250-252. doi:10.1038/334250a0

Kelley, W. M., Miezin, F. M., McDermott, K. B., Buckner, R. L., Raichle, M. E., Cohen, N. J., . . . Petersen, S. E. (1998). Hemispheric specialization in human dorsal frontal cortex and medial temporal lobe for verbal and nonverbal memory encoding. *Neuron, 20*(5), 927-936. doi:10.1016/s0896-6273(00)80474-2

Klose, U. (1990). In vivo proton spectroscopy in presence of eddy currents. *Magn Reson Med, 14*(1), 26-30. doi:10.1002/mrm.1910140104

Kobald, S. O., Getzmann, S., Beste, C., & Wascher, E. (2016). The impact of simulated MRI scanner background noise on visual attention processes as measured by the EEG. *Sci Rep, 6*, 28371. doi:10.1038/srep28371

Koch, I., Ruge, H., Brass, M., Rubin, O., Meiran, N., & Prinz, W. (2003). Equivalence of cognitive processes in brain imaging and behavioral studies: evidence from task switching. *Neuroimage, 20*(1), 572-577.

Kreis, R. (2016). The trouble with quality filtering based on relative Cramer-Rao lower bounds. *Magn Reson Med, 75*(1), 15-18. doi:10.1002/mrm.25568

Kreis, R., Ernst, T., & Ross, B. D. (1993). Absolute quantification of water and metabolites in the human brain. II. Metabolite concentrations. *J Magn Reson, 102*, 10.

Lavenex, P., & Amaral, D. G. (2000). Hippocampal-neocortical interaction: a hierarchy of associativity. *Hippocampus, 10*(4), 420-430. doi:10.1002/1098-1063(2000)10:4<420::AID-HIPO8>3.0.CO;2-5

Letzkus, J. J., Wolff, S. B., & Luthi, A. (2015). Disinhibition, a Circuit Mechanism for Associative Learning and Memory. *Neuron, 88*(2), 264-276. doi:10.1016/j.neuron.2015.09.024

Lin, A. L., & Rothman, D. L. (2014). What have novel imaging techniques revealed about metabolism in the aging brain? *Future Neurology, 9*(3), 14.

Luebke, J. I., Chang, Y. M., Moore, T. L., & Rosene, D. L. (2004). Normal aging results in decreased synaptic excitation and increased synaptic inhibition of layer 2/3 pyramidal

cells in the monkey prefrontal cortex. *Neuroscience, 125*(1), 277-288. doi:10.1016/j.neuroscience.2004.01.035

Lueken, U., Muehlhan, M., Evens, R., Wittchen, H. U., & Kirschbaum, C. (2012). Within and between session changes in subjective and neuroendocrine stress parameters during magnetic resonance imaging: A controlled scanner training study. *Psychoneuroendocrinology, 37*(8), 1299-1308. doi:10.1016/j.psyneuen.2012.01.003

Lynch, M. A. (2004). Long-term potentiation and memory. *Physiol Rev, 84*(1), 87-136. doi:10.1152/physrev.00014.2003

Lynn, J., Woodcock, E. A., Anand, C., Khatib, D., & Stanley, J. A. (2018). Differences in steady-state glutamate levels and variability between 'non-task-active' conditions: Evidence from (1)H fMRS of the prefrontal cortex. *Neuroimage, 172*, 554-561. doi:10.1016/j.neuroimage.2018.01.069

Magnusson, K. R., Brim, B. L., & Das, S. R. (2010). Selective Vulnerabilities of N-methyl-D-aspartate (NMDA) Receptors During Brain Aging. *Front Aging Neurosci, 2*, 11. doi:10.3389/fnagi.2010.00011

Majdi, M., Ribeiro-da-Silva, A., & Cuello, A. C. (2009). Variations in excitatory and inhibitory postsynaptic protein content in rat cerebral cortex with respect to aging and cognitive status. *Neuroscience, 159*(2), 896-907. doi:10.1016/j.neuroscience.2008.11.034

Makin, S. (2018). The amyloid hypothesis on trial. *Nature, 559*(7715), S4-S7. doi:10.1038/d41586-018-05719-4

Mangia, S., Tkac, I., Gruetter, R., Van de Moortele, P. F., Maraviglia, B., & Ugurbil, K. (2007). Sustained neuronal activation raises oxidative metabolism to a new steady-state level:

evidence from ^{1}H NMR spectroscopy in the human visual cortex. *J Cereb Blood Flow Metab, 27*(5), 1055-1063. doi:10.1038/sj.jcbfm.9600401

Maylor, E. A., & Badham, S. P. (2018). Effects of time of day on age-related associative deficits. *Psychol Aging, 33*(1), 7-16. doi:10.1037/pag0000199

McEntee, W. J., & Crook, T. H. (1993). Glutamate: its role in learning, memory, and the aging brain. *Psychopharmacology (Berl), 111*(4), 391-401.

McGlynn, F. D., Smitherman, T. A., Hammel, J. C., & Lazarte, A. A. (2007). Component fears of claustrophobia associated with mock magnetic resonance imaging. *J Anxiety Disord, 21*(3), 367-380. doi:10.1016/j.janxdis.2006.06.003

Menard, C., Quirion, R., Vigneault, E., Bouchard, S., Ferland, G., El Mestikawy, S., & Gaudreau, P. (2015). Glutamate presynaptic vesicular transporter and postsynaptic receptor levels correlate with spatial memory status in aging rat models. *Neurobiol Aging, 36*(3), 1471-1482. doi:10.1016/j.neurobiolaging.2014.11.013

Mergenthaler, P., Lindauer, U., Dienel, G. A., & Meisel, A. (2013). Sugar for the brain: the role of glucose in physiological and pathological brain function. *Trends Neurosci, 36*(10), 587-597. doi:10.1016/j.tins.2013.07.001

Minkeviciene, R., Ihalainen, J., Malm, T., Matilainen, O., Keksa-Goldsteine, V., Goldsteins, G., . . . Tanila, H. (2008). Age-related decrease in stimulated glutamate release and vesicular glutamate transporters in APP/PS1 transgenic and wild-type mice. *J Neurochem, 105*(3), 584-594. doi:10.1111/j.1471-4159.2007.05147.x

Morris, R. G., Anderson, E., Lynch, G. S., & Baudry, M. (1986). Selective impairment of learning and blockade of long-term potentiation by an N-methyl-D-aspartate receptor antagonist, AP5. *Nature, 319*(6056), 774-776. doi:10.1038/319774a0

Morris, R. G., & Kopelman, M. D. (1986). The memory deficits in Alzheimer-type dementia: a review. *Q J Exp Psychol A, 38*(4), 575-602. doi:10.1080/14640748608401615

Morrison, J. H., & Hof, P. R. (1997). Life and death of neurons in the aging brain. *Science, 278*(5337), 412-419. doi:10.1126/science.278.5337.412

Mosconi, L. (2005). Brain glucose metabolism in the early and specific diagnosis of Alzheimer's disease. FDG-PET studies in MCI and AD. *Eur J Nucl Med Mol Imaging, 32*(4), 486-510. doi:10.1007/s00259-005-1762-7

Müller, W. E., Scheuer, K., & Stoll, S. (1994). Glutamatergic treatment strategies for age-related memory disorders. *Life Sci, 55*(25-26), 2147-2153. doi:10.1016/0024-3205(94)00395-5

Müller, W. E., Stoll, S., Scheuer, K., & Meichelbock, A. (1994). The function of the NMDA-receptor during normal brain aging. *J Neural Transm Suppl, 44*, 145-158. doi:10.1007/978-3-7091-9350-1_11

Mullins, P. G. (2018). Towards a theory of functional magnetic resonance spectroscopy (fMRS): A meta-analysis and discussion of using MRS to measure changes in neurotransmitters in real time. *Scand J Psychol, 59*(1), 91-103. doi:10.1111/sjop.12411

Naveh-Benjamin, M. (2000). Adult age differences in memory performance: tests of an associative deficit hypothesis. *J Exp Psychol Learn Mem Cogn, 26*(5), 1170-1187.

Naveh-Benjamin, M., & Mayr, U. (2018). Age-related differences in associative memory: Empirical evidence and theoretical perspectives. *Psychol Aging, 33*(1), 1-6. doi:10.1037/pag0000235

Nicoll, R. A. (2017). A Brief History of Long-Term Potentiation. *Neuron, 93*(2), 281-290. doi:10.1016/j.neuron.2016.12.015

Nikolova, S., Stark, S. M., & Stark, C. E. L. (2017). 3T hippocampal glutamate-glutamine complex reflects verbal memory decline in aging. *Neurobiol Aging, 54*, 103-111. doi:10.1016/j.neurobiolaging.2017.01.026

Old, S. R., & Naveh-Benjamin, M. (2008). Differential effects of age on item and associative measures of memory: a meta-analysis. *Psychol Aging, 23*(1), 104-118. doi:10.1037/0882-7974.23.1.104

Oldfield, R. C. (1971). The assessment and analysis of handedness: the Edinburgh inventory. *Neuropsychologia, 9*(1), 97-113.

Park, D. C., Smith, A. D., Lautenschlager, G., Earles, J. L., Frieske, D., Zwahr, M., & Gaines, C. L. (1996). Mediators of long-term memory performance across the life span. *Psychol Aging, 11*(4), 621-637. doi:10.1037//0882-7974.11.4.621

Piekema, C., Kessels, R. P., Mars, R. B., Petersson, K. M., & Fernandez, G. (2006). The right hippocampus participates in short-term memory maintenance of object-location associations. *Neuroimage, 33*(1), 374-382. doi:10.1016/j.neuroimage.2006.06.035

Provencher, S. W. (1993). Estimation of metabolite concentrations from localized in vivo proton NMR spectra. *Magn Reson Med, 30*(6), 672-679.

Radloff, L. S. (1977). The CES-D scale: A self-report depression scale for research in the general population. *Appl Psychol Meas, 1*(3), 7.

Rapp, P. R., & Gallagher, M. (1996). Preserved neuron number in the hippocampus of aged rats with spatial learning deficits. *Proc Natl Acad Sci U S A, 93*(18), 9926-9930. doi:10.1073/pnas.93.18.9926

Ravishankar, M., Morris, A., Burgess, A., Khatib, D., Stanley, J. A., & Diwadkar, V. A. (2019). Cortical-hippocampal functional connectivity during covert consolidation sub-serves

associative learning: Evidence for an active "rest" state. *Brain Cogn, 131,* 45-55. doi:10.1016/j.bandc.2017.10.003

Raz, N., & Daugherty, A. M. (2018). Pathways to Brain Aging and Their Modifiers: Free-Radical-Induced Energetic and Neural Decline in Senescence (FRIENDS) Model - A Mini-Review. *Gerontology, 64*(1), 49-57. doi:10.1159/000479508

Raz, N., & Lindenberger, U. (2011). Only time will tell: cross-sectional studies offer no solution to the age-brain-cognition triangle: comment on Salthouse (2011). *Psychol Bull, 137*(5), 790-795. doi:10.1037/a0024503

Raz, N., & Rodrigue, K. M. (2006). Differential aging of the brain: patterns, cognitive correlates and modifiers. *Neurosci Biobehav Rev, 30*(6), 730-748. doi:10.1016/j.neubiorev.2006.07.001

Ribot, T. (1882). *Diseases of memory: An essay in the positive psychology*: D. Appleton.

Richter-Levin, G., Canevari, L., & Bliss, T. V. (1995). Long-term potentiation and glutamate release in the dentate gyrus: links to spatial learning. *Behav Brain Res, 66*(1-2), 37-40. doi:10.1016/0166-4328(94)00121-u

Rolls, E. T., Stringer, S. M., & Trappenberg, T. P. (2002). A unified model of spatial and episodic memory. *Proc Biol Sci, 269*(1496), 1087-1093. doi:10.1098/rspb.2002.2009

Rönnlund, M., Nyberg, L., Backman, L., & Nilsson, L. G. (2005). Stability, growth, and decline in adult life span development of declarative memory: cross-sectional and longitudinal data from a population-based study. *Psychol Aging, 20*(1), 3-18. doi:10.1037/0882-7974.20.1.3

Rosenzweig, E. S., & Barnes, C. A. (2003). Impact of aging on hippocampal function: plasticity, network dynamics, and cognition. *Prog Neurobiol, 69*(3), 143-179. doi:10.1016/s0301-0082(02)00126-0

Rothman, D. L., Behar, K. L., Hyder, F., & Shulman, R. G. (2003). In vivo NMR studies of the glutamate neurotransmitter flux and neuroenergetics: implications for brain function. *Annu Rev Physiol, 65*, 401-427. doi:10.1146/annurev.physiol.65.092101.142131

Rothman, D. L., De Feyter, H. M., De Graaf, R. A., Mason, G. F., & Behar, K. L. (2011). 13C MRS studies of neuroenergetics and neurotransmitter cycling in humans. *NMR Biomed, 24*(8), 943-957. doi:10.1002/nbm.1772

Rothman, D. L., Petroff, O. A., Behar, K. L., & Mattson, R. H. (1993). Localized 1H NMR measurements of gamma-aminobutyric acid in human brain in vivo. *Proc Natl Acad Sci U S A, 90*(12), 5662-5666. doi:10.1073/pnas.90.12.5662

Rupsingh, R., Borrie, M., Smith, M., Wells, J. L., & Bartha, R. (2011). Reduced hippocampal glutamate in Alzheimer disease. *Neurobiol Aging, 32*(5), 802-810. doi:10.1016/j.neurobiolaging.2009.05.002

Sailasuta, N., Ernst, T., & Chang, L. (2008). Regional variations and the effects of age and gender on glutamate concentrations in the human brain. *Magn Reson Imaging, 26*(5), 667-675. doi:10.1016/j.mri.2007.06.007

Salamé, P., & Baddeley, A. (1989). Effects of Background Music on Phonological Short-term Memory *The Quarterly Journal of Experimental Psychology, 41A(1),* 16.

Salthouse, T. A. (1994). Aging associations: influence of speed on adult age differences in associative learning. *J Exp Psychol Learn Mem Cogn, 20*(6), 1486-1503. doi:10.1037//0278-7393.20.6.1486

Salthouse, T. A. (1996). The processing-speed theory of adult age differences in cognition. *Psychol Rev, 103*(3), 403-428. doi:10.1037/0033-295x.103.3.403

Schacter, D. L., & Wagner, A. D. (1999). Medial temporal lobe activations in fMRI and PET studies of episodic encoding and retrieval. *Hippocampus, 9*(1), 7-24. doi:10.1002/(SICI)1098-1063(1999)9:1<7::AID-HIPO2>3.0.CO;2-K

Schaller, B., Mekle, R., Xin, L., Kunz, N., & Gruetter, R. (2013). Net increase of lactate and glutamate concentration in activated human visual cortex detected with magnetic resonance spectroscopy at 7 tesla. *J Neurosci Res, 91*(8), 1076-1083. doi:10.1002/jnr.23194

Schaller, B., Xin, L., O'Brien, K., Magill, A. W., & Gruetter, R. (2014). Are glutamate and lactate increases ubiquitous to physiological activation? A (1)H functional MR spectroscopy study during motor activation in human brain at 7Tesla. *Neuroimage, 93 Pt 1*, 138-145. doi:10.1016/j.neuroimage.2014.02.016

Scoville, W. B., & Milner, B. (1957). Loss of recent memory after bilateral hippocampal lesions. *J Neurol Neurosurg Psychiatry, 20*(1), 11-21. doi:10.1136/jnnp.20.1.11

Segovia, G., Porras, A., Del Arco, A., & Mora, F. (2001). Glutamatergic neurotransmission in aging: a critical perspective. *Mech Ageing Dev, 122*(1), 1-29. doi:10.1016/s0047-6374(00)00225-6

Shen, J., Petersen, K. F., Behar, K. L., Brown, P., Nixon, T. W., Mason, G. F., . . . Rothman, D. L. (1999). Determination of the rate of the glutamate/glutamine cycle in the human brain by in vivo 13C NMR. *Proc Natl Acad Sci U S A, 96*(14), 8235-8240.

Shing, Y. L., Werkle-Bergner, M., Li, S. C., & Lindenberger, U. (2008). Associative and strategic components of episodic memory: a life-span dissociation. *J Exp Psychol Gen, 137*(3), 495-513. doi:10.1037/0096-3445.137.3.495

Sibson, N. R., Dhankhar, A., Mason, G. F., Rothman, D. L., Behar, K. L., & Shulman, R. G. (1998). Stoichiometric coupling of brain glucose metabolism and glutamatergic neuronal activity. *Proc Natl Acad Sci U S A, 95*(1), 316-321. doi:10.1073/pnas.95.1.316

Simons, J. S., & Spiers, H. J. (2003). Prefrontal and medial temporal lobe interactions in long-term memory. *Nat Rev Neurosci, 4*(8), 637-648. doi:10.1038/nrn1178

Snodgrass, J. G., & Vanderwart, M. (1980). A standardized set of 260 pictures: norms for name agreement, image agreement, familiarity, and visual complexity. *J Exp Psychol Hum Learn, 6*(2), 174-215.

Sokoloff, L., Reivich, M., Kennedy, C., Des Rosiers, M. H., Patlak, C. S., Pettigrew, K. D., . . . Shinohara, M. (1977). The [14C]deoxyglucose method for the measurement of local cerebral glucose utilization: theory, procedure, and normal values in the conscious and anesthetized albino rat. *J Neurochem, 28*(5), 897-916. doi:10.1111/j.1471-4159.1977.tb10649.x

Sonnay, S., Duarte, J. M., Just, N., & Gruetter, R. (2016). Compartmentalised energy metabolism supporting glutamatergic neurotransmission in response to increased activity in the rat cerebral cortex: A 13C MRS study in vivo at 14.1 T. *J Cereb Blood Flow Metab, 36*(5), 928-940. doi:10.1177/0271678X16629482

Spencer, W. D., & Raz, N. (1995). Differential effects of aging on memory for content and context: a meta-analysis. *Psychol Aging, 10*(4), 527-539. doi:10.1037//0882-7974.10.4.527

Spurny, B., Seiger, R., Moser, P., Vanicek, T., Reed, M. B., Heckova, E., . . . Lanzenberger, R. (2020). Hippocampal GABA levels correlate with retrieval performance in an associative learning paradigm. *Neuroimage, 204*, 116244. doi:10.1016/j.neuroimage.2019.116244

Stanley, J. A. (2002). In vivo magnetic resonance spectroscopy and its application to neuropsychiatric disorders. *Can J Psychiatry, 47*(4), 315-326.

Stanley, J. A., Burgess, A., Khatib, D., Ramaseshan, K., Arshad, M., Wu, H., & Diwadkar, V. (2017). Functional dynamics of hippocampal glutamate during associative learning assessed with in vivo ^{1}H functional magnetic resonance spectroscopy. *Neuroimage*(153), 189-197. doi:doi: 10.1016/j.neuroimage.2017.03.051.

Stanley, J. A., Drost, D. J., Williamson, P. C., & Thompson, R. T. (1995). The use of a priori knowledge to quantify short echo in vivo 1H MR spectra. *Magn Reson Med, 34*, 8. doi:doi:10.1002/mrm.1910340105

Stanley, J. A., Pettegrew, J. W., & Keshavan, M. S. (2000). Magnetic resonance spectroscopy in schizophrenia: methodological issues and findings--part I. *Biol Psychiatry, 48*(5), 357-368.

Stanley, J. A., & Raz, N. (2018). Functional Magnetic Resonance Spectroscopy: The "New" MRS for Cognitive Neuroscience and Psychiatry Research. *Front Psychiatry, 9*, 76. doi:10.3389/fpsyt.2018.00076

Stephens, M. L., Quintero, J. E., Pomerleau, F., Huettl, P., & Gerhardt, G. A. (2011). Age-related changes in glutamate release in the CA3 and dentate gyrus of the rat hippocampus. *Neurobiol Aging, 32*(5), 811-820. doi:10.1016/j.neurobiolaging.2009.05.009

Suzuki, W. A. (2007). Making new memories: the role of the hippocampus in new associative learning. *Ann N Y Acad Sci, 1097*, 1-11. doi:10.1196/annals.1379.007

Tabone, C. J., & Ramaswami, M. (2012). Is NMDA receptor-coincidence detection required for learning and memory? *Neuron, 74*(5), 767-769. doi:10.1016/j.neuron.2012.05.008

Tang, Y. P., Shimizu, E., Dube, G. R., Rampon, C., Kerchner, G. A., Zhuo, M., . . . Tsien, J. Z. (1999). Genetic enhancement of learning and memory in mice. *Nature, 401*(6748), 63-69. doi:10.1038/43432

Tatti, R., Haley, M. S., Swanson, O. K., Tselha, T., & Maffei, A. (2017). Neurophysiology and Regulation of the Balance Between Excitation and Inhibition in Neocortical Circuits. *Biol Psychiatry, 81*(10), 821-831. doi:10.1016/j.biopsych.2016.09.017

Thielen, J. W., Hong, D., Rohani Rankouhi, S., Wiltfang, J., Fernandez, G., Norris, D. G., & Tendolkar, I. (2018). The increase in medial prefrontal glutamate/glutamine concentration during memory encoding is associated with better memory performance and stronger functional connectivity in the human medial prefrontal-thalamus-hippocampus network. *Hum Brain Mapp, 39*(6), 2381-2390. doi:10.1002/hbm.24008

Tkáć, I., & Gruetter, R. (2005). Methodology of ^{1}H NMR spectroscopy of the human brain at very high magnetic fields. *Appl Magn Reson, 29*, 19. doi:10.1007/BF03166960

Tromp, D., Dufour, A., Lithfous, S., Pebayle, T., & Despres, O. (2015). Episodic memory in normal aging and Alzheimer disease: Insights from imaging and behavioral studies. *Ageing Res Rev, 24*(Pt B), 232-262. doi:10.1016/j.arr.2015.08.006

Tulving, E. (1983). *Elements of episodic memory*: Oxford University Press.

Ungerleider, L. G. (1995). Functional brain imaging studies of cortical mechanisms for memory. *Science, 270*(5237), 769-775.

van der Graaf, M. (2010). In vivo magnetic resonance spectroscopy: basic methodology and clinical applications. *Eur Biophys J, 39*(4), 527-540. doi:10.1007/s00249-009-0517-y

van Maanen, L., Forstmann, B. U., Keuken, M. C., Wagenmakers, E. J., & Heathcote, A. (2016). The impact of MRI scanner environment on perceptual decision-making. *Behav Res Methods, 48*(1), 184-200. doi:10.3758/s13428-015-0563-6

VanPetten, C. (2004). Relationship between hippocampal volume and memory ability in healthy individuals across the lifespan: review and meta-analysis. *Neuropsychologia, 42*, 20. doi:10.1016/j.neuropsychologia.2004.04.006

Verhaeghen, P., & Marcoen, A. (1993). Memory aging as a general phenomenon: episodic recall of older adults is a function of episodic recall of young adults. *Psychol Aging, 8*(3), 380-388. doi:10.1037//0882-7974.8.3.380

Vieira, S., & Hoffman, R. (1977). Comparison of the Logistic and the Gompertz Growth Functions Considering Additive and Multiplicative Error Terms. *Appl Statist, 26*(2), 6.

Wadehra, S., Pruitt, P., Murphy, E. R., & Diwadkar, V. A. (2013). Network dysfunction during associative learning in schizophrenia: Increased activation, but decreased connectivity: an fMRI study. *Schizophr Res, 148*(1-3), 38-49. doi:10.1016/j.schres.2013.05.010

Walsh, D. M., & Selkoe, D. J. (2004). Deciphering the molecular basis of memory failure in Alzheimer's disease. *Neuron, 44*(1), 181-193. doi:10.1016/j.neuron.2004.09.010

West, M. J. (1993). Regionally specific loss of neurons in the aging human hippocampus. *Neurobiol Aging, 14*(4), 287-293. doi:10.1016/0197-4580(93)90113-p

West, M. J., Amaral, D. J., & Rapp, P. R. (1993). *Preserved hippocampal cell number in aged monkeys with recognition memory deficits.* Paper presented at the Soc. Neurosci. .

Williams, K., Pinto, J., Irwin, D., Jones, D., & Murphy, K. (2009). Age-related changes in the inhibitory:excitatory balance in macaque monkey primary visual cortex [Abstract]. *Journal of Vision, 9*(8).

Winsor, C. P. (1932). The Gompertz curve as a growth curve. . *Proc Natl Acad Sci U S A, 18*, 8.

Woodcock, E. A., Anand, C., Khatib, D., Diwadkar, V. A., & Stanley, J. A. (2018). Working Memory Modulates Glutamate Levels in the Dorsolateral Prefrontal Cortex during (1)H fMRS. *Front Psychiatry, 9*, 66. doi:10.3389/fpsyt.2018.00066

Woodcock, E. A., White, R., & Diwadkar, V. A. (2015). The dorsal prefrontal and dorsal anterior cingulate cortices exert complementary network signatures during encoding and retrieval in associative memory. *Behav Brain Res, 290*, 152-160. doi:10.1016/j.bbr.2015.04.050

Yankner, B. A., Lu, T., & Loerch, P. (2008). The aging brain. *Annu Rev Pathol, 3*, 41-66. doi:10.1146/annurev.pathmechdis.2.010506.092044

Zahr, N. M., Mayer, D., Rohlfing, T., Chanraud, S., Gu, M., Sullivan, E. V., & Pfefferbaum, A. (2013). In vivo glutamate measured with magnetic resonance spectroscopy: behavioral correlates in aging. *Neurobiol Aging, 34*(4), 1265-1276. doi:10.1016/j.neurobiolaging.2012.09.014

Zhang, X., Liu, H., Wu, J., Zhang, X., Liu, M., & Wang, Y. (2009). Metabonomic alterations in hippocampus, temporal and prefrontal cortex with age in rats. *Neurochem Int, 54*(8), 481-487. doi:10.1016/j.neuint.2009.02.004

Zhang, Y., Brady, M., & Smith, S. (2001). Segmentation of brain MR images through a hidden Markov random field model and the expectation-maximization algorithm. *IEEE Trans Med Imaging, 20*, 45-57.

Zola-Morgan, S., Squire, L. R., & Amaral, D. G. (1986). Human amnesia and the medial temporal region: enduring memory impairment following a bilateral lesion limited to field CA1 of the hippocampus. *J Neurosci, 6*(10), 2950-2967.

Zwietering, M. H., Jongenburger, I., Rombouts, F. M., & van 't Riet, K. (1990). Modeling of the bacterial growth curve. *Appl Environ Microbiol, 56*(6), 1875-1881.

ABSTRACT

AGE DIFFERENCES IN HIPPOCAMPAL GLUTAMATE MODULATION DURING ASSOCIATIVE LEARNING AND MEMORY: A PROTON FUNCTIONAL MAGNETIC RESONANCE SPECTROSCOPY (^{1}H fMRS) STUDY

by

CHAITALI ANAND

August 2020

Advisors: Dr. Naftali Raz and Dr. Jeffrey Stanley

Major: Neuroscience (Translational)

Degree: Doctor of Philosophy

Episodic and associative memory decline is one of the earliest cognitive impairments in normal aging and among the defining cognitive features of Alzheimer's disease (AD). Since, age-related cognitive decline gradually devolves into AD, with neuropathology preceding cognitive changes by many years, the identification of biomarkers of early disease progression is crucial. Reduction in glutamate, the main excitatory neurotransmitter involved in associative memory, in key brain regions such as the hippocampus, has been theorized as one of the cellular mechanisms underlying cognitive decline in aging and AD. A few neuroimaging studies that demonstrated a link between older adults' weaker cognitive performance and lower hippocampal glutamate levels, correlated static levels of glutamate with out-of-scanner performance. The current study is the first to investigate age effects on temporal modulation of hippocampal glutamate during associative memory performance. Proton functional magnetic resonance spectroscopy (^{1}H fMRS) was used to examine hippocampal glutamate modulation in healthy young and old adults during associative memory performance. Proton spectra from unilateral hippocampi were acquired during task performance and during a preceding non-task-active

control condition. Young adults demonstrated better associative memory performance than the old. Despite no age differences in glutamate levels during the control condition, significant age differences were detected in the temporal modulation of glutamate during the associative memory task that were specific to memory encoding. Young adults evinced higher glutamate levels earlier during encoding, that later reduced when the capacity to encode had presumably approached saturation. Conversely, old adults failed to demonstrate significant glutamate modulation in either memory stage. However, within the older group, associative memory performance seemed to depend on the timing of glutamate elevation during encoding. Specifically, old adults who displayed earlier glutamate elevation demonstrated a trend towards a later inflection point and a slower rate of learning. These results indicate that early glutamatergic response during memory encoding reflects early engagement of the hippocampus leading to better associative memory performance. This study provides the first *in vivo* demonstration of age differences in hippocampal glutamate modulation during associative memory performance and is the first step towards better elucidation of glutamatergic contribution to age-related cognitive differences.

AUTOBIOGRAPHICAL STATEMENT

I am grateful for the things that have made me uncomfortable and forced me to adapt and grow.